

2009

Development of Amphipathic Beta-Strand Mimics as Potential Membrane Active Antibiotics

Jessica L. Watson

Follow this and additional works at: <https://ir.lib.uwo.ca/digitizedtheses>

Recommended Citation

Watson, Jessica L., "Development of Amphipathic Beta-Strand Mimics as Potential Membrane Active Antibiotics" (2009). *Digitized Theses*. 3908.
<https://ir.lib.uwo.ca/digitizedtheses/3908>

This Thesis is brought to you for free and open access by the Digitized Special Collections at Scholarship@Western. It has been accepted for inclusion in Digitized Theses by an authorized administrator of Scholarship@Western. For more information, please contact wlsadmin@uwo.ca.

**Development of Amphipathic
Beta-Strand Mimics as Potential Membrane
Active Antibiotics**

(Spine Title: Amphipathic Beta-Strand Mimics as Potential
Antibiotics)

(Thesis Format: Monograph)

By

Jessica L. Watson

Graduate Program in Chemistry

**Submitted in partial fulfillment
of the requirements for the degree of
Master of Science**

The School of Graduate and Postdoctoral Studies

University of Western Ontario

London, Ontario, Canada

October, 2009

©Jessica Watson 2009

ABSTRACT

In recent years, there have been increasing numbers of bacterial strains emerging that are resistant to the currently available antibiotics. In the search for new antibiotics, attention has been focused on natural antimicrobial peptides that act by selectively disrupting the membranes of bacterial cells, a mechanism that is thought to be non-conducive to the development of resistance. It is desirable to mimic the structures and activities of these peptides, while introducing properties such as resistance to proteolytic degradation, which make molecules more ideal for development as drugs. Described here is the design and synthesis of β -strand mimetic oligomers based on alternating α -amino acids and azacyclohexenone units that segregate cationic lysine and hydrophobic valine side chains on opposite faces of the β -strand. ^1H NMR dilution studies demonstrated that despite the incorporation of alternating D- and L-amino acids in order to obtain facial amphiphilicity, these oligomers are capable of dimerizing to β -sheet mimics in a manner similar to the oligomers containing all L-amino acids. The ability of the molecules to disrupt phospholipid vesicles mimicking the membranes of both bacterial and mammalian cells was investigated using a fluorescent dye leakage assay. Several of the oligomers were found to exhibit activity and selectivity for the bacterial over mammalian membranes. Overall, these studies demonstrate the promise of this class of molecules for the development of new potential antibiotics, and provide information on the structural features that are important for activity.

KEY WORDS

β -strand mimic, antimicrobial peptides, membranes, facial amphiphilicity, dimers, dye leakage assay.

ACKNOWLEDGMENTS

I would like to thank my supervisor Dr. Elizabeth Gillies, for giving me this great opportunity to conduct this research, and for all of her help, guidance, support and encouragement throughout my time here. Her knowledge and dedication has made my experience in this group enjoyable and rewarding.

I would also like to thank all of the past and present members of the Gillies group. It has been a great pleasure to work with all of them, and I could not have done it without all of their friendship and support. Special thanks go out to Amanda Martin, Matt Dewit, Katelyn Atkins, Mike Maris, Barb Bajtos and Nick Morra, as well as Darryl Knight and Aneta Borecki for instrument assistance. Also, I would like to thank Dr. Mathew Willans for providing NMR assistance and Dr. Doug Hairsine for help with mass spectrometry.

Lastly I'd like to thank my family and friends for all of their support and love.

CONTENTS

	Page
CERTIFICATE OF EXAMINATION	ii
ABSTRACT	iii
ACKNOWLEDGEMENTS	iv
TABLE OF CONTENTS	v
LIST OF SCHEMES	vii
LIST OF FIGURES	viii
LIST OF EQUATIONS	xi
LIST OF ABBREVIATIONS	xii
Part One: Introduction	1
1.1 The Need for New Antibiotics	2
1.2 Naturally Occuring Peptide Antibiotics	2
1.2.1 Magainins	3
1.2.2 Cecropins	4
1.2.3 Protegrins	4
1.2.4 Defensins	5
1.3 Mechanism of Action	7
1.4 Synthetic Mimics of Natural Antimicrobial Peptides	8
1.5 Helical Peptidomimetics	10
1.5.1 12-Helix Forming β -Peptide Antimicrobial Mimics	12
1.5.2 14-Helix Forming β -Peptide Antimicrobial Mimics	15
1.5.3 α/β -Peptide Antimicrobial Mimics	16
1.6 Antimicrobial Peptides with Undefined Conformations	19
1.7 Other Synthetic Oligomer Backbones	22
1.8 Elongated Antimicrobial Mimics Containing Aryl Backbone	
Monomers	25

1.9 β -Strand Mimics as Potential Antibiotics	30
Part Two: Results and Discussion	34
2.1 Thesis Goals	35
2.2 Primary Design of First Generation β -Strand Peptidomimetics	35
2.3 Synthesis of First Generation β -Strand Peptidomimetics	37
2.4 Self Association of @-Tide 8 in CDCl ₃ /CD ₃ OH Mixtures	40
2.5 Assessment of Membrane Disruptive Potential Using a Vesicle Leakage Assay	45
2.6 Design of Second Generation β -Strand Peptidomimetics	58
2.7 Synthesis of Second Generation β -Strand Peptidomimetics	60
2.8 Assessment of Membrane Disruptive Potential Using a Vesicle Leakage Assay	65
Part Three: Conclusions	75
3.1 Contributions	76
Part Four: Experimental	79
4.1 General Procedures and Materials	80
4.2 Experimental Section	81
Part Five: References	95
Part Six: Appendix (NMR Spectra)	102
Curriculum Vitae	114

LIST OF SCHEMES

Scheme 1. Synthesis of alternating D-/L- amino acid @-tide tetramer 6	38
Scheme 2. Synthesis of alternating D-/L- pentamers 8 and 10 and hexamers 9 and 11	39
Scheme 3. Synthesis of the first series (more valine residues) of the second generation	61
Scheme 4. Synthesis of the second series (all lysine residues) of the second generation	63
Scheme 5. Synthesis of the third series (aliphatic tail addition) of the second generation	64

LIST OF FIGURES

Figure 1. Schematic of Magainin-2, a helical antimicrobial peptide with hydrophobic side chains shown as green and polar (cationic) side chains shown as blue.	4
Figure 2. Protegrin-1 ($X_{6,8,13,15}$ are cysteine residues, X_{10} is an arginine residue).	5
Figure 3. The corresponding cysteines in both α - and β -defensins are indicated by dotted lines, with the disulfide linkages indicated by solid lines. Human β -defensin 2 in its monomeric form shows the general shape (defensin-fold).	6
Figure 4. Mechanisms of antimicrobial action. a) The barrel-stave mechanism b) The carpet mechanism c) The toroidal pore mechanism and d) The disordered toroidal pore mechanism.	8
Figure 5. a) Gellman's <i>trans</i> -ACHC as a 14-helix; b) Building blocks of both oligomers (<i>trans</i> -ACHC and <i>trans</i> -ACPC, respectively).	11
Figure 6. Seebach's β -substituted β -peptide.	12
Figure 7. a) The structure of β -17; b) The 12-helix schematic.	13
Figure 8. Example β -peptide containing cyclic β -residues and noncyclic β^3 -residues.	14
Figure 9. β -peptide H-(β^3 -HVal- β^3 -HLys- β^3 -HLeu) ₄ -OH in the 14-helix conformation.	15
Figure 10. a) Amphiphilic peptide in 11-helix (left column); b) Amphiphilic peptide in 14/15-helix (right column); c) Scrambled in both conformations.	17
Figure 11. a) Standard hypothesis for peptides that involve a folding pattern upon interaction with a bacterial membrane. b) Alternative hypothesis that involves induction of globally amphiphilic but irregular conformations in the presence of bacterial membranes.	20
Figure 12. a) Examples of β -lactam monomers (hydrophobic and cationic, respectively); b) Example of nylon-3 polymer.	21
Figure 13. a) Globally amphiphilic segregated copolymer; b) Facially amphiphilic copolymer containing norbornene monomer; c) Facially amphiphilic copolymer containing furan ring.	23
Figure 14. Basic arylamide structure.	25
Figure 15. Arylamide with ether groups at the 4 and 6 position of the middle ring, generating increased intramolecular hydrogen bonding and overall rigidity.	26

Figure 16. The most active aryl amide reported.	27
Figure 17. Aryl urea trimer.	28
Figure 18. Tri(phenylene ethynylene) facially amphiphilic oligomer.	29
Figure 19. Artificial β -sheet containing Hao artificial amino acid and urea β -turn.	32
Figure 20. Linear α -tide containing alternating α units and L-amino acids.	33
Figure 21. Structure of an α -tide comprising a) all L-amino acids alternating with azacyclohexenone units and b) hydrophobic D-amino acids and hydrophilic L-amino acids alternating with azacyclohexenone units.	36
Figure 22. Chemical shifts of the farthest downfield N-H proton of pentamer 8 in ^1H NMR spectroscopy, as a function of solvent and concentration. The concentration dependence is indicative of dimerization of 8 to β -sheet mimics.	43
Figure 23. Chemical shifts of an N-H proton of tetramer 6 in ^1H NMR spectroscopy, as a function of solvent and concentration.	44
Figure 24. Chemical shifts of an N-H proton of hexamer 9 in ^1H NMR spectroscopy, as a function of solvent and concentration.	44
Figure 25. Detection of membrane lysis based on the leakage of encapsulated HPTS/DPX from vesicles by oligomer 10 assessed in vesicles of 80/20 DOPE/DOPG (bacterial mimic).	48
Figure 26. Detection of membrane lysis based on the leakage of encapsulated HPTS/DPX from vesicles by oligomer 11 assessed in vesicles of 80/20 DOPE/DOPG (bacterial mimic).	49
Figure 27. Detection of membrane lysis based on the leakage of encapsulated HPTS/DPX from vesicles by oligomer 6 assessed in vesicles of 80/20 DOPE/DOPG (bacterial mimic).	49
Figure 28. Detection of membrane lysis based on the leakage of encapsulated HPTS/DPX from vesicles by pentamer 8 assessed in vesicles of 80/20 DOPE/DOPG (bacterial mimic).	50
Figure 29. Detection of membrane lysis based on the leakage of encapsulated HPTS/DPX from vesicles by oligomer 9 assessed in vesicles of 80/20 DOPE/DOPG (bacterial mimic).	50
Figure 30. Summary of lysis activity for oligomers 6, 8, 9, 10, and 11 based on alternating D- and L-amino acids assessed in vesicles of 80/20 DOPE/DOPG (bacterial mimic) at 100 $\mu\text{g/mL}$.	51
Figure 31. Detection of membrane disruption based on the leakage of encapsulated HPTS and its quencher DPX from vesicles for oligomers 6, 8, 9, 10, and 11 based	

on alternating D- and L-amino acids assessed in vesicles of DOPC (mammalian mimic) at 100 $\mu\text{g}/\text{mL}$ in each case.	52
Figure 32. Detection of membrane lysis based on the leakage of encapsulated HPTS/DPX from vesicles by tetramer 6' assessed in vesicles of 80/20 DOPE/DOPG.	54
Figure 33. Detection of membrane lysis based on the leakage of encapsulated HPTS/DPX from vesicles by pentamer 8' assessed in vesicles of 80/20 DOPE/DOPG.	54
Figure 34. Detection of membrane lysis based on the leakage of encapsulated HPTS/DPX from vesicles by hexamer 9' assessed in vesicles of 80/20 DOPE/DOPG.	55
Figure 35. Detection of membrane lysis based on the leakage of encapsulated HPTS/DPX from vesicles by pentamer 10' assessed in vesicles of 80/20 DOPE/DOPG.	55
Figure 36. Detection of membrane lysis based on the leakage of encapsulated HPTS/DPX from vesicles by hexamer 11' assessed in vesicles of 80/20 DOPE/DOPG.	56
Figure 37. Summary of lysis activity for oligomers 6', 8', 9', 10', and 11' based on all L-amino acids assessed in vesicles of 80/20 DOPE/DOPG (bacterial mimic) at 100 $\mu\text{g}/\text{mL}$.	56
Figure 38. Detection of membrane disruption based on the leakage of encapsulated HPTS and its quencher DPX from vesicles for oligomers 6', 8', 9', 10', and 11' based on all L-amino acids assessed in vesicles of DOPC (mammalian mimic) at 100 $\mu\text{g}/\text{mL}$ in each case.	57
Figure 39. Target nonamer @-tide with a larger ratio of valine residues to lysine residues.	58
Figure 40. Target all lysine nonamer@-tide	59
Figure 41. Target nonamer @-tide with additional aliphatic tail for hydrophobicity.	60
Figure 42. Detection of membrane lysis based on the leakage of encapsulated HPTS/DPX from vesicles: (a) oligomer 14 assessed in vesicles of 80/20 DOPE/DOPG (bacterial mimic); (b) oligomer 14 assessed in vesicles of DOPC (mammalian mimic).	66
Figure 43. Detection of membrane lysis based on the leakage of encapsulated HPTS/DPX from vesicles: (a) oligomer 13 assessed in vesicles of 80/20 DOPE/DOPG (bacterial mimic); (b) oligomer 13 assessed in vesicles of DOPC (mammalian mimic).	67
Figure 44. Detection of membrane lysis based on the leakage of encapsulated HPTS/DPX from vesicles: (a) oligomer 16 assessed in vesicles of 80/20 DOPE/DOPG (bacterial mimic); (b) oligomer 16 assessed in vesicles of DOPC (mammalian mimic).	69

Figure 45. Detection of membrane lysis based on the leakage of encapsulated HPTS/DPX from vesicles: (a) oligomer 15 assessed in vesicles of 80/20 DOPE/DOPG (bacterial mimic); (b) oligomer 15 assessed in vesicles of DOPC (mammalian mimic). 70

Figure 46. Dicationic tetramer 16. The blue region indicates the polar part of the molecule and the green region indicates the hydrophobic part of the molecule. 71

Figure 47. Detection of membrane lysis based on the leakage of encapsulated HPTS/DPX from vesicles: (a) oligomer 20 assessed in vesicles of 80/20 DOPE/DOPG (bacterial mimic); (b) oligomer 20 assessed in vesicles of DOPC (mammalian mimic). 72

LIST OF EQUATIONS

Equation 1: Determination of dissociation constants 45

LIST OF ABBREVIATIONS

<i>trans</i> -ACHC	<i>trans</i> -2-aminocyclohexanecarboxylic acid
<i>trans</i> -ACPC	<i>trans</i> -2-aminocyclopentanecarboxylic acid
AIDS	acquired immunive deficiency syndrome
AP	β -amino-D-proline
<i>trans</i> -APC	<i>trans</i> -4-aminopyrrolidine-3-carboxylic acid
<i>trans</i> -3,4-APC	<i>trans</i> -3-aminopyrrolidine-4-carboxylic acid
AMP	antimicrobial peptide
ATP	adenosine triphosphate
Boc	tert-butyloxycarbonyl
Cbz	benzyl carbamate
CD	circular dichroism
COSY	correlation spectroscopy
DCC	dicyclohexylcarbodiimide
DIPEA	<i>N,N</i> -diisopropylethylamine
DMAP	dimethylaminopyridine
DMF	dimethylformamide
DMSO	dimethylsulfoxide
DNA	deoxyribonucleic acid
DOPC	1,2-dioleoyl- <i>sn</i> -glycero-3-phosphocholine
DOPE	1,2-dioleoyl- <i>sn</i> -glycero-3-phosphoethanolamine
DOPG	1,2-dioleoyl- <i>sn</i> -glycero-3-[phospho- <i>rac</i> -(1-glycerol)](sodium salt)
DPTS	4-(dimethyleamino)pyridinium 4-toluene-sulfonate
DPX	<i>p</i> -xylene-bis(<i>N</i> -pyridinium bromide)
HATU	<i>O</i> -(7-azabenzotriazol-1-yl)- <i>N,N,N',N'</i> -tetramethyluronium hexafluorophosphate
HMBC	heteronuclear multiple bond correlation
HPLC	high pressure liquid chromatography
HPTS	8-hydroxypyrene-1,3,6-trisulfonic acid trisodium salt
hRBC	human red blood cell
HRMS	high resolution mass spectrometry
IC ₅₀	half of the maximum inhibitory concentration
IR	infrared
K _d	dissociation constant
LUV	large unilamellar vesicles
MDR	multi-drug-resistant
MDRTB	multi-drug resistant <i>Mycobacterium tuberculosis</i>
MeCN	acetonitrile
MIC	minimum inhibitory concentration
MRSA	Methicillin-resistant <i>Staphylococcus aureus</i>
NMR	nuclear magnetic resonance spectroscopy
NOE	nuclear overhauser effect
PAON	polyamine oxanorbornene
PDZ	Post synaptic density protein (PSD95), <i>Drosophila disc large</i>

PHB	tumor suppressor (DlgA), and Zonula occludens-1 protein (zo-1)
SUV	poly(hydroxybutyrate)
TFA	small unilamellar vesicles
THF	trifluoroacetic acid
TLC	tetrahydrofuran
VRE	thin layer chromatography
	vancomycin-resistant enterococci

Part One: Introduction

1.1 The Need for New Antibiotics

The emergence of bacterial resistance to commercial antibiotics has increasingly become a major concern. Methicillin-resistant *Staphylococcus aureus* (MRSA), vancomycin-resistant enterococci (VRE), multi-drug resistant *Mycobacterium tuberculosis* (MDRTB) and multi-drug-resistant (MDR) Gram-negative bacteria have become extremely common hospital acquired resistant strains.¹ This resistance makes current antibiotics ineffective and the rate at which new antibiotics are being discovered is much slower than the rate of increasing resistance. Antibiotics generally act as inhibitors of intracellular bacterial enzymes. For example, sulfonamides inhibit folic acid production and rifamycin inhibits RNA polymerase but bacteria are developing methods to resist these actions. Essentially, bacteria are overcoming the action of these drugs by many mechanisms such as reduced antibiotic uptake, drug degradation, modification of specific target sites, overproduction of the target or bypass of the antibiotic-sensitive step by duplication of the target sites.²⁻⁵

1.2 Naturally Occurring Peptide Antibiotics

The development of novel and alternative antibiotics has recently become an important area of interest in order to overcome the problem of resistance. One relatively new approach is to mimic the structures and activities of naturally produced antibiotics which are often the first line of defense against bacteria.^{6, 7} Many naturally occurring peptide antibiotics such as magainins,⁸ cecropins,⁹ protegrins,¹⁰ defensins¹¹ and indolucidins¹² exhibit a diverse range of structures and activities. They show good antibacterial properties against some of the resistant strains of bacteria. A common

feature underlying these peptides is their ability to adopt conformations in which hydrophobic and cationic amino acid side chains are spatially clustered in distinct regions or faces of the molecule. This feature is referred to as amphipathicity. It is proposed that these molecules interact strongly and selectively with the negatively charged phospholipids and teichoic acids on the surfaces of the bacterial membranes as opposed to the neutral cholesterol and zwitterionic phospholipids on the surface of mammalian membranes. These naturally occurring antimicrobial peptides are found in a wide range of species, including plants, frogs, worms and humans.¹³

1.2.1 Magainins

The magainins (Figure 1) are a family of cationic peptides which are rich in lysine, contain 20-23 α -amino acid residues, and adopt an amphiphilic α -helical conformation in the presence of membranes.¹⁴ They were the first host-defense peptides to be isolated from a vertebrate by Zasloff in 1987.⁸ These peptides are proposed to act as antibiotics by disrupting bacterial membranes as well as by dissipating the electric potential across various energy-transducing membranes thus uncoupling respiration from other free-energy-requiring processes.^{15, 16, 17, 18, 19, 20, 21}

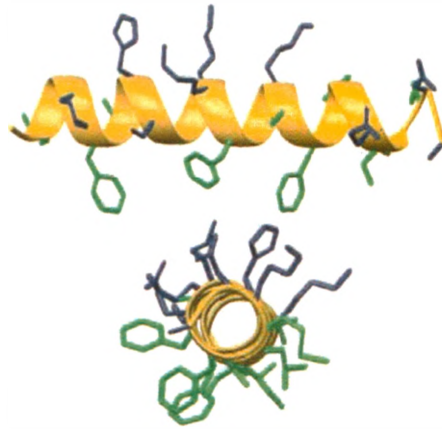


Figure 1. Schematic of Magainin-2, a helical antimicrobial peptide with hydrophobic side chains shown as green and polar (cationic) side chains shown as blue in both a side and head on view.²²

1.2.2 Cecropins

Insects produce cecropins as a response to the injection of bacteria.²³ Cecropins are a family of antimicrobial peptides isolated from the silk moth. They typically have 35-37 residues and also form amphipathic α -helices. As a mechanism of action, it is thought that cecropins form membrane channels and cause subsequent lysis.²³

1.2.3 Protegrins

Protegrins, in contrast to these examples, are a family of short cationic peptides of 16-18 amino acid residues isolated from porcine leukocytes²⁴ that adopts rigid two-stranded β -sheet conformation due to the stability of two disulfide bonds from cysteine residues. They show potent antimicrobial activity against a variety of gram-negative and gram-positive bacteria. They also resemble other antimicrobial peptides in that they are cationic due to their high arginine content. A hydrophobic cluster of amino acid residues

which differ in the length of peptide segments between the cysteine residues as well as the pairing between the cysteines that are connected by the disulphide bonds. Both families of defensins consist of triple stranded β -sheets with a characteristic defensin fold (Figure 3).¹¹ Clusters of positively charged amino acids, with arginine and lysine as the cationic residues, are characteristic of most α - and β -defensins, but where the clusters are distributed in the molecule is variable.^{28, 29, 30} Permeabilization of target membranes is the proposed mode of action in defensin-mediated antimicrobial activity. Conditions that interfered with permeabilization also prevented the loss of bacterial viability, indicating that it is essential for bacteriostatic and bacteriocidal activity.¹¹ Cell-generated transmembrane potentials and electrostatic interactions, between the cationic peptide and vesicles composed of negatively charge phospholipids, have also been experimentally shown to be a very important influence for initial activity and peptide insertion.^{31, 32, 33, 34}

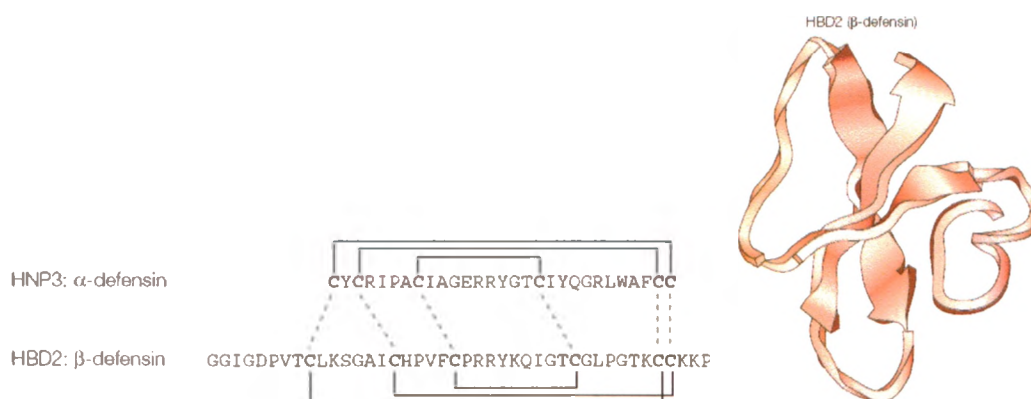


Figure 3. The corresponding cysteines in both α - and β -defensins are indicated by dotted lines, with the disulfide linkages indicated by solid lines. Human β -defensin 2 in its monomeric form shows the general shape (defensin-fold).¹¹

1.3 Mechanism of Action

The overall mechanism of action of natural peptide antibiotics is quite different than the more common receptor or enzyme targeted mechanisms. It is proposed that these peptide antibiotics and their mimics adhere or bind to the surfaces of the membranes, either by insertion or electrostatic forces, and form transmembrane pores.³⁵ These pores then act like ion channels. The passage of ions lowers the proton gradient and destroys the membrane potential, stopping ATP production and all cellular metabolism, resulting in cell death.²⁰ They also act as leakage sites for the internal components of the cell, which again would result in cell death.³⁶ Studies have also shown that all D-amino acid enantiomers of various peptides that were synthesized exhibited the same antimicrobial activities as their all-L native peptide counterparts,³⁷⁻⁴⁰ implying that the action of antimicrobial peptides does not involve stereospecific protein receptors.²⁰ There are a few different methods proposed for pore formation, including the barrel-stave, toroidal pore, disordered toroidal pore and carpet mechanism (Figure 4).²⁰ The barrel-stave model involves the insertion of amphipathic peptides perpendicularly into the bilayer, parallel to the lipids, with their hydrophobic side facing towards the lipids and the hydrophilic side facing the inside of the channel. The toroidal pore model involves the peptides inserting themselves perpendicularly into the bilayer, like the barrel-stave; however, they embed themselves in the lipid head group region, inducing a membrane curvature. The headgroups then bend from top to bottom to form a shape like the inside of a torus, which expands the headgroup region compared to the tails. This space is then further filled with the antimicrobial peptides to form a pore. The disordered toroidal pore mechanism is a recent modification to the toroidal pore hypothesis in which

a less rigid peptide conformation and orientation is formed. The carpet mechanism is one where the peptides adsorb to the lipid bilayer and, after a sufficient amount of coverage, produce a detergent-like effect which disintegrates the membrane.¹¹ Different antibiotic peptides may exhibit different mechanisms of action. Overall, these modes of action are of particular interest for novel antimicrobial therapeutics as they are thought to be relatively non specific and therefore not conducive to the development of resistance.^{11,41,42}

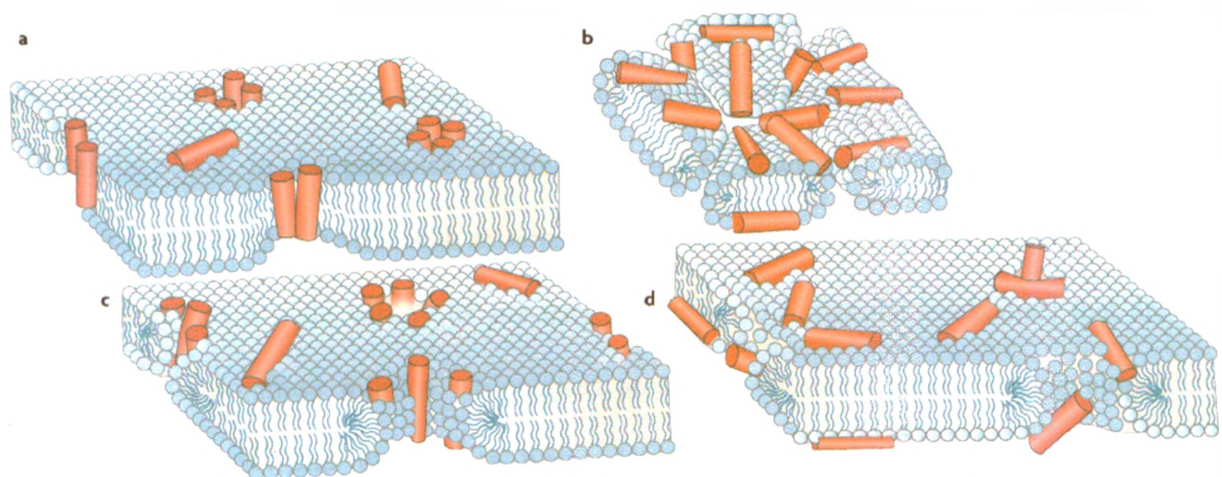


Figure 4. Mechanisms of antimicrobial action. a) The barrel-stave mechanism b) The carpet mechanism c) The toroidal pore mechanism and d) The disordered toroidal pore mechanism.⁴²

1.4 Synthetic Mimics of Natural Antimicrobial Peptides

Inspired by the structures and activities of naturally occurring antimicrobial peptides (AMPs), there has been significant interest in the development of several synthetic AMP mimics. These new molecules are providing insight into the mechanism of action of host-defense membrane-disruptive peptides⁴³⁻⁴⁵ while at the same time introducing simplified sequences and resistance to proteolytic degradation,⁴⁶ a problem

that plagues natural α -peptides as potential drug candidates. Thus far, the majority of efforts have been focused on the creation of new helical forming multimers, mimicking the structures of the magainins and cecropins. A number of groups have reported additional synthetic mimics of these AMPs which are designed to act by the mechanism of natural AMPs, such as peptides composed of α -amino acids,^{8, 47, 48} β -amino acids (“ β -peptides”),^{49, 50} both α - and β -amino acids (“ α/β -peptides”),^{51, 52} N-alkyl glycines (“peptoids”),⁵³ aromatic oligomers⁵⁴⁻⁵⁸ and synthetic polymers.^{59-61, 51} These molecules adopt either helical or β -sheet-like amphipathic conformations in the presence of bacteria or under conditions that are thought to mimic the environment provided by a bacterial cell surface (i.e. in the presence of lipid vesicles or detergent micelles).⁵¹ Research towards bacteriostatic AMPs with minimal hemolytic properties has also recently led to the discovery of a wide variety of successfully designed molecular backbones that are incorporated into these mimics. Elongated aromatic oligomers have been developed based on amides⁵⁴ and ureas,⁶² as well, oligo(phenyleneethynylenes)⁶³ that exhibit extended conformations have also been investigated, providing promising results. Recent work has also shown that through careful balance of the cationic charge and hydrophobicity, amphiphilic polymers can provide desired activities.^{55, 59, 60, 63, 64} Naturally helical AMPs and synthetic mimics that exhibit selective toxicity towards bacterial cells over mammalian cells typically display a cationic residue:lipophilic residue ratio between 1:1 and 1:2, depending on the primary sequence and residue compositions.⁶⁵ However there are many characteristics that determine antibacterial activity and selectivity, including size, conformational stability, net charge, net

hydrophobicity, amphiphilicity and the widths of the hydrophobic and hydrophilic helix faces.⁶⁵

1.5 Helical Peptidomimetics

Gellman and coworkers^{45, 51, 66, 67} have synthesized and tested, as antimicrobials, many different globally amphipathic peptides containing α -amino acids, β -amino acids, and a combination of both, mainly focusing on those that form helical oligomers or random oligomers that mimic host-defense peptides. These efforts have resulted in the discovery of several compounds with excellent antibiotic activity and specificity. Their initial focus was on the design of peptides containing unnatural backbones that fold into compact and specific conformations like their naturally occurring counterparts. These unnatural peptides were termed “foldamers” which were defined as any polymer or oligomer with a strong tendency to adopt a specific compact conformation.⁶⁸ These conformations consist of secondary peptide structures, such as α -helices, β -turns, β -strands and β -sheets. β -amino acids were chosen as the backbone building blocks because they were shown to be less conducive to nearest-neighbour H-bonding, which is not favourable in compact folding patterns.⁶⁹ *Trans*-2-aminocyclohexanecarboxylic acid (*trans*-ACHC) and *trans*-2-aminocyclopentanecarboxylic acid (*trans*-ACPC) (Figure 5b) were used as initial monomeric units and formed a 14- (defined by 14 membered ring C=O(*i*)---H-N(*i* - 2) hydrogen bonds) (Figure 5a) and 12-helix (12-membered ring C=O(*i*)---H-N(*i* + 3) hydrogen bonds), respectively.⁷⁰ The α -helix found in natural peptides is defined by a 13-membered ring with the same directionality relative to the termini.⁷¹

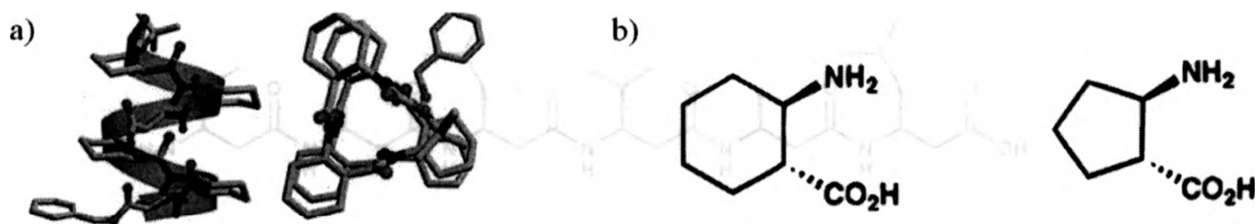


Figure 5. a) Gellman's *trans*-ACHC as a 14-helix; b) Building blocks of both oligomers (*trans*-ACHC and *trans*-ACPC, respectively).⁶⁸

Seebach and coworkers also reported at the same time β -peptide foldamers, but starting from a different class of β -amino acid building blocks.^{72, 73, 74, 75, 76} Their work stemmed from the study of poly(hydroxybutyrate) (PHB).⁷⁷ They proposed that PHB could adopt a helical conformation and that substitution of the ester linkages with amide linkages would reinforce the stability of the conformation through H-bonding. They further developed a method of incorporating optically active β -substituted residues into these peptides and found them to adopt a 14-helix in polar solution.⁷⁴ Further characterization of β -amino acid foldamers gave interesting results. Seebach and coworkers showed that β -peptides comprised of β -substituted (Figure 6) residues⁷⁵ or α -substituted residues⁷³ adopt the 14-helix. The effects of substituent position and configuration on the 14-helix folding^{73, 74} were carefully examined and it was shown that β -peptides were resistant to the actions of proteases,⁷⁶ which is excellent for medicinal applications. They also showed that β -peptides with alternating sequences of α - and β -substituted residues displayed a 12/10/12-helix, which contained both 12- and 10-membered rings.⁷⁸ Fleet and coworkers showed that oligomers containing β -amino acids constrained by *cis*-substituted oxetane rings adopt a 10-helical conformation.⁷⁹

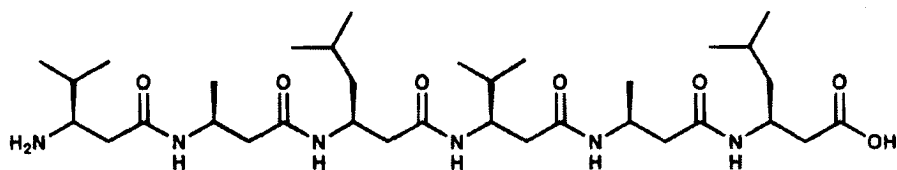


Figure 6. Seebach's β -substituted β -peptide.

1.5.1 12-Helix Forming β -Peptide Antimicrobial Mimics

Unnatural helix-forming peptides can then be employed for a variety of applications, specifically in the context of antimicrobial design. These oligomeric backbones can serve as scaffolds for displaying desired residues or functional groups in specific three-dimensional orientations. With this approach, molecules have been generated that bind specifically to other molecules and/or manifest selective biological activity.⁸⁰ As in the previous example with the *trans*-ACPC, Gellman and coworkers have shown that partial replacement of the *trans*-ACPC residues with cationic cyclic residues to create an amphipathic oligomer is possible. *Trans*-4-aminopyrrolidine-3-carboxylic acid (*trans*-APC) was employed as this cationic residue to construct a β -17 residue oligomer (Figure 7a) that was 40% cationic and 60% hydrophobic.⁵⁰ Because there are about 2.5 residues per turn in the 12-helix, the oligomer could be constructed to be amphipathic upon formation of the helix, with all the hydrophobic groups on one face and all the cationic groups on the opposite face (Figure 7b). The antimicrobial activities were compared to those of a synthetic magainin derivative, that is more effective than its precursor⁸¹ and were evaluated in 4 strains of bacteria (both gram positive and negative), two of which are resistant strains. The β -17 oligomer proved to have comparable activity to the magainins against all species.⁵⁰ To be considered as a potential therapeutic, the oligomer must also be compatible and non hemolytic with humans cells. This is

the nitrogen in the pyrrolidine ring, and β^3 -homolysine were also introduced. Additional β^3 -residues, such as homoleucine, homoalanine, homophenylalanine, homoserine, homovaline, were introduced to provide a more hydrophobic surface (Figure 8).⁸⁶ These oligomers were examined at varying lengths and ratios of cationic : hydrophobic residues. The projected helix

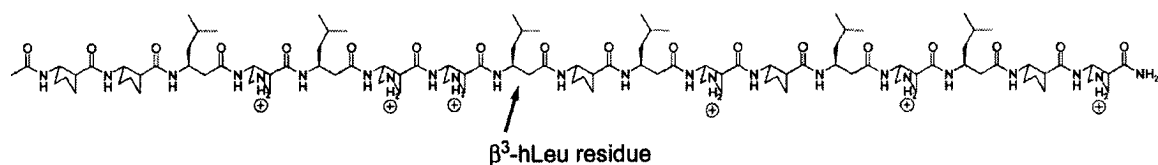


Figure 8. Example β -peptide containing cyclic β -residues and noncyclic β^3 -residues.

again formed an amphipathic conformation. Upon bacterial testing, the minimum inhibitory concentrations (MICs) were comparable to those of the β -17 oligomer as well as host defense peptides, like magainins, but were found to be slightly more hemolytic.⁸⁰ Scrambled oligomers were also prepared to assess the necessity of the amphipathic characteristic of these oligomers.^{67, 71, 87} In all cases, none were as potent as the original β -17 oligomer with the scrambled oligomer showing little to no activity. However, there was a trend found, that oligomers having a 40% cationic face were the most active. Hemolysis studies showed that there was only lytic activity for the most active oligomers at concentrations much higher than the MIC values, which is a desired trait to show selectivity for bacterial cells. Leakage studies, involving large unilamellar vesicles (LUVs) that mimic bacterial membranes and red blood cells, were also conducted for these compounds along with the magainins (host-defense and derivative) and the results showed that the β -oligomers acted by a membrane-disrupting mechanism similar to that of the naturally occurring peptides.⁷¹ However, the details of membrane interactions

varied between the β -peptides and α -peptides.¹⁴ Cyclic β -peptides of this kind have never been studied for proteolytic degradation before, however acyclic β -peptides have been shown to be very stable to many endogenous proteases.^{46, 76, 88} A heptamer was examined against a variety of proteases that are known to denature α -peptides and no significant change was observed.⁸³

1.5.2 14-Helix Forming β -Peptide Antimicrobial Mimics

Antimicrobial activity has also been observed for the 14-helical β -peptides. DeGrado^{49, 84} and coworkers have prepared versions of β -peptides 6-18 residues long by linking hydrophobic-cationic-hydrophobic residue triads to one another with the resulting helix circumference being comprised of approximately one third cationic surface (Figure 9). Although initially they did

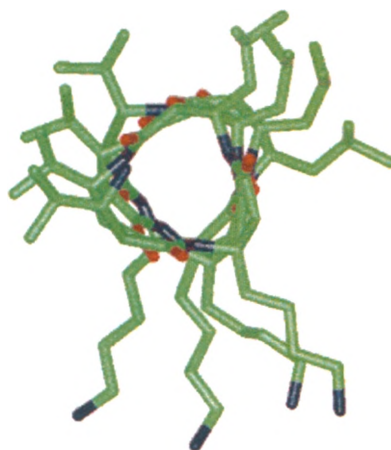


Figure 9. β -peptide H-(β^3 -HVal- β^3 -HLys- β^3 -HLeu)₄-OH in the 14-helix conformation.⁴⁹

show potent antibacterial activity but no selectivity, upon optimization of the net hydrophobicity by testing different hydrophobic residues (β^3 -hLeu and β^3 -hVal changed to β^3 -hAla), selectivity was achieved, with longer oligomers being more potent than

shorter ones. However, none of the reported oligomers were as potent as the β -17 peptide. Gellman also reported six-, nine- and ten-residue β -peptides in which the proportion of cyclohexane-constrained and acyclic (β -substituted) residues (β^3 -homovaline, homoleucine, and homolysine) were varied (zero to two-thirds cyclic residues).^{67, 86, 89} Those that contained only acyclic residues did not form the 14-helix in solution. This allowed for the ability to examine the effect of very high helical propensity on biological activity, as there has been much debate on the relationship between stability of the helical conformation and its resulting biological activity.^{90, 18, 91, 81, 92} Antimicrobial activity was seen for all compounds with nearly all of them being comparable to or more potent than synthetic magainin despite their vastly different extents of helical structure, leading them to believe that there is little relationship between conformational stability and antimicrobial activity for these peptides. The oligomers however did not follow a consistent trend for hemolytic activity, resulting in uncertain conclusions.⁶⁷

1.5.3 α/β -Peptide Antimicrobial Mimics

Incorporating α -amino acids into these β -peptides (generating α/β -peptides) as alternating residues has also been examined.^{93, 94} Work by Gellman and coworkers indicated that β -residues with a five-membered ring constraint led to short α/β -peptides that equilibrate between two internally H-bonded helices: the 11-helix (with about 3 residues per turn) and the 14/15-helix (with about 4.5 residues per turn).⁹⁴ Similar lengths and cationic/hydrophobic proportions of the β -peptides were used as guidelines for the design of the α/β -peptides. These peptides were designed to be amphipathic for

either the 11-helix or 14/15-helix or scrambled conformations for both (Figure 10). Upon bacterial tests, of the three classes, the 14/15-helix showed the least amount of antibacterial activity, which was unexpected as it was believed to be the most preferred conformation (by HPLC and NOE) compared to the 11-helix. The scrambled class along with the 11-helix showed greater activity, comparable to that of the synthetic magainin analogue, than the 14/15-helix. This was perplexing, as the scrambled version was not designed to be globally amphiphilic for either helix conformation. Further to this, scrambled α -peptides have been shown to have significantly diminished activity compared to their amphiphilic counterparts⁹⁵ and so have β -peptides, as described above. The scrambled α/β -peptide showed little hemolysis, comparable to that of the magainin analogue, but the other two classes showed

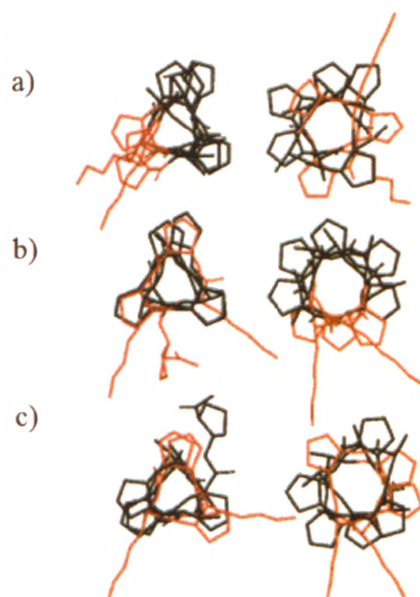


Figure 10. a) Amphiphilic peptide in 11-helix (left column); b) Amphiphilic peptide in 14/15-helix (right column); c) Scrambled in both conformations.⁵²

equal hemolytic activity to melittin. This hemolysis trend, in contrast to the antimicrobial trend, parallels the effects of sequence scrambling on hemolytic behaviour among helix forming α - and β -peptides.^{67, 71, 95} This phenomenon is explained by the fact that the amphiphilic 14/15- and 11-helix have a greater net hydrophobicity, therefore displaying a large hydrophobic patch whereas the scrambled peptide would have smaller patches.⁹⁶ Because erythrocytes are essentially devoid of anionic lipids and mainly consist of zwitterionic lipids,⁹⁷ the hydrophobic patches of the 14/15-helix interact readily with them.⁹⁸ It was then desirable to test this by creating new molecules that had reduced overall hydrophobicity by switching the hydrophobic α -amino acid residues to less hydrophobic ones (Leu to Ala). Upon this change, antimicrobial activity was drastically enhanced for the two different helical amphipathic oligomers, but reduced slightly for the scrambled one. Also, hemolytic activity was greatly reduced for all.⁵¹ This confirmed that the first three oligomers were too lipophilic, as it had been previously shown that high lipophilicity can lead to high hemolytic activity among antibacterial α -peptides.⁶⁵ These results also showed that designed amphiphilicity may not necessarily be essential for antibacterial activity and that the net lipophilicity may be the more important factor over that of designed conformation.⁵¹ Resistance to proteolytic degradation is additionally a concern for molecules containing α -amino acids, as α -peptides are readily degraded by proteases. All the α/β -peptides were tested against three different proteases and only one (the most catalytically active protease, pronase) caused trace amounts of cleavage after incubation and prolonged treatment. This result confirmed the expectation that oligomers containing 1:1 alternation of α - and β - residues are highly resistant to proteolytic degradation.⁵¹

1.6 Antimicrobial Peptides with Undefined Conformations

One possible explanation for the high activity of the scrambled α/β -polymers is that, under appropriate conditions, such as interaction with a membrane, they could adopt irregular, nonhelical conformations that result in a random global segregation of lipophilic and cationic side chains. The increased flexibility of the α - or β -residues would assist in this irregular conformation, as conformationally restricted residues in scrambled sequences show propensities to form the desired secondary structure.^{67, 71} Rathinakumar and Wimley⁹⁹ reported that the design of host-defense peptide analogues based on a specific structures and sequences were not as effective as a design based on the overall amino acid composition of the peptide. A combinatorial library was generated of short peptides with fixed amino acid residues at regular intervals while varying the hydrophobicity at the remaining sites. These peptides were shown to share very little sequence similarity, outside of the fixed residues, but were nevertheless highly membrane-lytic. This hypothesis posed an interesting concept for the design

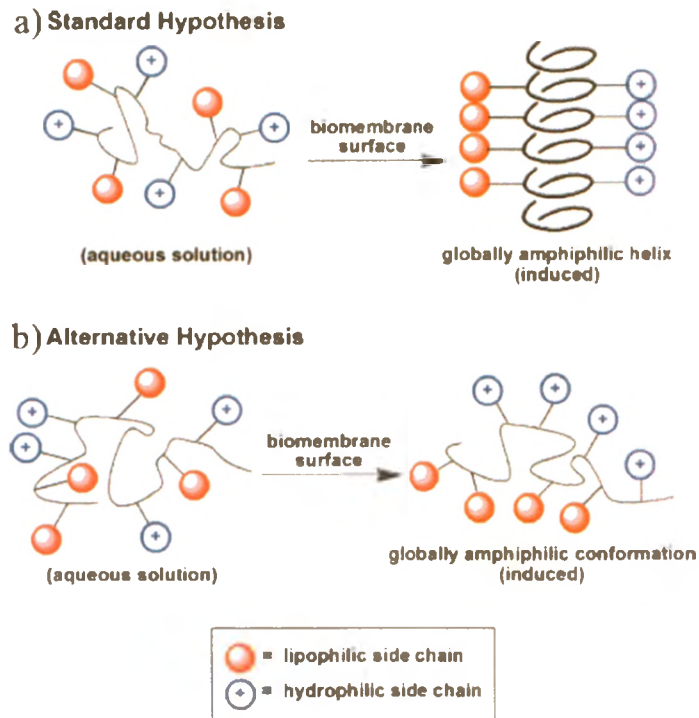


Figure 11. a) Standard hypothesis for peptides that involve a folding pattern upon interaction with a bacterial membrane. b) Alternative hypothesis that involves induction of globally amphiphilic but irregular conformations in the presence of bacterial membranes.⁶⁴

of new antimicrobial peptides, showing promise for developing antimicrobial agents that are inexpensive to make and can be prepared in large quantities.

Initial endeavours into this field began with polymers containing a polystyrene backbone that contained tertiary (would require protonation) and quaternary amines.¹⁰⁰⁻¹⁰⁴ Although these polystyrenes displayed antimicrobial activity, Gellman et al.⁶¹ were the first to show that these polystyrenes were highly hemolytic. Thus, the lack of selectivity for prokaryotic over eukaryotic cells was explained by the fact that the overall hydrophobicity of the polymers was too high, a previously shown trend among other

host-defense mimic peptides.⁶⁵ DeGrado et al. also examined poly(methyl methacrylate) copolymers⁵⁷ but were unable to identify examples that displayed significant antibacterial activity in the absence of hemolytic activity.

Polymers based on the nylon-3 family, comprised of hydrophobic and cationic β -lactams (synthesized via ring-opening copolymerization¹⁰⁵) have been designed as random copolymers to adopt a globally amphiphilic conformation induced by the presence of membranes (Figure 12).^{64, 106-109} Different percentages of the cationic and lipophilic residues were tested, and a ratio of about 40:60 lipophilic:cationic showed the most favourable antimicrobial activity without excessive hemolytic activity. The length of polymer was also optimized, which showed an average of 10-30 subunits to have very weak tendencies to induce hemoglobin release from

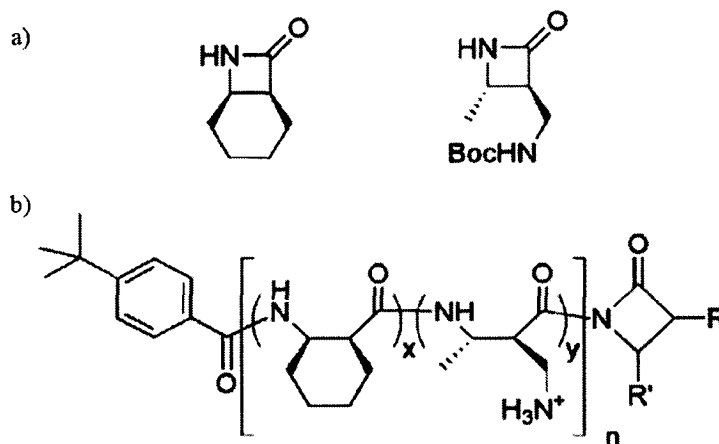


Figure 12. a) Examples of β -lactam monomers (hydrophobic and cationic, respectively);
b) Example of nylon-3 polymer.

hRBCs, but those longer were very hemolytic. When compared to other host-defense peptides (magainin and cecropins) as well as an improved magainin derivative, the nylon-

3 polymer showed greater antibacterial activity than those naturally occurring host-defense peptides and comparable results to the magainin derivative. It also showed decreased lytic activity toward hRBCs compared to the magainin derivative, however both were much more hemolytic than the host-defense peptides. Nevertheless, the 40:60 polymer showed substantial selectivity for bacteria relative to hRBCs. Upon model leakage studies, disruption and permeabilization of the bacterial membranes but not mammalian membranes was observed¹⁰⁷ which supported the previous selectivity derived from the bacterial studies.⁶⁴ These results were also consistent with the hypothesis that a polar backbone is important in minimizing hemolytic activity.⁶¹ In this regard, it is noteworthy that the polymers had a backbone rich in secondary amides, as do proteins. However, unlike proteins or conventional peptides, polymers in this nylon-3 family are not susceptible to degradation by proteases.⁴⁶

1.7 Other Synthetic Oligomer Backbones

Independent from antimicrobial peptide research, a second thrust has involved studies of other synthetic cationic polymers that exhibited varying degrees of antibacterial activities;⁶⁰ however, those attempts did not provide nonhemolytic, highly antibacterial polymers that acted by the disruption of membranes. For example, Tew and coworkers have studied materials generated via ring-opening alkene metathesis polymerization with norbornene units to generate the backbone.^{60, 110} These units can either be designed to be facially amphiphilic with a "lysine like" residue off of one face and a hydrophobic group of varying degrees of hydrophobicity off of the opposite face^{60, 63, 111-120} or have the hydrophobic and cationic groups on separate monomers creating

segregated copolymers¹²¹ (Figure 13), much like the random conformations observed for the α/β -peptides described above. No preformed or stable secondary structure was expected from these molecules. Starting from the monomer unit of polyamine oxanorbornene (PAON), homopolymers were examined for antibacterial and hemolytic activity and little to no activity was found. New copolymers from segregated monomers were designed to assess a wide range of amphiphilicities. The monomeric units were a *tert*-butyloxycarbonyl (Boc)-protected amine oxanorbornene and eleven other monomers carrying various alkyl chains.

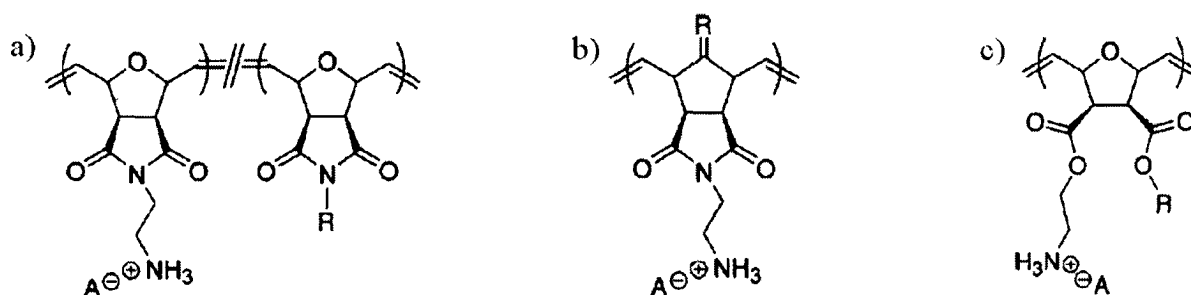


Figure 13. a) Globally amphiphilic segregated copolymer; b) Facially amphiphilic copolymer containing norbornene monomer; c) Facially amphiphilic copolymer containing furan ring.

They were synthesized in a manner to allow the copolymers to have a broad range of amphiphilicities, but approximately the same number of amines, and thus charges, at a high and low molecular weight. Fair antibacterial activity was seen for the copolymers with intermediate hydrophobicity at the low molecular weight, but not as effective as natural host defense peptide magainin. The most hydrophobic and hydrophilic copolymers showed negligible activity, as expected. Undesirable hemolytic activities

were observed, indicating that the hydrophobicity was likely too high. Tuning of these copolymers was attempted to help improve the activity and selectivity by adjusting the ratio of charged and hydrophobic monomers within the copolymer. Surprisingly, the dramatic anticipated improvement was not observed. This suggests that the spatial arrangement of charged and non-polar groups is important and not just the overall global amphiphilicity. The facially amphiphilic copolymers were also examined and compared to the segregated ones. These monomers consisted of either a norbornene or oxanorbornene with an alkylamine off the imide on one side and various hydrophobic groups off the opposite side or an oxanorbornene with hydrophobic and hydrophilic ester groups off the 3- and 4- positions of the furan ring (Figure 13c). Many different substituents were tested for the imide containing norbornene and oxanorbornene, such as ethyl amine, guanidinium, isopropyl, isobutyl, and methylacetylene to name a few. Some showed reasonable antimicrobial activity and selectivity that surpassed that of the magainin derivative. Additionally they proved to be bacteriocidal. With these results in hand though, none compared to the copolymer of the oxanorbornene monomer containing the cationic and hydrophobic (methyl to hexyl) ester residues, which is the most efficient of this type to date. When lipid vesicle studies were run on some of these facially amphiphilic copolymers, it was discovered that these peptides caused little to no damage to the membrane. This must mean that their ability to effectively kill bacteria likely occurs via a different mechanism than gross membrane trauma. It was then demonstrated that they have the ability to traverse membranes as well as other properties reminiscent of cell-penetrating peptides and then interact with an anionic macromolecule inside the cell.¹²²

1.8 Elongated Antimicrobial Mimics Containing Aryl Backbone Monomers

Oligomers composed of arylamides, designed by DeGrado et al., have been shown to mimic the properties of membrane-interactive antimicrobial peptides.^{54, 55} These oligomers however were conformationally different from the previously reported helical conformations by employing intramolecular hydrogen bonding¹²³⁻¹²⁵ of a thioether to both adjacent amide protons (Figure 14). This interaction could potentially help to rigidify the structure as well as prevent uncontrolled intermolecular H-bonding aggregation. The thioether also allowed for a convenient point of attachment for the basic residues. These oligomers were proposed to form an elongated linear facially amphiphilic conformation with the cationic and lipophilic functional groups protruding to the top and bottom of the molecule. Bacterial studies indicated that this class of oligomers was bactericidal and not just bacteriostatic. Hemolytic IC₅₀s (concentration which gives 50% of maximum inhibitory effect) were shown to be approximately

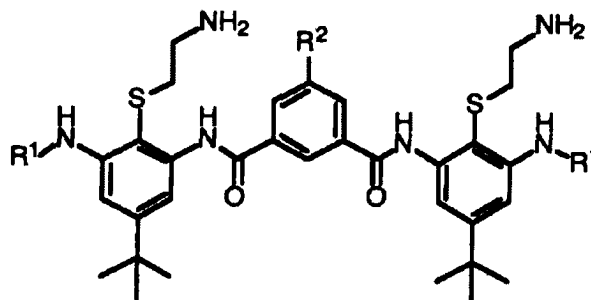


Figure 14. Basic arylamide structure.

10-fold higher than the MIC values for the bacteria, an insufficient selectivity for an antimicrobial agent of this type. To help eliminate this problem, the end groups (R¹ of Figure 14) of the short triaryl amide were varied with both polar and hydrophobic groups. Increasing the hydrophobicity resulted in increased activity toward erythrocytes, but

increasing the polarity, specifically to an arginine residue, resulted in substantial antibacterial activity, similar to that of a superior magainin analog, as well as significantly greater selectivity. Encouraged by these results, an additional polar positively charged alkylamino substituent was introduced to the central isophthaloyl group (R^2 of Figure 14) which even further enhanced the selectivity without greatly altering the potency. Vesicle leakage, evaluated using fluorescent dye assays further confirmed the mode of action of these oligomers by releasing about 90% of the dye at concentrations near the reported MIC values. These results indicated that short oligomers can also have strong antibiotic activity as well as selectivity, and also allowed for a simple cost effective synthesis.

To further optimize this class of oligomers, rigidity of the backbone was increased through hydrogen-bonding, and/or new substituents were introduced.¹²⁶ Hydrogen bonding in the backbone does not appear to be essential however, as the phenylene ethynylene backbone, introduced by Tew et al., was highly active.^{111, 114, 127} The two ether groups on the 4 and 6 position (R'' of Figure 15) of the isophthalic amide linker also hydrogen bond to the adjacent amide or terminal amine protons, forming

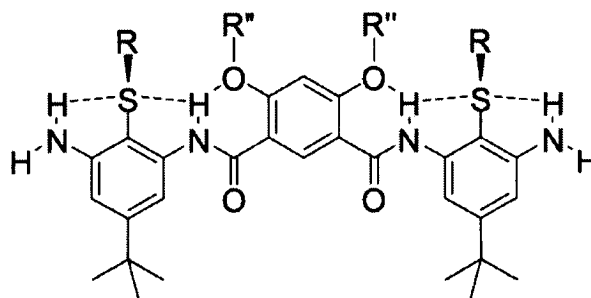


Figure 15. Arylamide with ether groups at the 4 and 6 position of the middle ring, generating increased intramolecular hydrogen bonding and overall rigidity.

3-centre intramolecular hydrogen bonds that rigidify the entire aryl amide trimer.¹³ Increased affinity and selectivity were observed upon this increase of rigidity of the molecule. Guanidinylation of the aniline groups also increased activity for both gram negative and gram positive species without affecting the hemolytic potency. Changes of the ether substituents on the isophthalic ring to add varying cationic substituents showed that the trimer could be selectively targeted to be preferably active towards one strain of bacteria over another. This additional introduction of cationic charge also decreased toxicity towards erythrocytes. Two additional changes of the isophthalic ring to a pyrimidine ring (position X of Figure 16) and the tert-butyl substituent to a less hydrophobic trifluoromethyl group (R^2 of Figure 16) minimized toxicity without loss of antibacterial potency. This is the most active arylamide oligomer to date (Figure 16), with activities comparable to that of vancomycin at its maximum tolerated dose.¹³ Like antimicrobial peptides, the arylamides cause rapid depolarization of lipid membranes (of mimicking vesicles) in a concentration-dependent manner at concentrations close to those required to the MIC. Interestingly, only partial depolarization is required to

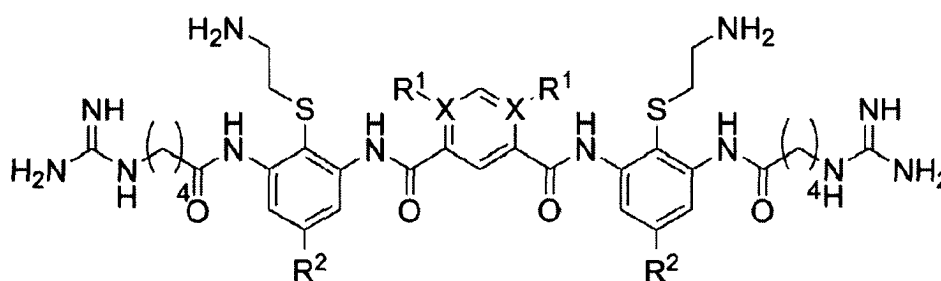


Figure 16. The most active aryl amide reported.

lead to cell death, which occurs in a slower process that can take up to several hours at concentrations near the MIC. This behaviour suggests that many AMPs and AMP

mimics act by mixed mechanisms; at high concentrations they disrupt membranes sufficiently to lead to cell death, whereas at lower concentrations, other slower mechanisms become important.¹³ Because these arylamides are too short to span the hydrophobic length of the phospholipid bilayer, it is suggested that these oligomers work in part by a mechanism that resembles the “carpet” mechanism of AMP activity. Their relatively small size and conformationally constrained structures may aid in their ability to penetrate various physical barriers in Gram-positive and Gram-negative bacteria. Once they gain access to the membranes, they must bind with sufficiently favourable free energy of association to allow disruption of the bilayer.

Tew et al.⁶² further explored this arylamide design with aryl urea oligomers which also have the intramolecular hydrogen bonding of amide or aniline hydrogens to a thioether substituent (Figure 17). The length of these oligomers was optimized for overall activity and selectivity and it was found that 3 monomer units were most favourable. In contrast to the preliminary arylamides reported above, these aryl ureas have hydrogen bonding interactions on every ring. Antibacterial and hemolysis activity was determined and the urea trimer proved to be extremely active and somewhat selective. Upon comparison to the magainin derivative

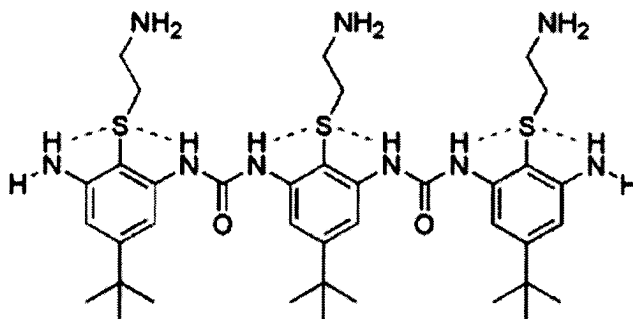


Figure 17. Aryl urea trimer.

and most active aryl amide, the antibacterial activity of the aryl urea far surpassed that of the magainin and was comparable to the aryl amide, but was not nearly as selective.

Oligomers without any hydrogen bonding amide motifs along the backbone were also studied. Oligo(phenylene ethynylene) backbones (Figure 18) were introduced and were shown to adopt facially amphiphilic conformations when properly designed.^{112, 114, 128-132} The tri(phenylene ethynylene) showed the most impressive results compared to longer versions for both antimicrobial activity as well as selectivity. They also showed potential as a new clinical treatment for antibiotic-resistant bacterial infections.¹¹¹ This oligomer was screened against a large set of bacteria and other microorganisms and was extremely potent against *E. coli*, with the lowest MIC reported thus far. Along with this, it was found that the measured selectivity showed extremely encouraging results. It also demonstrated good activity towards antibiotic resistant bacterial strains MRSA and VRE and showed no indication of inducing resistance. Studies on the behaviours of these phenylene ethynylene oligomers on membranes were also performed⁴⁴ which showed that the observed antibacterial activity correlates with an induced transition of

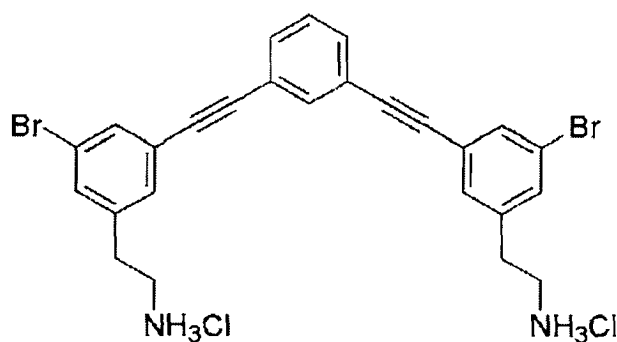


Figure 18. Tri(phenylene ethynylene) facially amphiphilic oligomer.

SUVs into an inverted hexagonal phase, in which hexagonal arrays of water channels are formed. Upon addition of the tri(phenylene ethynylene) to phospholipid vesicles, selective permeability was demonstrated.

Overall, the above described studies demonstrate that a diverse array of chemical structures is capable of exhibiting membrane disruptive antimicrobial properties. While amphiphilicity or amphipathicity appear to be the common features required for activity, the mechanism of action of many of the molecules is still poorly understood and new antibiotic molecules are still badly needed.

1.9 β -Strand Mimics as Potential Antibiotics

While most of the AMP mimics developed so far have focused on helices or molecules lacking well defined conformations as described above, the prior successes using the linear aromatic oligomers^{54, 56, 130} as well as an example of a highly active α -peptide capable of adopting an amphipathic β -sheet structure¹³³ suggest that β -strand mimics may provide a successful design for antimicrobial peptide mimics. Although synthetic analogues of protegrins have been developed to mimic their rigid anti-parallel two-stranded β -sheet structure which is stabilized by disulfide bonds, these structures have focused on the incorporation of the new turn inducing elements, and like the protegrins, they contain segregated domains of cationic groups at each end of the β -sheet.^{10, 134} The goal of this thesis was to develop the first example of an α -amino acid based β -strand peptidomimetic that is designed to have an amphipathic structure in which cationic amino acid side chains are directed to one face of the strand and hydrophobic

groups are directed towards the opposite face, with the aim of developing a new scaffold for membrane-disruptive antibiotics.

There is considerable interest presently in mimicking peptide and protein β -sheets and strands and their turn structures in hopes of duplicating and perhaps improving on their structural, functional and pharmacological properties.¹³⁵ β -sheets consist of extended polypeptide strands connected by a network of hydrogen bonds and occur widely in proteins. Intermolecular interactions between the hydrogen-bonding edges of β -sheets constitute a fundamental form of biomolecular recognition (like DNA base pairing) and are involved in protein quaternary structure, protein-protein interactions, and peptide and protein aggregation. The importance of β -sheet interactions in biological processes makes them potential targets for intervention and investigation in diseases such as AIDS, cancer, Alzheimer's disease, and specifically for our work, antimicrobial agents.¹³⁵

Nowick and co-workers have synthesized peptide-based artificial β -sheets that mimic parallel and antiparallel conformations. Their templates form folded, hydrogen-bonded structures and help prevent the formation of complex, ill-defined aggregates, selectively promoting the hydrogen bonding capabilities of one side of the molecule while blocking the hydrogen bonding capabilities of the opposite side. This negates the possibility of the molecule forming aggregates as well as promoting the formation of simple monomeric and dimeric species.¹³⁵ Their initial efforts began with turn structures that loosely resemble amide-based β -turn structures common in peptides and proteins.¹³⁶ They then developed a urea-based turn structure, which allowed two specific groups to be in close proximity to one another. The resemblance of these urea-based turns to β -turns

inspired them to combine their molecular scaffolds with amino acids to form structures that they termed “artificial β -sheets”.^{135, 137-139} Evaluation of the propensities of different amino acids to adopt β -sheet structures was examined, and it was determined that amino acids valine and leucine had the greatest propensities to adopt the β -sheet structure.¹⁴⁰ These results largely match those of the established propensities (the “Chou-Fasman parameters”).¹⁴¹ Following this, they began work on a second template to enhance folding and reduce uncontrolled intermolecular interactions that contained the unnatural amino acid Hao, which they developed¹⁴² (Figure 19). This template would mimic the hydrogen bonding pattern of one edge of a peptide in the β -strand conformation as well as increase the rigidity along the backbone; this was termed a “ β -strand mimic”.^{143, 144} Peptides containing the Hao group fold to form β -sheet structures, dimerize through edge to edge β -interactions and antagonize β -sheet aggregation (Figure 19).¹⁴⁵

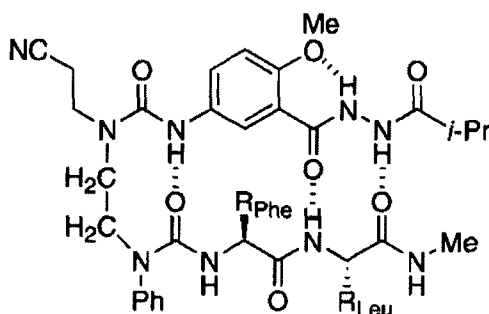


Figure 19. Artificial β -sheet containing Hao artificial amino acid and urea β -turn.

Bartlett and coworkers^{146, 147} have also recently reported artificial β -strand forming oligomers which consist of alternating amino acids and azacyclohexenone units or “@”¹⁴⁷ units (Figure 20). These oligomers have been termed @-tides. The replacement of alternating amino acids with the @-units provides conformational restriction which favours elongated conformations and the tertiary amide limits hydrogen

bonding to one edge of the strand, preventing uncontrolled aggregation. They also possess attractive features such as resistance to proteolytic degradation¹⁴⁸ and the easy incorporation of the @ unit by a flexible, modified peptide synthesis.^{146,149} Similar analogues have been demonstrated to bind to the PDZ domains of proteins more strongly than their natural β -sheet ligands.¹⁴⁸

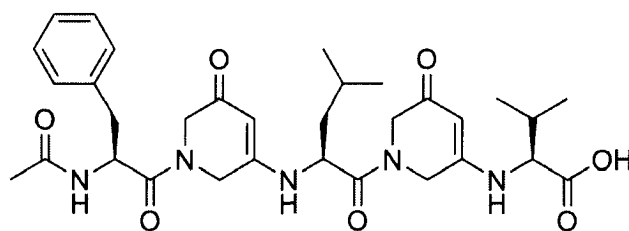


Figure 20. Linear @-tide containing alternating @ units and L-amino acids.

Part Two: Results and Discussion

2.1 Thesis Goals

The goals of this thesis were to design and synthesize new amphipathic @-tides and to evaluate their abilities to potentially serve as membrane active antibiotics by studying the release of encapsulated fluorescent dye molecules from phospholipid vesicle models of both bacterial and mammalian cell membranes. The propensity of these modified oligomers to assemble into β -sheet structures in solution is also described and compared to the results obtained for the original @-tides described by Bartlett and coworkers.¹⁴⁹ Several of the oligomers were found to exhibit membrane disruptive activity as well as selectivity for the bacterial over mammalian cell membrane models. These studies therefore introduce a promising new template for the development of potential antibiotics and provide important insights into the structural features that are critical for activity in this class of molecules.

2.2 Primary Design of First Generation β -Strand Peptidomimetics

The common structural feature of most membrane-disruptive antimicrobial peptides is the segregation of hydrophobic and cationic groups into different regions of the molecule, such as on opposite faces of a helix.⁶ In a β -strand based entirely on L- α -amino acids, the side chain groups will be naturally directed to opposite faces of the strand. However, in the @-tides, as every second amino acid is replaced by an azacyclohexenone unit, all of the side chains are expected to be directed to the same face of the strand in its linear conformation as shown in Figure 21a.¹⁴⁹ Therefore, the main design modification made to the previously reported @-tide template was to alternate L- and D-amino acids. By subsequently alternating hydrophobic and cationic amino

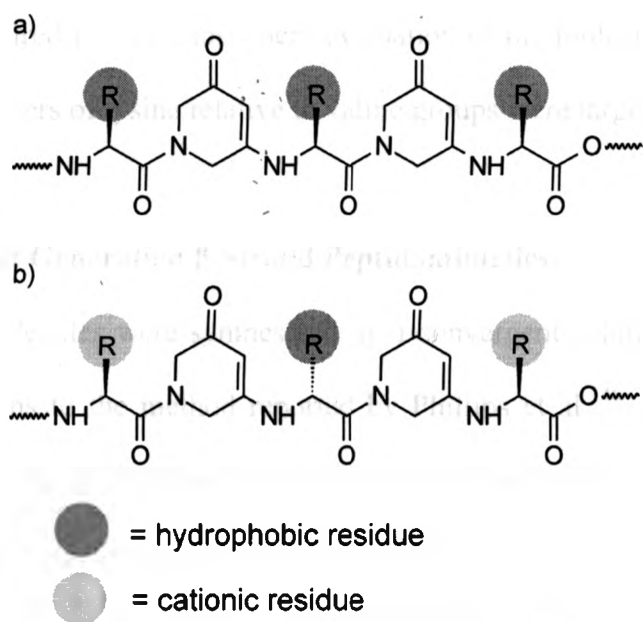


Figure 21. Structure of an @-tide comprising a) all L-amino acids alternating with azacyclohexenone units and b) hydrophobic D-amino acids and hydrophilic L-amino acids alternating with azacyclohexenone units.

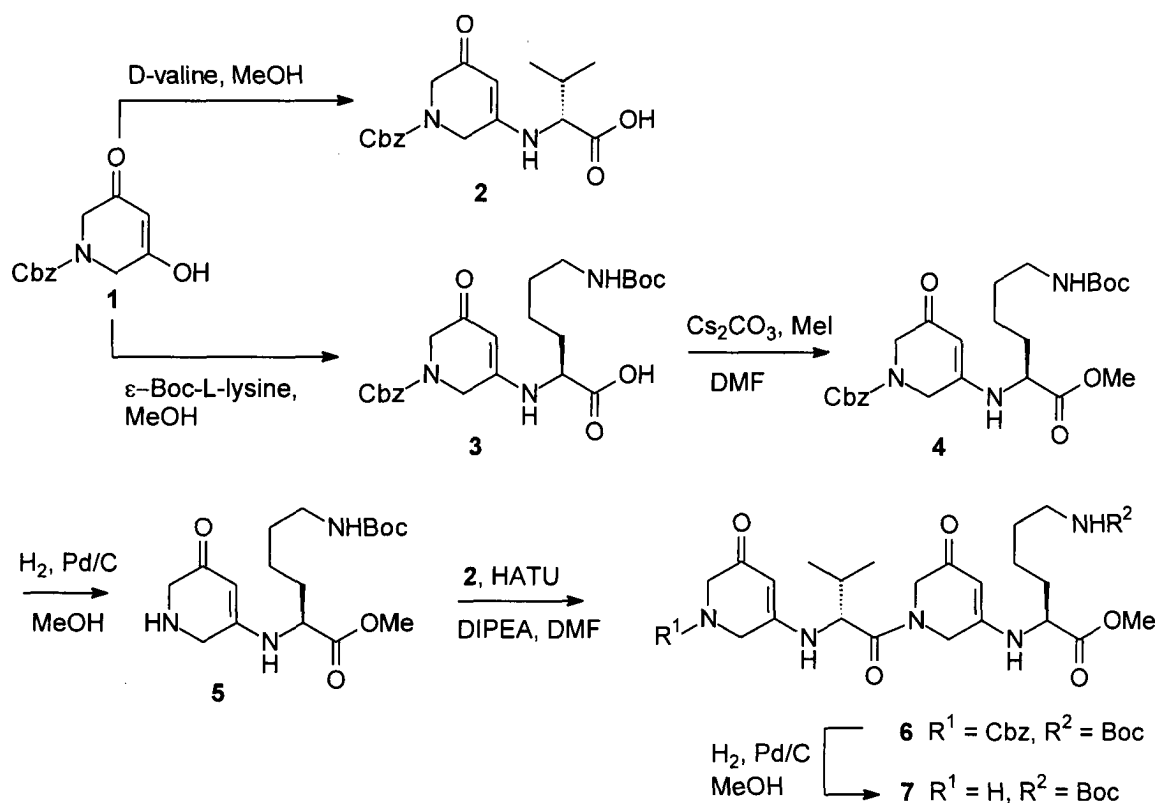
acids as shown in Figure 21b, it was anticipated that an amphipathic structure should be presented in the @-tide's linear conformation. As a cationic residue, L-lysine was selected because aliphatic amines have been one of the most commonly and successfully used cations in the development of antimicrobial peptidomimetics.^{54, 63, 150} D-Valine was selected as the hydrophobic residue because of its propensity to form β -strands and β -sheets.^{151, 152} The previously reported antimicrobial peptidomimetics have generally consisted of larger fractions of hydrophobic than hydrophilic residues.^{49, 71, 153} However, it was anticipated that the azacyclohexenone units in the @-tides would introduce significant hydrophobicity to the structures, so in order to obtain at least the minimal

water solubility required for the subsequent evaluation of the molecules, structures with equal or greater numbers of lysine relative to valine groups were targeted initially.

2.3 Synthesis of First Generation β -Strand Peptidomimetics

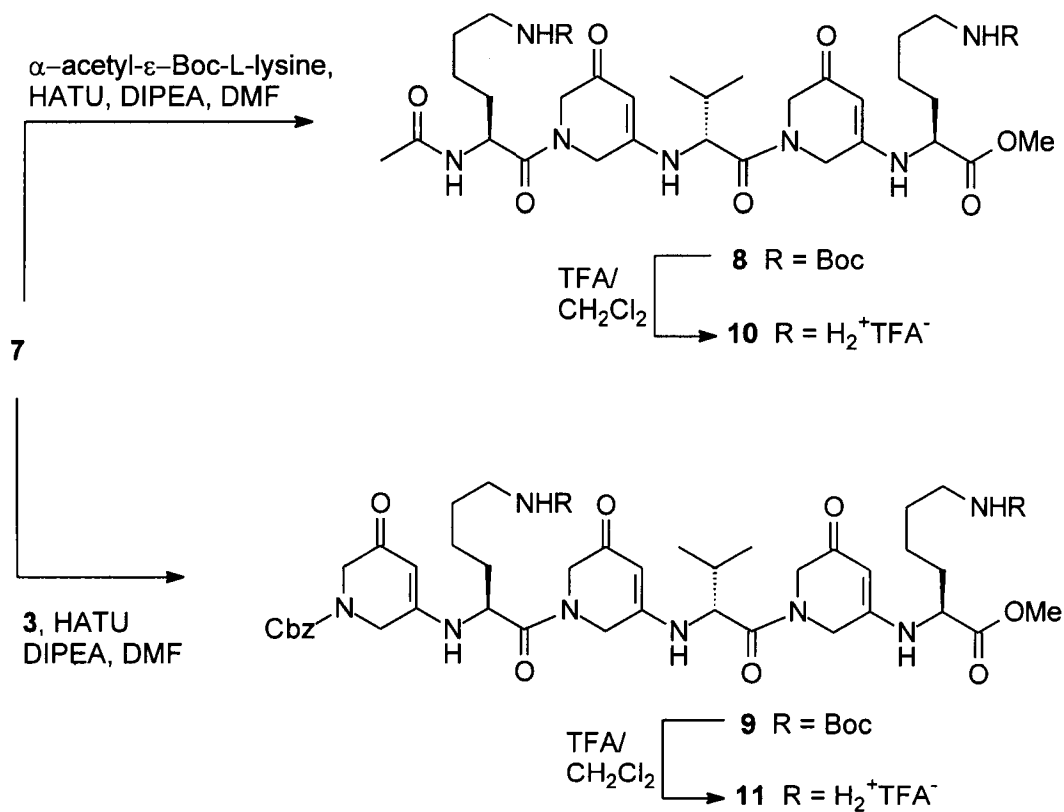
The target molecules were synthesized by a convergent solution phase approach based on modifications to the method reported by Phillips et al.¹⁴⁶ First, as shown in Scheme 1, the previously reported benzyl carbamate (Cbz) protected α -tide unit **1**¹⁴⁶ was reacted with either D-valine or ϵ -Boc-L-lysine to provide the corresponding condensation products **2** and **3** respectively which will be referred to as dimers throughout this discussion. Without further purification, the L-lysine derivative **3** was converted to the methyl ester **4**. After removal of the Cbz group by catalytic hydrogenolysis in methanol, the resulting dimer amine **5** was coupled with dimer acid **2** using *O*-(7-azabenzotriazol-1-yl)-*N,N,N',N'*-tetramethyluronium hexafluorophosphate (HATU) as the coupling agent, in *N,N*-diisopropylethylamine (DIPEA) and DMF to provide the tetramer **6**.

Scheme 1 Synthesis of alternating D-/L- amino acid @-tide tetramer **6**



The Cbz protecting group on the tetramer **6** was then removed by hydrogenolysis, providing **7**, which was then coupled to α -acetyl- ϵ -Boc-L-lysine¹⁵⁴ to provide the pentamer **8** as shown in Scheme 2. Alternatively, the tetramer was coupled with the dimer **3** to provide the hexamer **9**. Deprotected versions of the pentamer and hexamer were prepared for evaluation of the membrane-disruptive capabilities. The Boc protecting group on the pentamer **8** was removed by treatment with a 1/1 TFA/CH₂Cl₂ solution to provide the dicationic pentamer **10**. The Boc groups on the hexamer **9** were removed under the same conditions to provide the dicationic oligomer **11**.

Scheme 2 Synthesis of alternating D-/L- pentamers **8** and **10** and hexamers **9** and **11**



In addition, it was of interest to investigate the effect of incorporating the alternating D- and L-amino acids to potentially provide facially amphiphilic structures in the linear β -strand conformations, in comparison with oligomers containing all L-amino acids. Thus, molecules corresponding to **2**, **6**, **8**, **9**, **10**, and **11**, but containing only L-amino acids were prepared by the same methods described above. These molecules will be referred to as **2'**, **6'**, **8'**, **9'**, **10'**, and **11'** respectively. It is also noteworthy that while none of the oligomers described above are very long and do not possess highly charged states, high antibiotic activity and selectivity have been previously observed for aromatic amide and urea-based oligomers of similar lengths.^{54, 56, 114} Therefore, this initial series

of molecules was expected to give valuable insights into the activity of this class of molecules.

Oligomers up to the tetramer length (6, 6') were characterized by the standard methods used for small molecules, using techniques including proton nuclear magnetic resonance (^1H NMR) spectroscopy, carbon nuclear magnetic resonance (^{13}C NMR) spectroscopy, and infra-red (IR) spectroscopy as well as high resolution mass spectrometry (HRMS). All characterization data were consistent with the proposed structures. Due to the increasing broadness and complexity of the NMR spectra with increasing length, and solubility constraints, the pentamers and hexamers were characterized mainly by high performance liquid chromatography (HPLC) and HRMS, techniques that are standard for the characterization of oligopeptides, along with ^1H NMR spectroscopy.

2.4 Self Association of @-Tide 8 in $\text{CDCl}_3/\text{CD}_3\text{OH}$ Mixtures

Phillips et al. have reported extensive studies to demonstrate that @-tides of various lengths and compositions assemble in organic and aqueous solutions to form β -sheets.^{149, 155} While the formation of such assemblies is probably not critical to achieving membrane-disruptive activity, it is nevertheless of interest to investigate the effect of alternating the amino acid stereochemistry on this potential dimerization, as it can provide some insight into the conformational preferences of the molecules and their potential to assume amphipathic conformations in the presence of membranes. Therefore, the approximate self-association constants for several oligomers in CDCl_3 and $\text{CDCl}_3/\text{CD}_3\text{OH}$ mixtures were determined.

These studies were carried out using the NMR dilution method.¹⁵⁶ First, a solution of **8** was prepared and was gradually diluted. The chemical shifts of the most downfield N-H proton were measured in pure CDCl₃, 99/1 CDCl₃/CD₃OH, and 97.5/2.5 CDCl₃/CD₃OH as a function of concentration and are shown in Figure 22. Unfortunately, despite the use of 2D NMR experiments including nuclear overhauser enhancement spectroscopy (NOESY), correlation spectroscopy (COSY) and heteronuclear multiple bond correlation (HMBC) it was not possible to unambiguously assign this peak to a specific N-H of **8** due to the high symmetry of the molecule relative to those previously reported,¹⁴⁹ as well as the broadness and overlap of many of the peaks in the spectra. However, to determine the dissociation constant K_d for the dimerization, the NMR chemical shift data was fit to eq 1 using a nonlinear curve-fitting procedure,¹⁵⁶ where δ_s is the chemical shift of the nondimerized oligomer, $\Delta\delta$ is the difference in chemical shifts between the dimerized and nondimerized oligomer, and c_o is the concentration of the oligomer. This provided K_d s of 0.2 ± 0.4 mM, 0.7 ± 0.4 mM, and 1.6 ± 0.6 mM in pure CDCl₃, 99/1 CDCl₃/CD₃OH, and 97.5/2.5 CDCl₃/CD₃OH respectively. The increasing K_d s with increasing CD₃OH content is consistent with the disruptive effect of CD₃OH on the expected hydrogen-bonded dimers. To investigate the effect of oligomer length, the K_d s determined from the N-H shifts for both the tetramer **6** (Figure 23) and hexamer **9** (Figure 24) were also measured using the same method. In 97.5/2.5 CDCl₃/CD₃OH their respective K_d s were 34 ± 3 mM and 5.7 ± 1.3 mM. The higher K_d for the tetramer **6** was expected because its shorter length allows for the formation of a maximum of four hydrogen bonds in the dimerized state. In contrast, both the pentamer **8** and the hexamer **9** are capable of forming a maximum of six hydrogen bonds in the dimerized state and

were therefore expected to exhibit similar K_{dS} , which was indeed observed. These values are of approximately the same order of magnitude as those obtained by Phillips et al. for the dimerization of α -tides of similar lengths in these solvents.¹⁴⁹

Overall, the magnitudes of the K_{dS} , their dependence on the CD_3OH concentration, and dependence on the oligomer length suggest that the oligomers containing alternating D- and L-amino acids are capable of dimerizing to form β -sheet mimics in the same manner as the previously well characterized α -tides containing all L-amino acids. This indicates that under some conditions, these oligomers should be capable of forming elongated amphipathic conformations. However, the relatively high dissociation constants and the strong effect of hydrogen bonding solvents observed in our studies and previously reported by Phillips et al.^{149, 155} for oligomers of these relatively short lengths suggest that they would not spontaneously assemble into dimers in aqueous solution at the concentrations relevant for antimicrobial activity, prior to their interactions with membranes. In addition, it should be noted that while circular dichroism (CD) spectroscopy has been previously used to elucidate the extent of α -tide

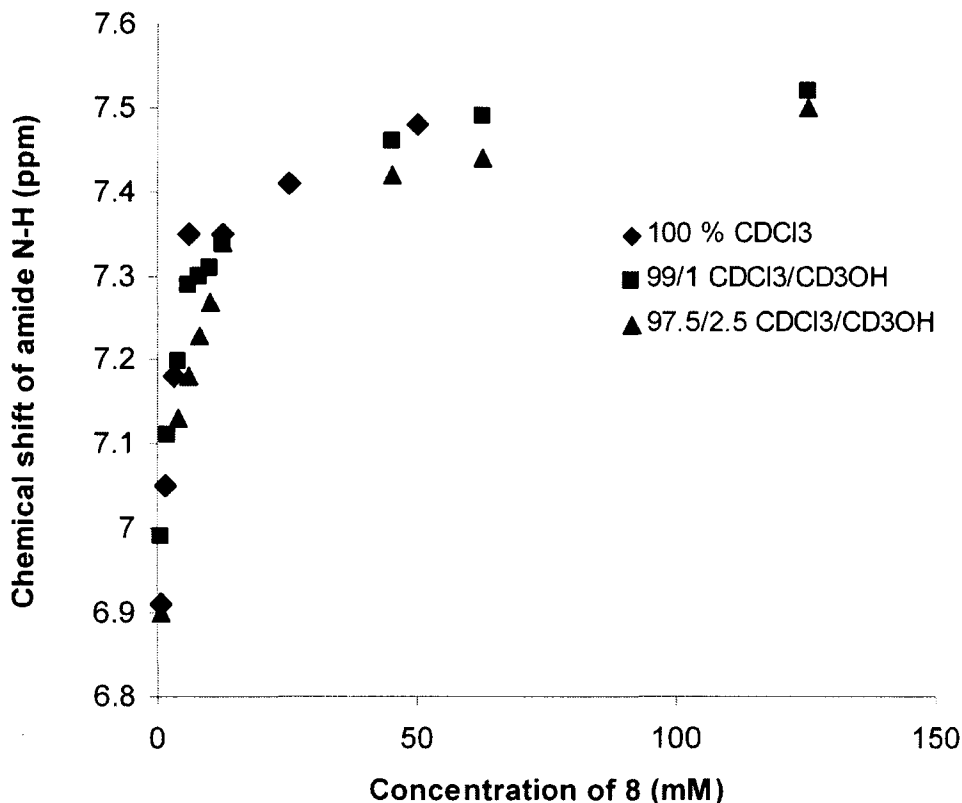


Figure 22. Chemical shifts of the farthest downfield N-H proton of pentamer **8** in ^1H NMR spectroscopy, as a function of solvent and concentration. The concentration dependence is indicative of dimerization of **8** to β -sheet mimics.

dimerization in a variety of solvents, this technique was not suitable for the analysis of oligomers containing D- and L-amino acids due to the requirement of having two L-amino acids surrounding the @-unit in order to observe the characteristic signal near 280 nm.^{149, 155}

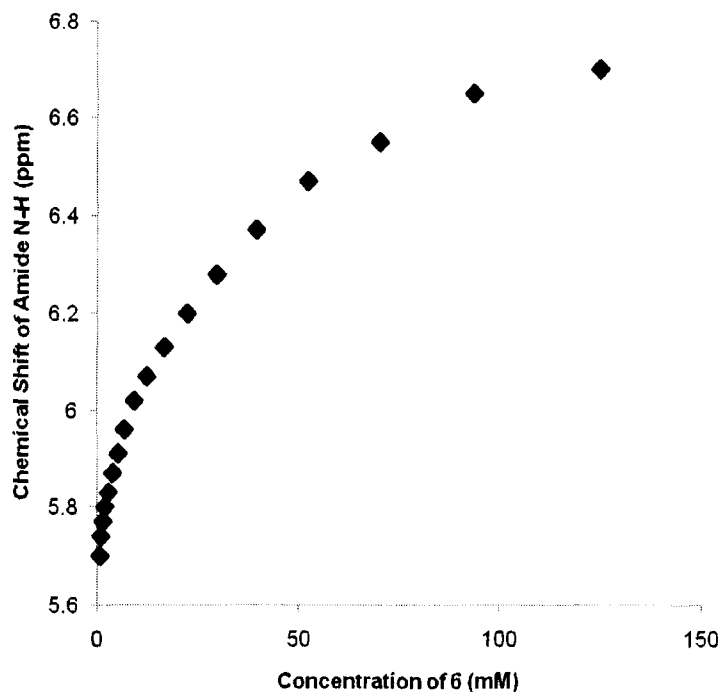


Figure 23. Chemical shifts of an N-H proton of tetramer **6** in ^1H NMR spectroscopy, as a function of solvent and concentration.

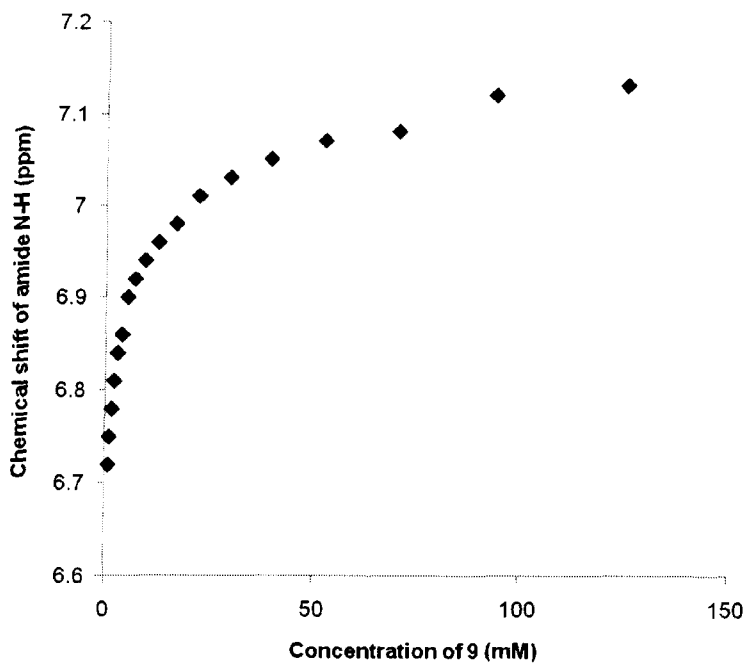


Figure 24. Chemical shifts of an N-H proton of hexamer **9** in ^1H NMR spectroscopy, as a function of solvent and concentration.

$$\delta_{obs} = \delta_s + \Delta\delta \left[1 + \frac{K_d}{2c_0} - \sqrt{\left(\frac{K_d}{2c_0}\right)^2 + \left(\frac{K_d}{c_0}\right)} \right] \quad (1)$$

2.5 Assessment of Membrane Disruptive Potential Using a Vesicle Leakage Assay

Numerous studies have demonstrated that the ability of membrane-disruptive antimicrobial peptides to kill bacterial cells via membrane lysis generally coincides with their ability to disrupt and lyse the phospholipid membranes of small unilamellar vesicles (SUVs).^{45, 54, 84, 114} Such studies have provided insight into the mechanism of action of these molecules. In addition, in order to predict the selectivity of the molecules for bacterial over mammalian cell membranes, it is possible to choose SUVs that mimic either bacterial or mammalian cell membranes.^{45, 54, 84, 114} In this study, as previously reported by Yang et al.,^{45, 54, 84, 114} an 80/20 ratio of the lipids 1,2-dioleoyl-*sn*-glycero-3-phosphoethanolamine (DOPE)/1,2-dioleoyl-*sn*-glycero-3-[phospho-rac-(1-glycerol)](sodium salt) (DOPG) were selected to mimic bacterial cell membranes. Most gram-negative bacterial membranes are rich in PE lipids, which have a relatively small head group and therefore a tendency to promote negative curvature.^{45, 54, 84, 114} DOPG is anionic, which is characteristic of bacterial membranes that contain negatively charged phospholipids, lipopolysaccharides, and teichoic acids on their surfaces.¹⁵⁷ The phospholipid 1,2-dioleoyl-*sn*-glycero-3-phosphocholine (DOPC) was chosen for the preparation of SUVs mimicking mammalian cell membranes as eukaryotic cell membranes are rich in PC lipids.¹¹⁴

Thus far, several techniques have been used to investigate the disruption of phospholipid membranes by antimicrobial peptides and peptidomimetics,^{43, 114} but by far

the most widely used methods involve fluorescence.^{45, 54, 84, 114} Generally, a water-soluble dye is entrapped in the vesicle core during vesicle formation at a concentration that is sufficiently high to provide fluorescence quenching. Upon the addition of the membrane-active molecules, and rapid disruption of the membranes, the dye molecules are released from the vesicles, resulting in a significant dilution and the recovery of their fluorescence. In the current work, the 8-hydroxypyrene-1,3,6-trisulfonic acid trisodium salt (HPTS) and *p*-xylene-bis(*N*-pyridinium bromide) (DPX) fluorescent probe system was selected.¹⁵⁸ HPTS undergoes efficient self-quenching at moderately high concentrations in the presence of DPX, a collisional quencher.¹⁵⁹ Thus, the new oligomers were added to the HPTS-DPX loaded vesicles at varying concentrations from DMSO solutions. Small volumes of DMSO were used to dissolve the oligomers due to difficulties in dissolving some of the more hydrophobic molecules directly in the aqueous buffer. However, none of the oligomers were found to precipitate upon addition of the DMSO solutions to the aqueous buffer at the concentrations evaluated. The initial fluorescence intensity was taken as 0% HPTS-DPX release, and it was verified that the small quantities of DMSO that were used to dissolve the @-tides for their addition to the vesicles did not lead to any changes in fluorescence. At the end of each experiment, triton X-100, a well known membrane disruptive surfactant, was added to completely lyse the vesicles and the observed fluorescence intensity was used to indicate 100% HPTS-DPX release.

In preliminary work, it was found that @-tide oligomers with a carboxylic acid terminus did not lyse either the DOPE/DOPG or the DOPC vesicles to any measurable degree. This may be due to an insufficient cationic charge as the terminal carboxylic acid

would cancel the charge of one of the two lysines, leaving an overall positive charge of only +1 on the molecule. Alternatively, the presence of the charged carboxylate ion may make the molecule insufficiently hydrophobic for membrane disruptive activity. C-terminal capping has also previously been shown to enhance antimicrobial activity among conventional peptides.¹⁶⁰⁻¹⁶² Therefore, the current efforts focused on only the evaluation of the methyl ester derivatives. As shown in Figure 25, the pentamer **10**, with an overall positive charge of +2 exhibited concentration-dependent DOPE/DOPG membrane lysis with greater than 50% of the dye molecules released in 3 minutes. Hexamer **11** (Figure 26), also having an overall charge of +2, exhibited a similar degree of membrane lysis after 3 minutes, but the kinetics of dye release were somewhat slower than for the pentamer **10**. To investigate the role of the cationic ϵ -amines of lysine in the membrane disruptive activity, the protected tetramer **6** (Figure 27), pentamer **8** (Figure 28), and hexamer **9** (Figure 29) were also investigated. Quite unexpectedly, all of these molecules were found to be active in DOPE/DOPG vesicles. All three molecules provided approximately 80% release of HPTS-DPX after 3 minutes at the highest concentration, with the hexamer again exhibiting slower release kinetics than the tetramer or pentamer. A comparison of the membrane-disruptive activities of oligomers **6**, **8**, **9**, **10**, and **11** at a concentration of 100 $\mu\text{g/mL}$ is shown in Figure 30. Overall, these results indicate that a cationic charge is not essential for activity in this class of molecules, and that perhaps their activity may be enhanced by increasing their hydrophobicity. While **6**, **8**, and **9** are not cationic, they may still be amphipathic with the hydrogen-bonding edge of the molecule being relatively hydrophilic and the opposite edge with the valine side chain and the Boc protected amine groups being hydrophobic in the β -strand

conformation. The results thus far also suggest that there would not be significant benefits to the preparation of longer @-tide oligomers in terms of the degree of membrane disruption or the rate.

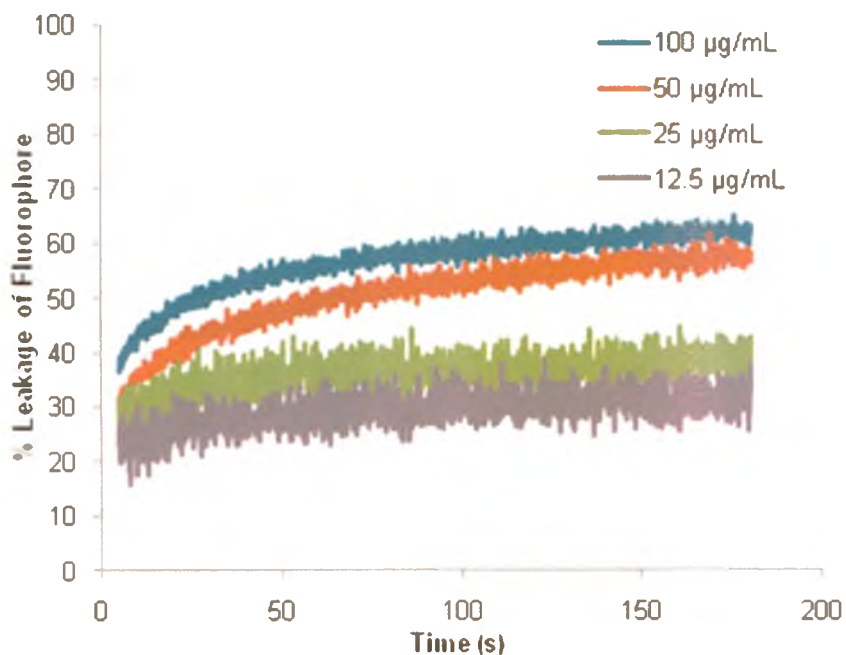


Figure 25. Detection of membrane lysis based on the leakage of encapsulated HPTS/DPX from vesicles by oligomer **10** assessed in vesicles of 80/20 DOPE/DOPG (bacterial mimic).

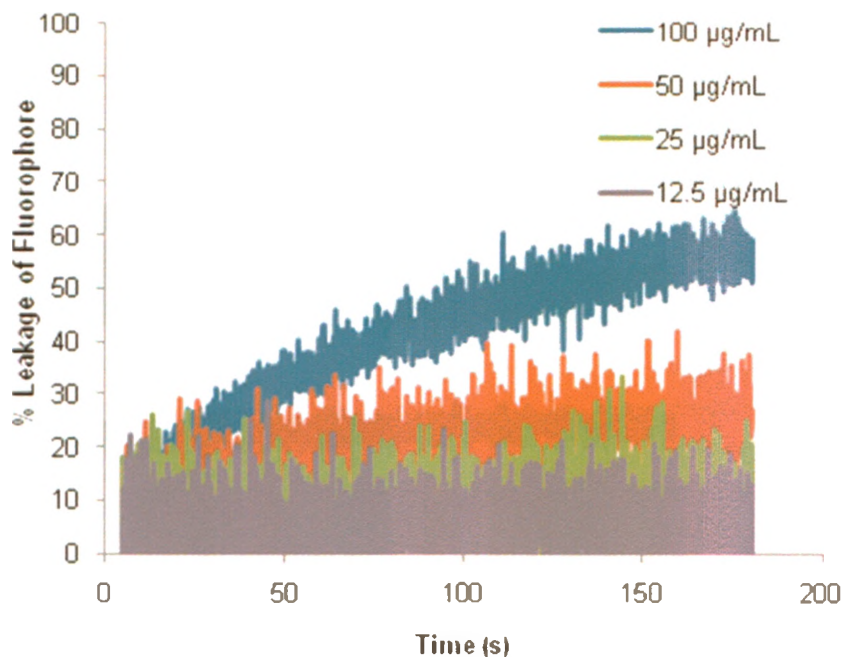


Figure 26. Detection of membrane lysis based on the leakage of encapsulated HPTS/DPX from vesicles by oligomer **11** assessed in vesicles of 80/20 DOPE/DOPG.

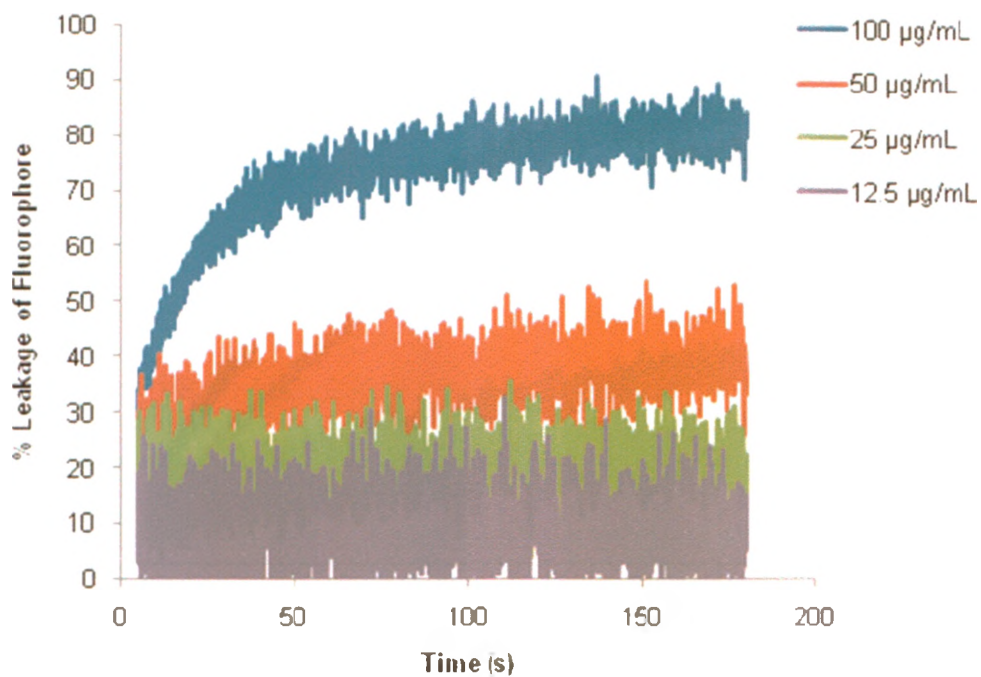


Figure 27. Detection of membrane lysis based on the leakage of encapsulated HPTS/DPX from vesicles by oligomer **6** assessed in vesicles of 80/20 DOPE/DOPG.

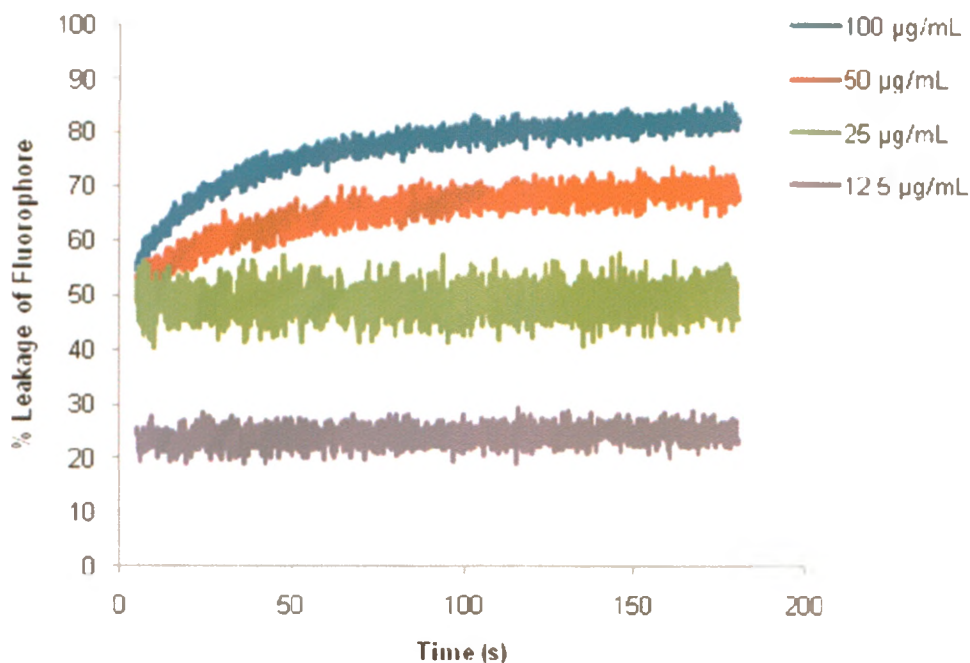


Figure 28. Detection of membrane lysis based on the leakage of encapsulated HPTS/DPX from vesicles by pentamer **8** assessed in vesicles of 80/20 DOPE/DOPG.

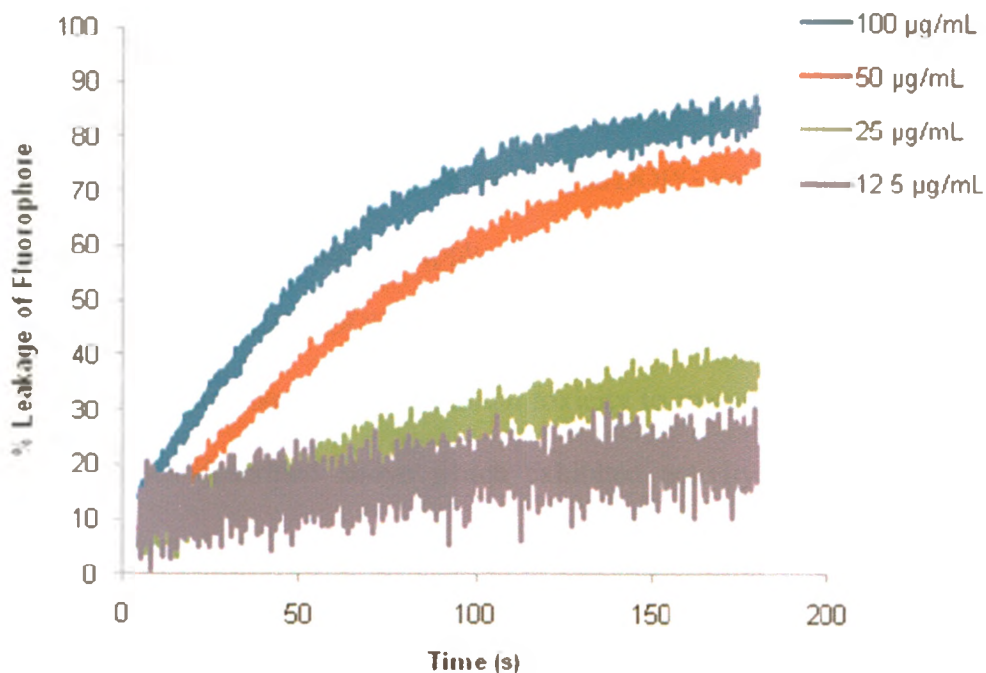


Figure 29. Detection of membrane lysis based on the leakage of encapsulated HPTS/DPX from vesicles by oligomer **9** assessed in vesicles of 80/20 DOPE/DOPG.

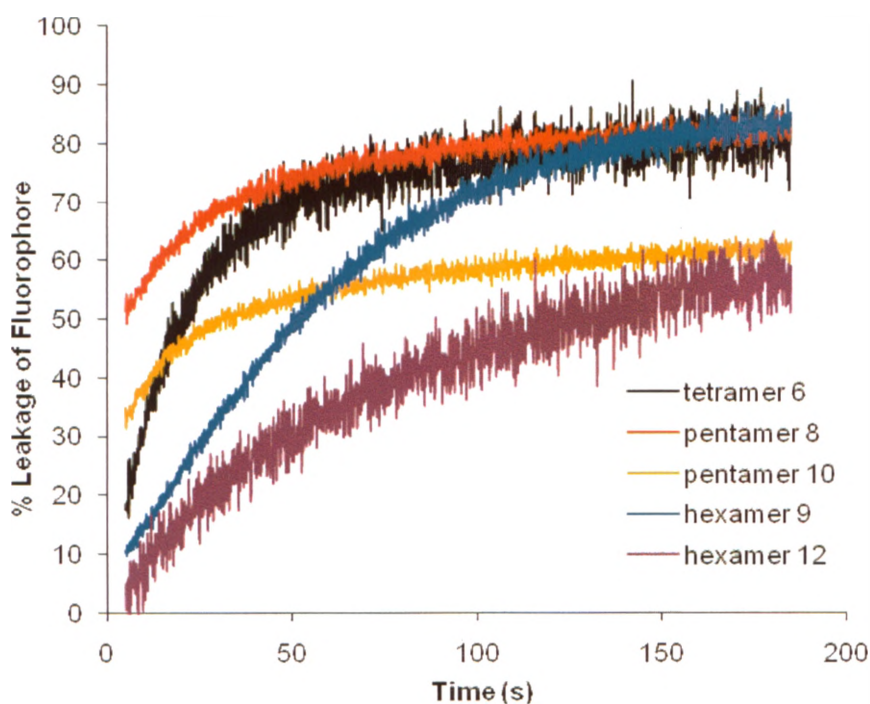


Figure 30. Summary of lysis activity for oligomers **6**, **8**, **9**, **10**, and **11** based on alternating D- and L-amino acids assessed in vesicles of 80/20 DOPE/DOPG (bacterial mimic) at 100 $\mu\text{g}/\text{mL}$.

While the ability of the molecules to lyse the DOPE/DOPG-based mimics of bacterial membranes is critical to their potential applications as antibiotics, it is also important to evaluate their ability to lyse the DOPC-based mimics of mammalian membranes, as this may provide early indications of their potential toxicity to mammalian cells. Therefore, all of the molecules described above which exhibited activity in the DOPE/DOPG vesicles were evaluated in DOPC vesicles with encapsulated HPTS-DPX. As shown in Figure 31, it was found that at a concentration of 100 $\mu\text{g}/\text{mL}$, the highest concentration evaluated, all of the molecules exhibited greatly reduced membrane-disruptive activity in the DOPC vesicles, with less than 10% of the HPTS- DPX released during the course of

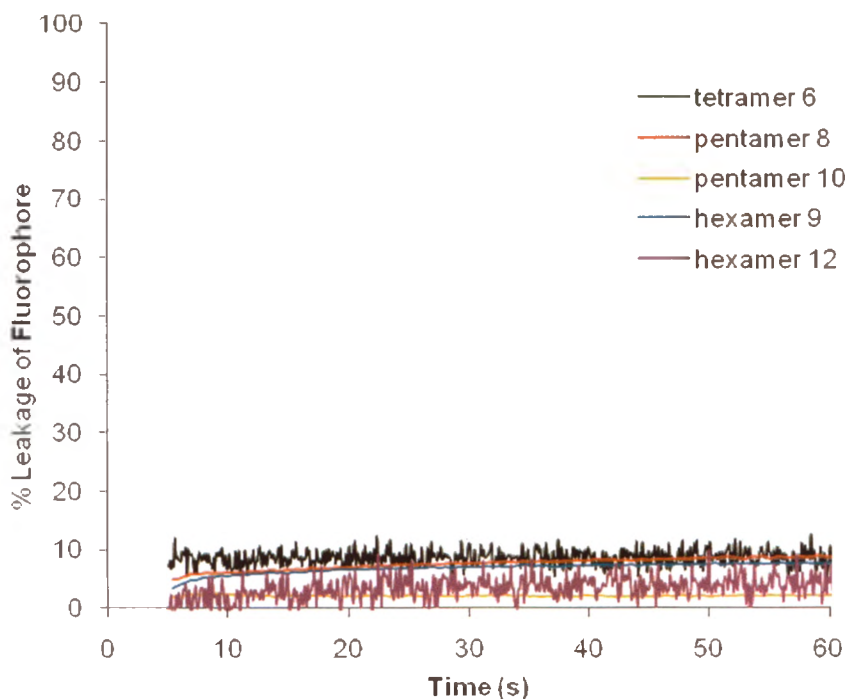


Figure 31. Detection of membrane disruption based on the leakage of encapsulated HPTS and its quencher DPX from vesicles for oligomers **6**, **8**, **9**, **10**, and **11** based on alternating D- and L-amino acids assessed in vesicles of DOPC (mammalian mimic) at 100 $\mu\text{g}/\text{mL}$ in each case.

the experiment. The reduced activities of the molecules in the DOPC vesicles may be due partly to the lack of anionic charge on these vesicle membranes. However, for the noncationic α -tides **6**, **8**, and **9**, the reduced activity cannot be attributed only to charge effects but may be due at least partly to the intrinsic negative curvature of the DOPE lipids relative to the DOPC lipids, and thus their increased susceptibility to lysis.

In order to evaluate the role of the three-dimensional structure on the membrane-disruptive activity, the analogues **6'**, **8'**, **9'**, **10'**, and **11'** (Figures 32-36, respectively), containing only L-amino acids were also tested in the vesicle lysis assay. As illustrated in Figure 21 and described above, it was not expected that these molecules would display

facially amphiphilic conformations, as all of the amino acid side chains would be directed to the same side of the β -strand in the linear conformation. As shown in the corresponding figures, all of these all L-amino acid analogues exhibited greatly reduced lysis activity in DOPE/DOPG vesicles relative to their alternating D-,L- counterparts, with the exception of the hexamer **11'** which had similar activity to **11**. A comparison of their activities at 100 $\mu\text{g/mL}$ is shown in Figure 37. This suggests that the designed amphipathicity of the molecules does have an important role in their activity, and that while the molecules would not be expected to preorganize into amphipathic β -sheet mimics in aqueous solution, they may be able to assume conformations resembling β -strands in the presence of membranes. In the case of natural antimicrobial peptides such as magainin, it has been found that while the molecules are capable of displaying amphipathic conformations, they are often unstructured in aqueous solution in the absence of membranes or membrane mimics.^{6, 163} Nevertheless, this result is surprising in light of the high activities of the protected oligomers **6**, **8**, and **9**, which suggested that the presence of hydrophobic and cationic residues on opposite faces of the molecule was not essential for activity and that instead an amphipathicity based on the hydrogen-bonding edge and the edge presenting the amino acid side chains might be sufficient. Compounds **6'**, **8'**, **9'**, **10'**, and **11'** (Figure 38) were all also evaluated in the DOPC vesicles to probe their selectivity for bacterial over mammalian cell membranes and as observed for the alternating D, L analogues less than 10% of the HTPS-DPX was released.

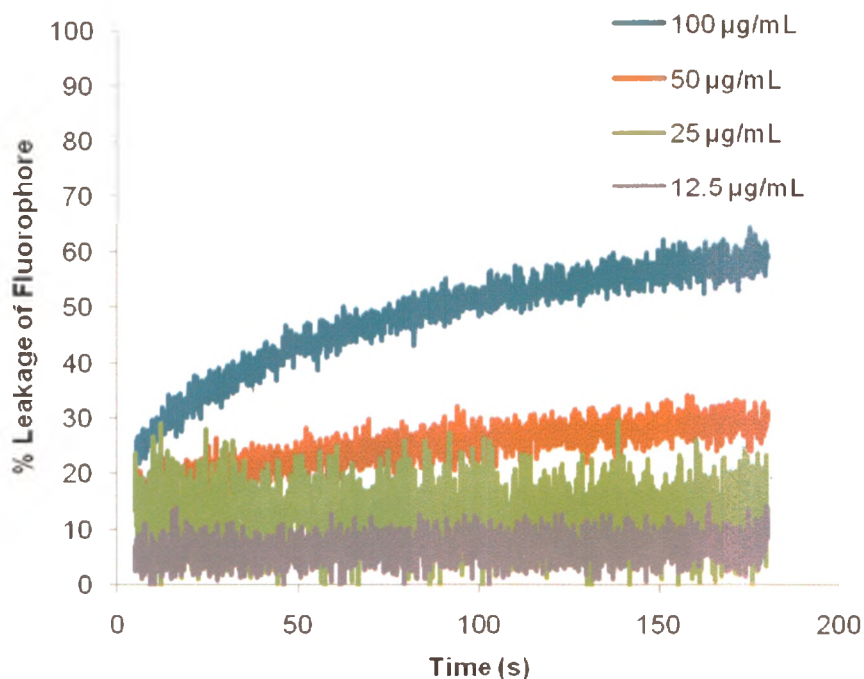


Figure 32. Detection of membrane lysis based on the leakage of encapsulated HPTS/DPX from vesicles by tetramer **6'** assessed in vesicles of 80/20 DOPE/DOPG.

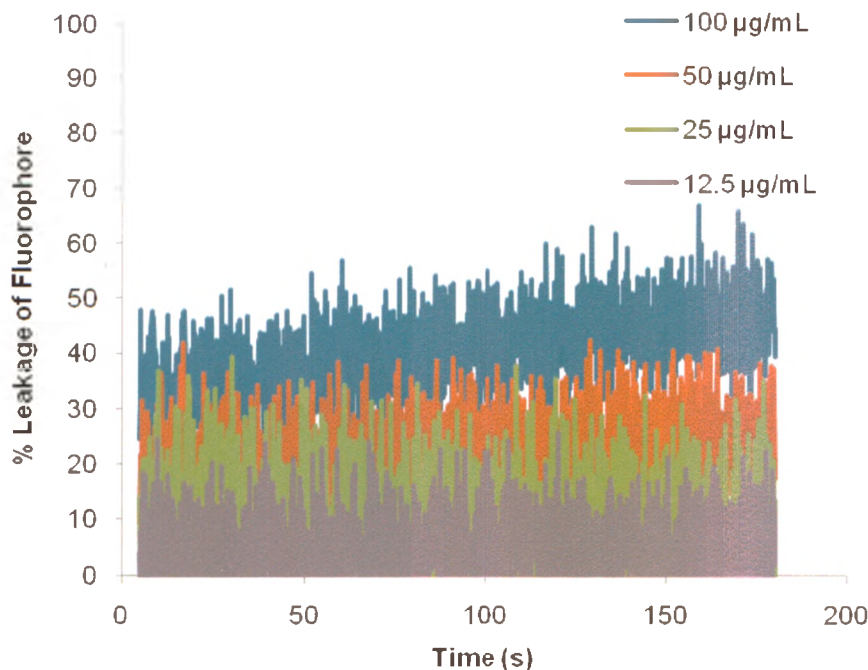


Figure 33. Detection of membrane lysis based on the leakage of encapsulated HPTS/DPX from vesicles by pentamer **8'** assessed in vesicles of 80/20 DOPE/DOPG.

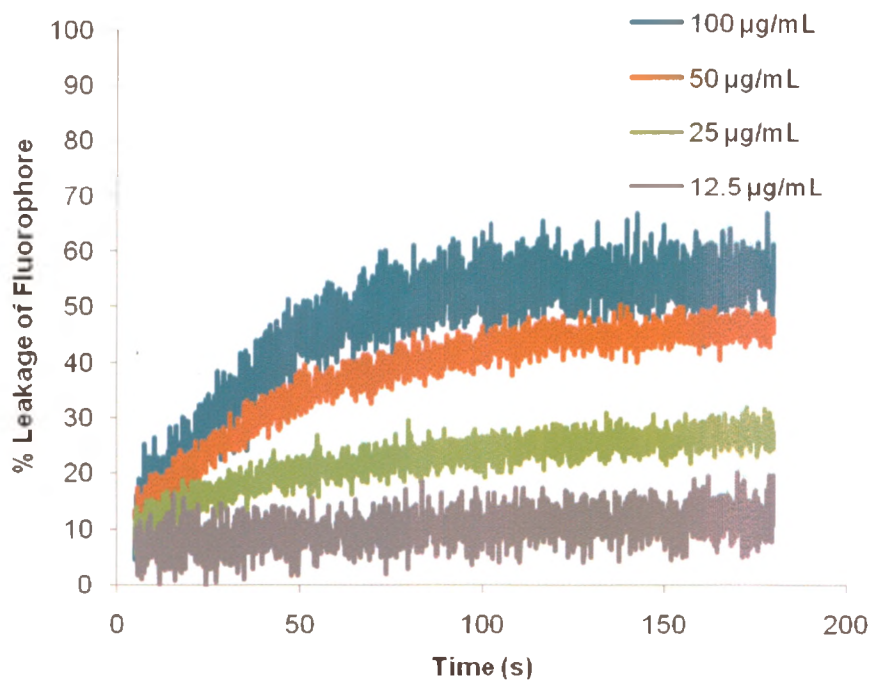


Figure 34. Detection of membrane lysis based on the leakage of encapsulated HPTS/DPX from vesicles by hexamer **9'** assessed in vesicles of 80/20 DOPE/DOPG.

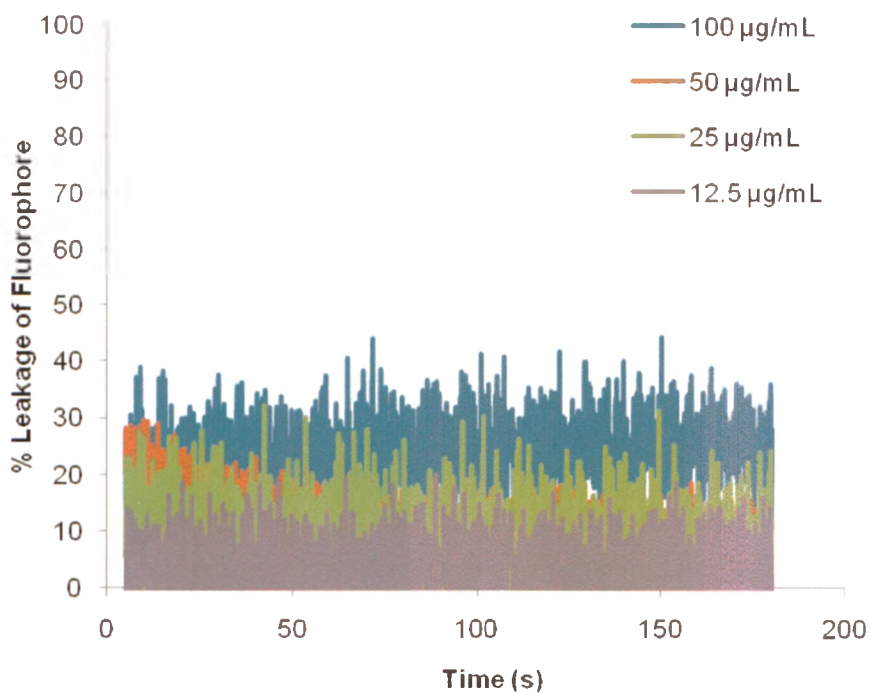


Figure 35. Detection of membrane lysis based on the leakage of encapsulated HPTS/DPX from vesicles by pentamer **10'** assessed in vesicles of 80/20 DOPE/DOPG.

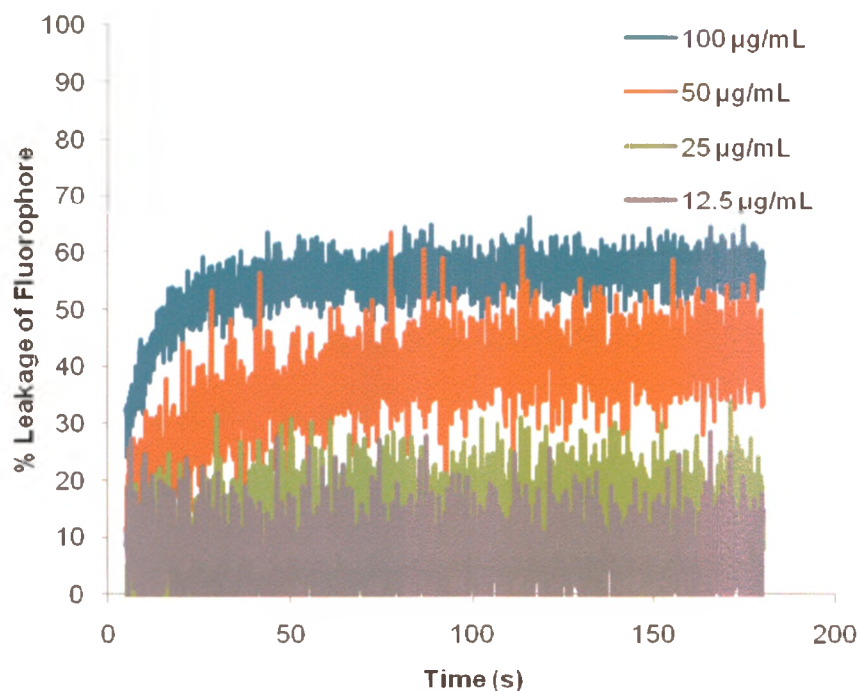


Figure 36. Detection of membrane lysis based on the leakage of encapsulated HPTS/DPX from vesicles by hexamer 11' assessed in vesicles of 80/20 DOPE/DOPG.

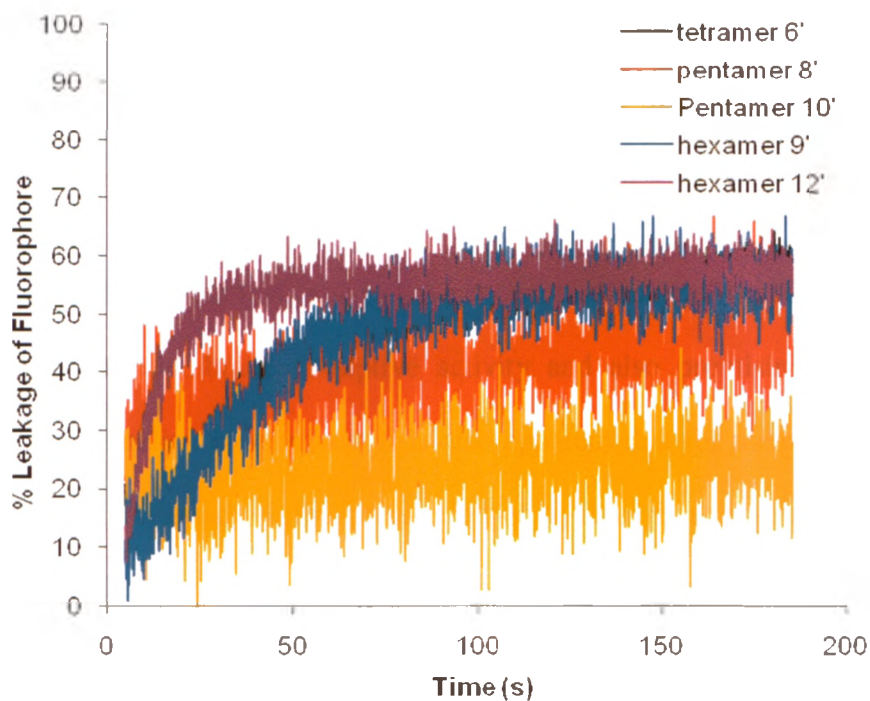


Figure 37. Summary of lysis activity for oligomers 6', 8', 9', 10', and 11' based on all L-amino acids assessed in vesicles of 80/20 DOPE/DOPG (bacterial mimic) at 100 µg/mL.

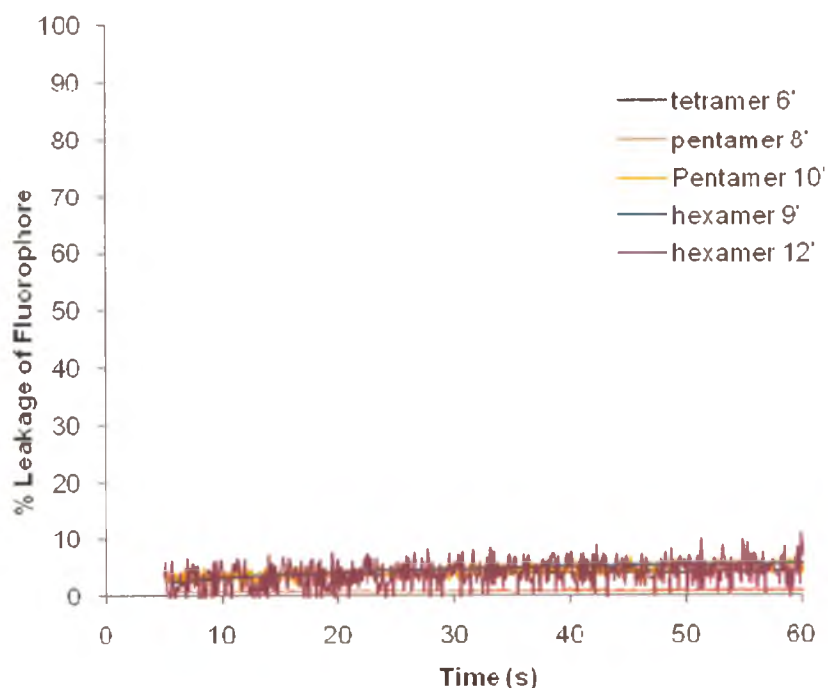


Figure 38. Detection of membrane disruption based on the leakage of encapsulated HPTS and its quencher DPX from vesicles for oligomers 6', 8', 9', 10', and 11' based on all L-amino acids assessed in vesicles of DOPC (mammalian mimic) at 100 $\mu\text{g}/\text{mL}$ in each case.

Overall, these vesicle lysis assays have shown that many of the @-tides described here have moderate membrane disruptive activity and also promising selectivity for bacterial over mammalian membranes. It is also apparent that for membrane disruptive activity there is an advantage to the preparation of @-tides from alternating D- and L-amino acids, such that alternating side chains diverge to opposite sides of the molecule in the linear conformation. The surprising activities of the protected oligomers suggest that the azacyclohexenone units of the @-tides may not contribute as much hydrophobicity as expected and that higher levels of activity might be achieved by the use of higher ratios

of hydrophobic:hydrophilic amino acid side chains as well as the incorporation of amino acids or terminal groups with higher hydrophobicity.

2.6 Design of Second Generation β -Strand Peptidomimetics

From the activities observed with the previous series of @-tide oligomers, it was thought that there were some features of these molecules which were responsible for the exhibition of activity and that slightly adjusting them would help to increase activity. From those results, especially the unexpected activities of the protected oligomers, it was thought that an increase in hydrophobicity would further increase the activity of these oligomers towards the microbial membrane mimics. Because the selectivity was very good for the previous series of molecules, it was speculated that a minimal addition of hydrophobicity would not be significant enough to cause a dramatic loss of selectivity or increase in activity of the @-tides towards the mammalian membrane mimics.

Three new series of @-tides were designed in an attempt to fine tune features of the moderately active @-tides described above. The first series was designed to increase hydrophobicity by incorporating more hydrophobic residues into the backbone. The two amino acids from the previous @-tides would remain the same, but the target molecules would contain larger portions of valine (Figure 39).

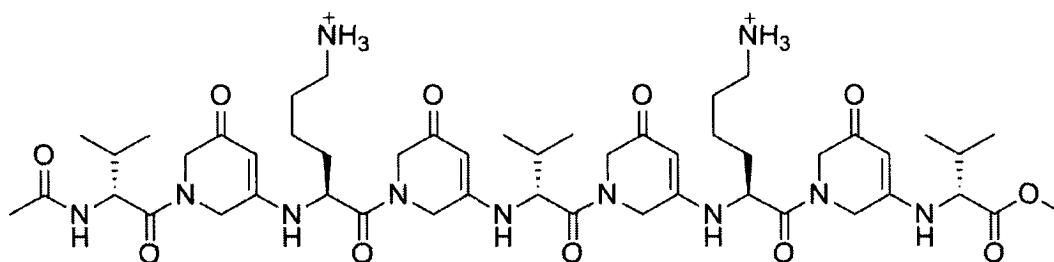


Figure 39. Target nonamer @-tide with a larger ratio of valine residues to lysine residues.

The design of the second series stemmed from the increased activity observed in the @-tides containing ϵ -Boc protected lysine residues compared to their deprotected analogues. A series containing only lysine residues, both D- and L-, was designed, with the target molecules being oligomers ranging from the tetramer to the nonamer shown in Figure 40. These lysine @-tides were designed to test the importance of the presence of this residue and protecting group along with the effect it was having on the activity towards both bacterial and mammalian membrane mimics.

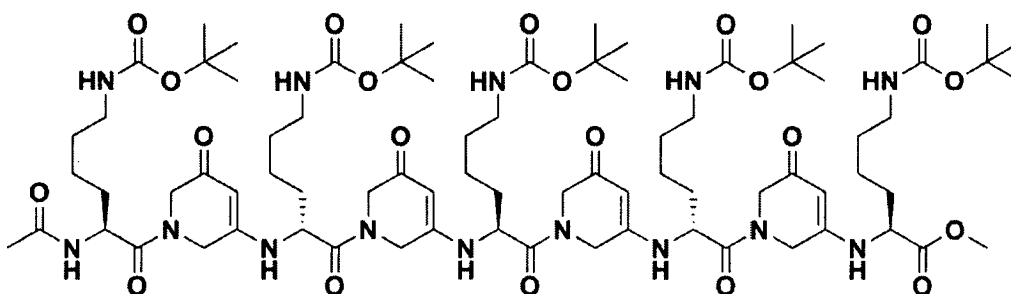


Figure 40. Target all lysine nonamer @-tide

For the third series, a larger increase in hydrophobicity was imparted by the addition of an aliphatic tail to the end of the previously described @-tides (Figure 41). This was designed to see if a greater degree of hydrophobicity would result in more activity, as well as to see if it was important if the hydrophobicity came from a residue on the backbone, or a hydrophobic group attached to an arbitrary position on the oligomer. This addition was also expected to aid in the purification of these molecules during synthesis, as chromatography had previously been challenging due to the high polarity of the molecules.

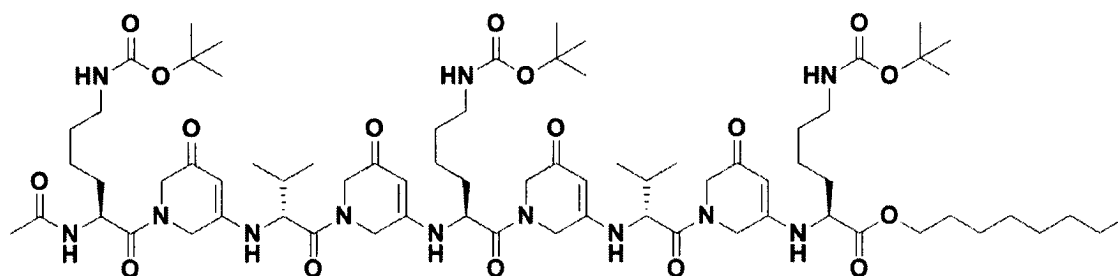


Figure 41. Target nonamer @-tide with additional aliphatic tail for hydrophobicity.

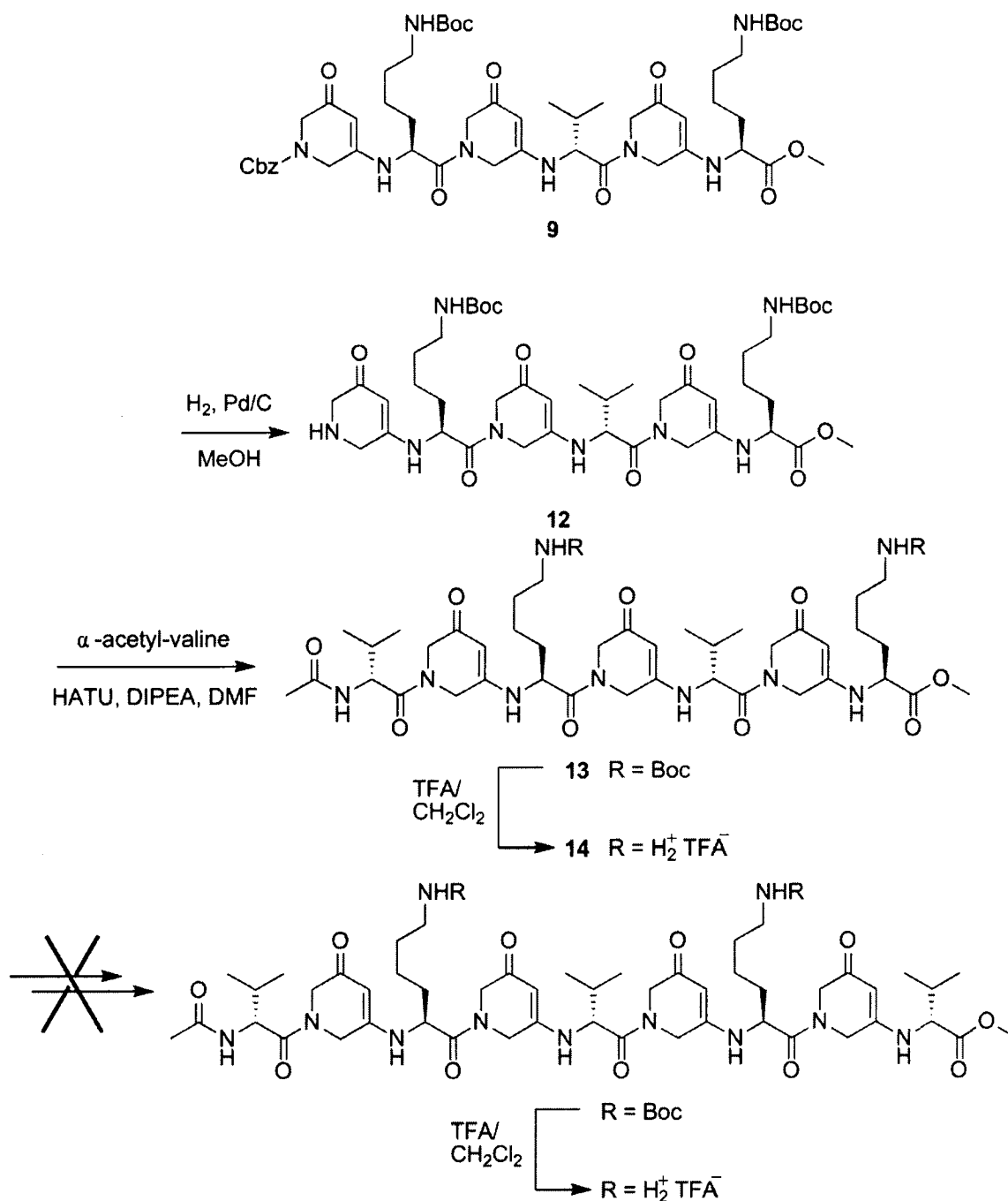
Due to the increased activity observed for the alternating D-/L- oligomers compared to their all L versions, the designed facial amphipathicity was retained as a constant component within these oligomers, as it proved to be the most active conformation.

2.7 Synthesis of Second Generation β -Strand Peptidomimetics

The three new series were synthesized in the same manner as the previously synthesized @-tides. The first series was synthesized with alternating D-valine and L-lysine amino acid residues to generate facially amphipathic oligomers, as shown in Scheme 3. Hexamer **9** was synthesized as described in Scheme 2. This hexamer was then subjected to catalytic hydrogenolysis in methanol, removing the Cbz protecting group, to yield **12**, which was then coupled with α -acetyl-valine¹⁶⁶ using HATU as the coupling reagent in DIPEA and DMF to provide the heptamer **13**, containing the acetyl, Boc and methyl ester protecting groups. A deprotected version was also prepared to evaluate the membrane disruptive capabilities. The Boc protecting groups were removed by treatment with 1/1 TFA/CH₂Cl₂ solution to provide the dicationic heptamer **14**. The synthesis of longer oligomers, such as a nonamer, was attempted by removing the methyl

ester protecting group at the C terminus followed by coupling to a Cbz deprotected methyl ester valine dimer. This attempt proved unsuccessful unfortunately and the

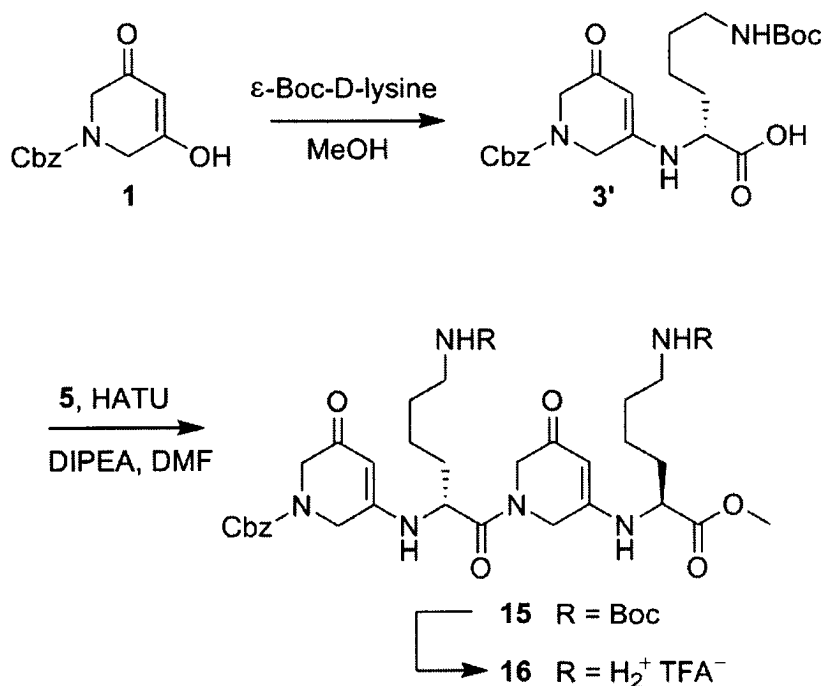
Scheme 3. Synthesis of the first series (more valine residues) of the second generation



desired nonamer was not formed. Difficulties in synthesizing long oligomers of this nature by these methods have been seen in our previous endeavours to synthesize @-tides by coupling two larger groups together. It was thought that perhaps synthesizing the oligomers by the addition of dimers one at a time might assist in the synthesis of larger molecules, however this was not the case when coupling to the carboxy terminus. In the future, a more successful approach might involve the coupling of a carboxylic acid functionalized dimer to the amino terminus of the @-tide, in an approach more analogous to traditional peptide synthesis.

The synthesis of the second series, containing only lysine residues, began with the synthesis of the dimer **3'** through the coupling of **1** with ϵ -Boc-D-lysine in methanol. The dimer acid **3'** was then coupled with **5** using HATU and DIPEA in DMF, as shown in Scheme 4. The resulting fully protected lysine tetramer @-tide **15** was found to be very unstable and degraded readily at room temperature, resulting in the recovery of minimal material. A Boc deprotected version, **16**, was also prepared using the same method as described for the first series. The synthesis of longer oligomers was also desired, however, due to the rapid degradation of material, this task seemed to be much more difficult than originally thought and only enough material was recovered and preserved to complete the testing of the tetramer. Even though this oligomer is not very long, membrane disruptive activity was observed for @-tides of similar lengths for the previously examined molecules. Testing was still conducted in hopes that these short oligomers would give some insight to the activities of this series.

Scheme 4. Synthesis of the second series (all lysine residues) of the second generation

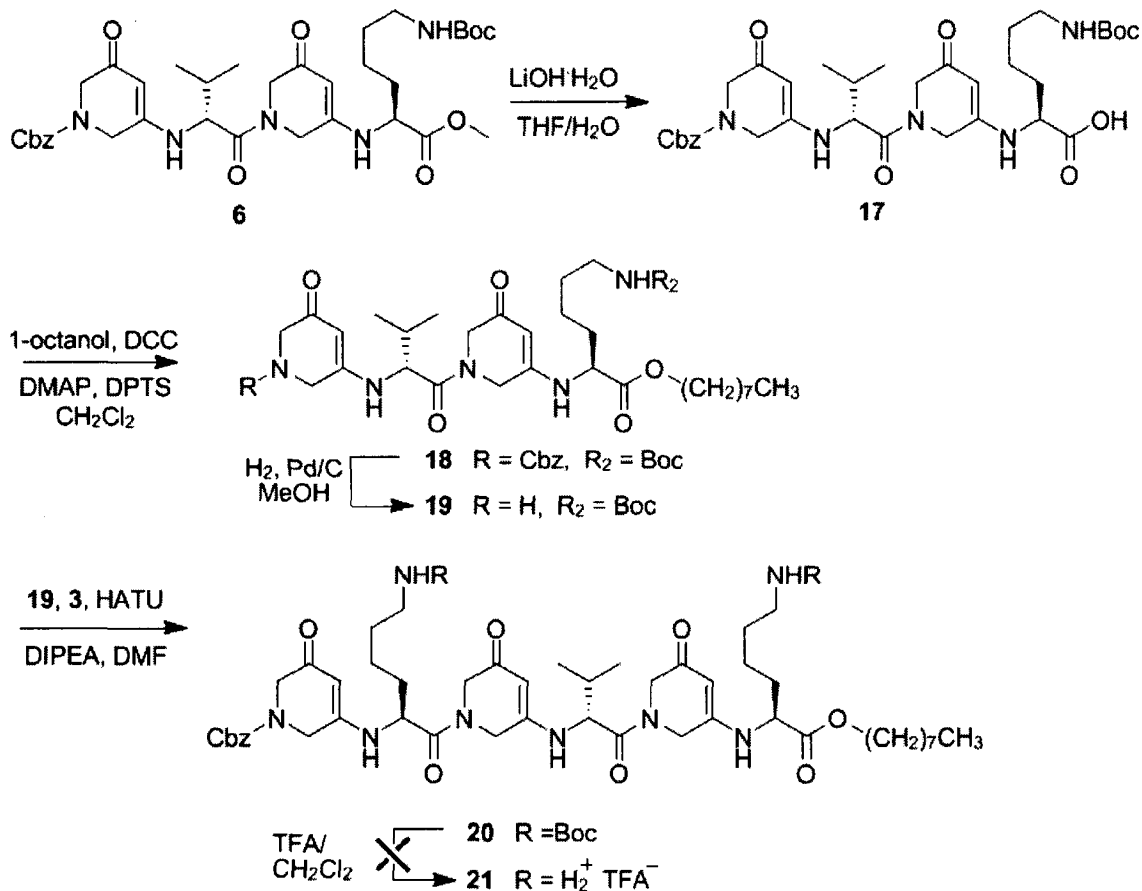


For preparation of the third series, shown in Scheme 5, the methyl ester protecting group of tetramer **6** was first removed with lithium hydroxide hydrate in a 1/1 solution of THF/water for 1 hour. The resulting acid **17** was then coupled to 1-octanol with DCC, DMAP and DPTS in dry CH₂Cl₂ for 24 hours, yielding tetramer **18**. 1-octanol was chosen as the aliphatic tail because a chain of that length had been previously shown to give the best antimicrobial activity and selectivity results in that it was not so hydrophobic as to cause significant interaction with the mammalian vesicle mimics, but hydrophobic enough to help increase interaction with bacterial vesicle mimics.¹⁰⁸ Catalytic hydrogenolysis was then performed on **18**, resulting in the formation of the amine **19** which was then coupled to the dimer **3** using the same coupling procedure as described for the synthesis of tetramer **18**. A Boc deprotection of the hexamer **20** was attempted to give the desired dicationic oligomer. However, upon treatment with TFA,

the molecule degraded and the desired product **21** was not formed, as confirmed by ¹H NMR and HRMS. The reasons for degradation of this oligomer, unlike the other oligomers, are not clear. In addition, considering this unexpected degradation and the availability of only small amounts of oligomer **20**, the synthesis of longer oligomers of this series was not possible.

The above described molecules were characterized by the same methods described for the α-tides described in the first part of this thesis, with the main characterization methods of the new molecules being ¹H NMR, HPLC and HRMS.

Scheme 5. Synthesis of the third series (aliphatic tail addition) of the second generation



2.8 Assessment of Membrane Disruptive Potential Using a Vesicle Leakage Assay

Vesicles containing an 80/20 ratio of lipids DOPE and DOPG, as described previously, were selected for the bacterial cell mimic membranes. DOPC lipids were chosen for the vesicles mimicking mammalian cell membranes. Due to the success observed previously using the HPTS/DPX fluorescent probe system, this method was used again here to evaluate the interactions and lysing abilities of the three new series of @-tide oligomers for the two different membrane mimics. Preparation methods for the vesicles remained the same as those previously described. As well, the oligomers were again dissolved in small amounts of DMSO and evaluated at the same concentrations as the previously examined @-tide oligomers. Upon evaluation of the new @-tides solubilities in the aqueous buffer solutions, although many of them were designed to be more hydrophobic and therefore less water soluble, it was again found that there was no precipitation observed upon the addition of the DMSO solutions to the buffer at all concentrations evaluated. Triton X-100 was used as a measure of complete lysis to indicate 100% dye release from the vesicles.

The molecules examined in the first series were heptamers **13** and **14**, in which the previously discussed alternating D-/L- facially amphiphilic @-tides were elongated by the addition of an acetylated valine residue. As shown in Figure 42a, heptamer **14**, with a dicationic charge and 2 valine residues, exhibited an extremely low degree of lysis, with the most concentrated dose generating less than 5% dye release in 3 minutes. This result was surprising as it showed a drastic drop in activity compared to that of hexamer **11**. Heptamer **13**, with an overall net charge of zero, also exhibited diminished activity compared to the fully protected hexamer **9**, as seen in Figure 43a. However, it was

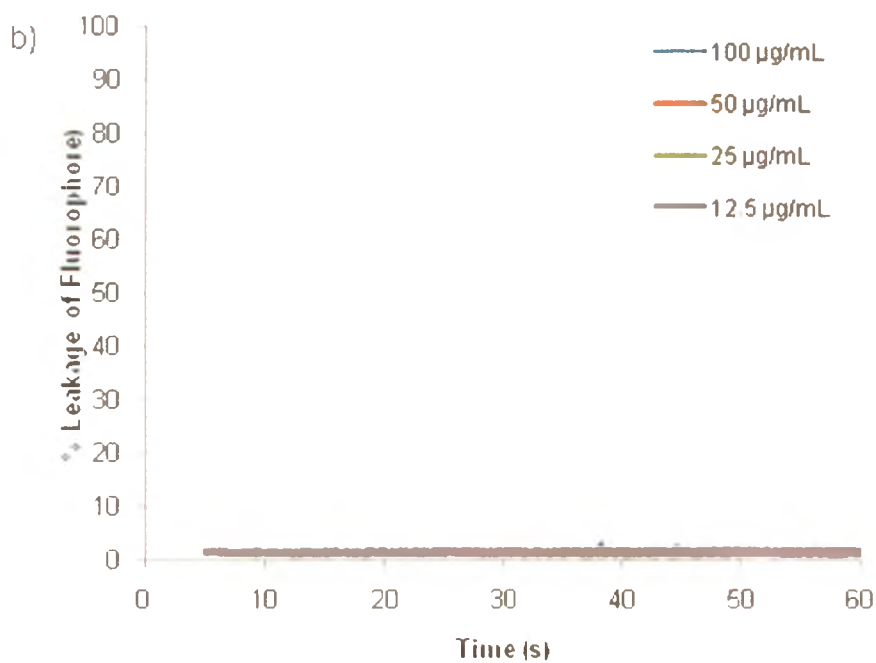
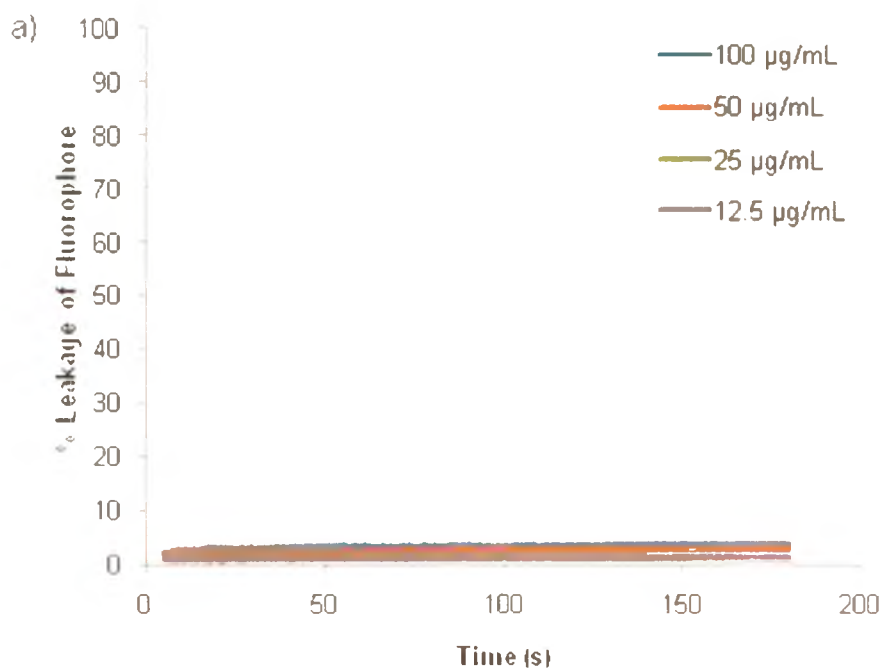


Figure 42. Detection of membrane lysis based on the leakage of encapsulated HPTS/DPX from vesicles: (a) oligomer **14** assessed in vesicles of 80/20 DOPE/DOPG (bacterial mimic); (b) oligomer **14** assessed in vesicles of DOPC (mammalian mimic).

slightly more active than its dicationic version **14**, as observed for all of the other oligomers previously examined. This result was quite perplexing, as it was hypothesized that the increased activity of the protected oligomers previously examined was due to the increased hydrophobicity imparted by the Boc group. Thus the increased hydrophobicity of this series was expected to provide increased activity. However, this appears to have in fact hindered their activity. This result may indicate that it is not a general or net increase of hydrophobicity that is required for activity, but rather specifically that the Boc protecting group provides the disruption of the membranes. When examining the activity of these heptamers towards the mammalian vesicle mimics, it was observed that the fully protected heptamer **13** (Figure 43b) showed slightly greater activity and **14** (Figure 42b) showed similar activity compared to the activities of these oligomers towards the bacterial vesicle mimics. This indicates that the degree of hydrophobicity may in fact be too great and results in the loss of selectivity.

The all lysine dicationic tetramer **16** exhibited marginal activity, with the highest concentration of 100 $\mu\text{g/mL}$ showing about 30% dye release after 3 minutes (Figure 44a). This deprotected tetramer showed approximately 10% more lysis than its completely protected version **15** (Figure 45a) at the same concentration. Although the results don't show a large degree of lysis, they do show a promising result that hasn't been seen yet for these α -tides. The cationic oligomers were more active towards the bacterial mimic membranes than the neutral oligomers. This result indicates that the presence of a net cationic charge must in fact aid in the attraction and ultimate disruption and lysis of the membrane mimics by these oligomers. Tetramers **16** and **15** (Figures 44b and 45b respectively) were also examined against the DOPC mammalian vesicle mimics. Both

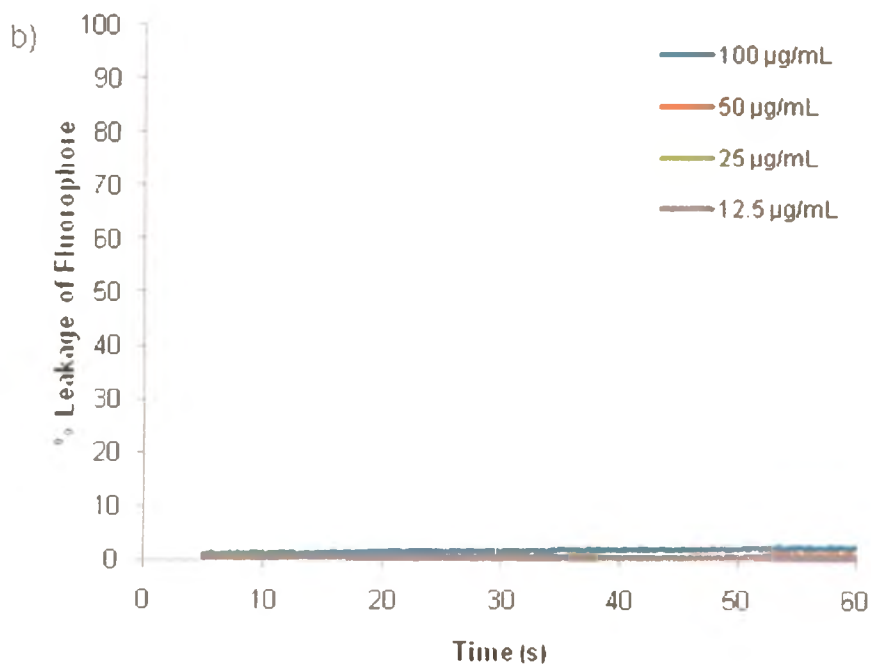
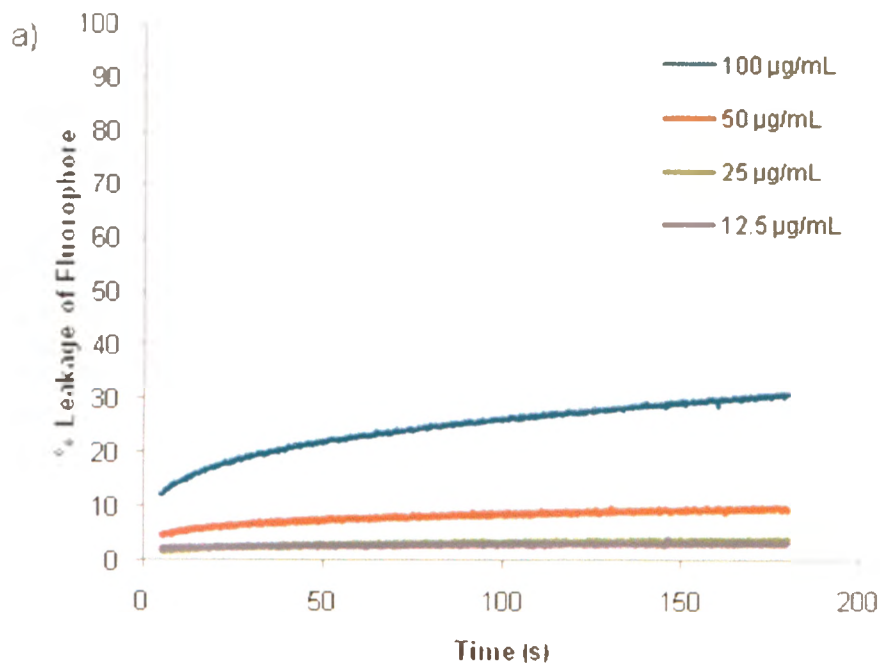


Figure 44. Detection of membrane lysis based on the leakage of encapsulated HPTS/DPX from vesicles: (a) oligomer **16** assessed in vesicles of 80/20 DOPE/DOPG (bacterial mimic); (b) oligomer **16** assessed in vesicles of DOPC (mammalian mimic).

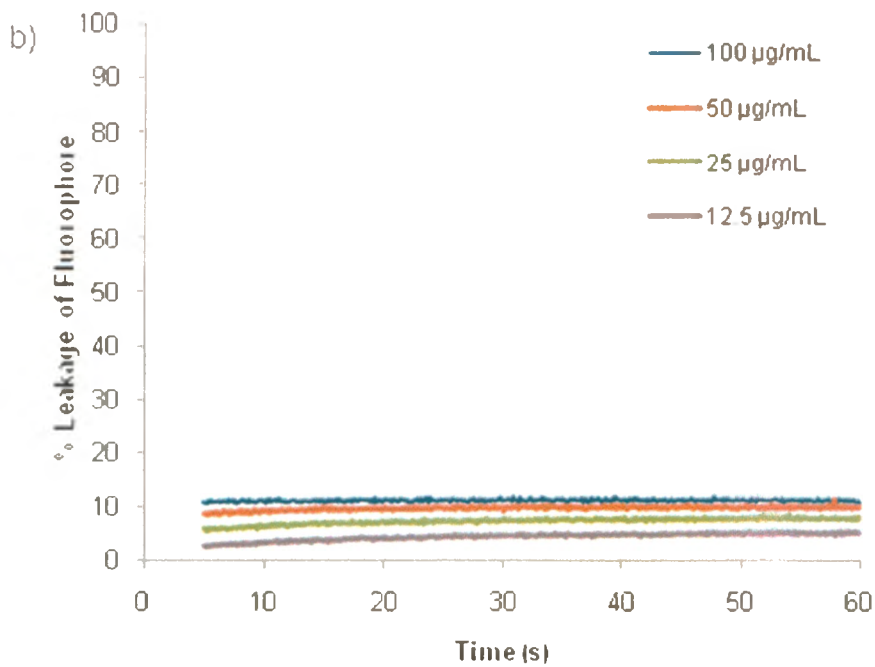
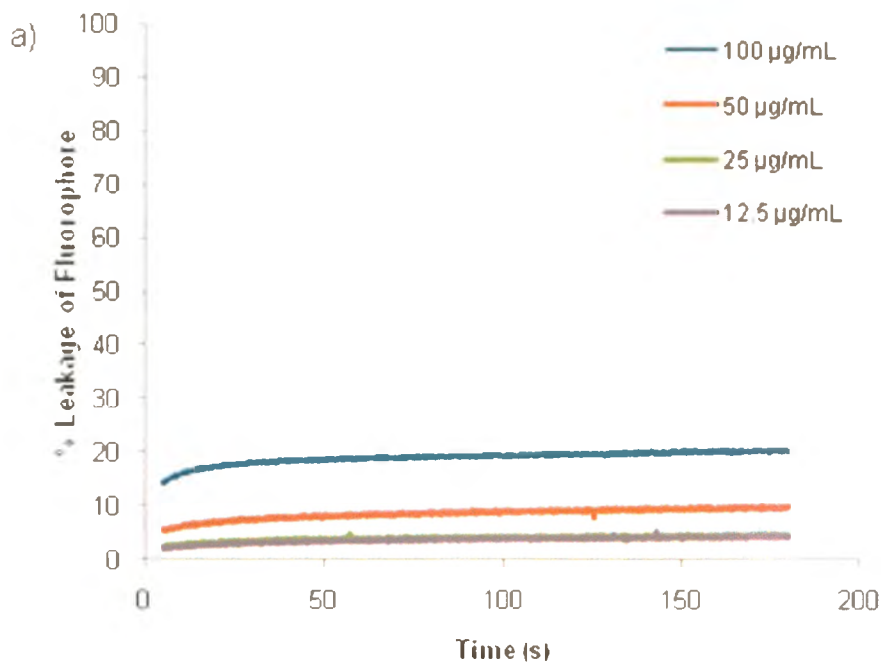


Figure 45. Detection of membrane lysis based on the leakage of encapsulated HPTS/DPX from vesicles: (a) oligomer **15** assessed in vesicles of 80/20 DOPE/DOPG (bacterial mimic); (b) oligomer **15** assessed in vesicles of DOPC (mammalian mimic).

tetramers showed diminished activity towards the mammalian mimics, but the best selectivity was observed for **16** with essentially negligible activity towards the mammalian mimics. This result again shows some promise and perhaps indicates that the designed amphipathicity is sufficient to provide the initial electrostatic attraction of the cationic oligomers to the negatively charged vesicles followed by insertion or disruption of the membranes by the oligomers. The displayed selectivity also indicates that the oligomer is not too hydrophobic to cause significant disruption of the mammalian vesicle mimics but is polar enough to cause some lysis of the bacterial vesicle mimics. With these results in hand, it is now questionable as to whether the alternating D-/L-lysine residue @-tides would still show greater activity and selectivity than its all L-lysine @-tide counterpart. This also might indicate that the amphipathicity arises from the primary cationic amines providing one face and the @-tide backbone the other face as demonstrated in Figure 46.

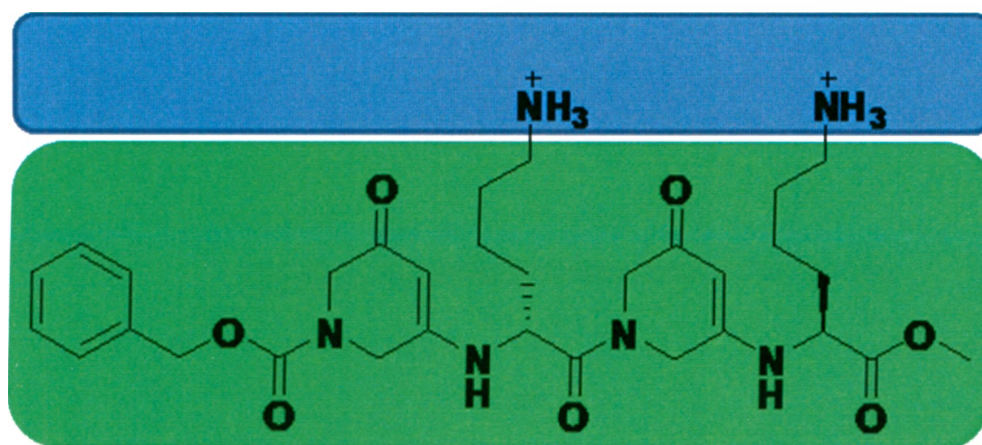


Figure 46. Dicationic tetramer **16**. The blue region indicates the polar part of the molecule and the green region indicates the hydrophobic part of the molecule.

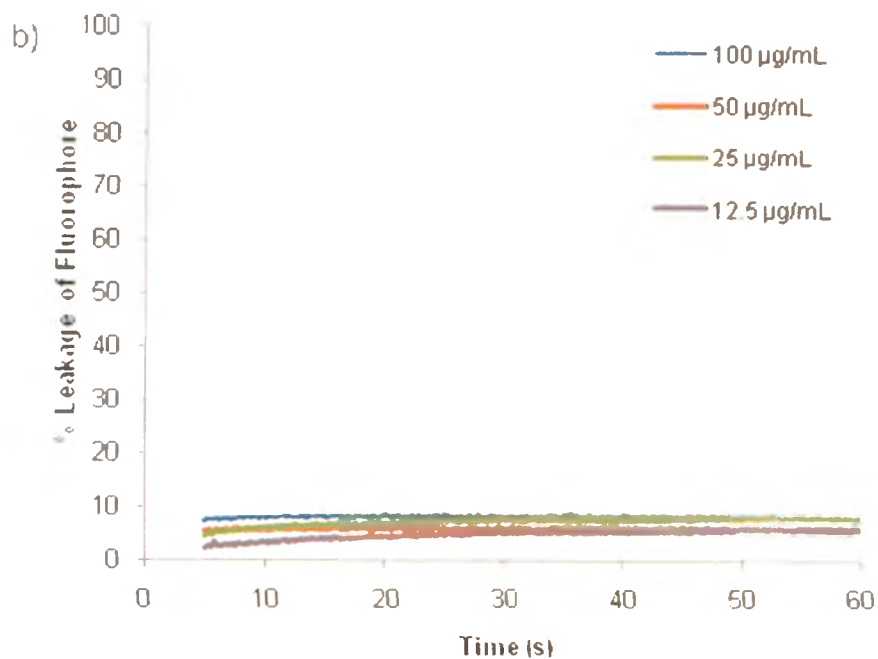
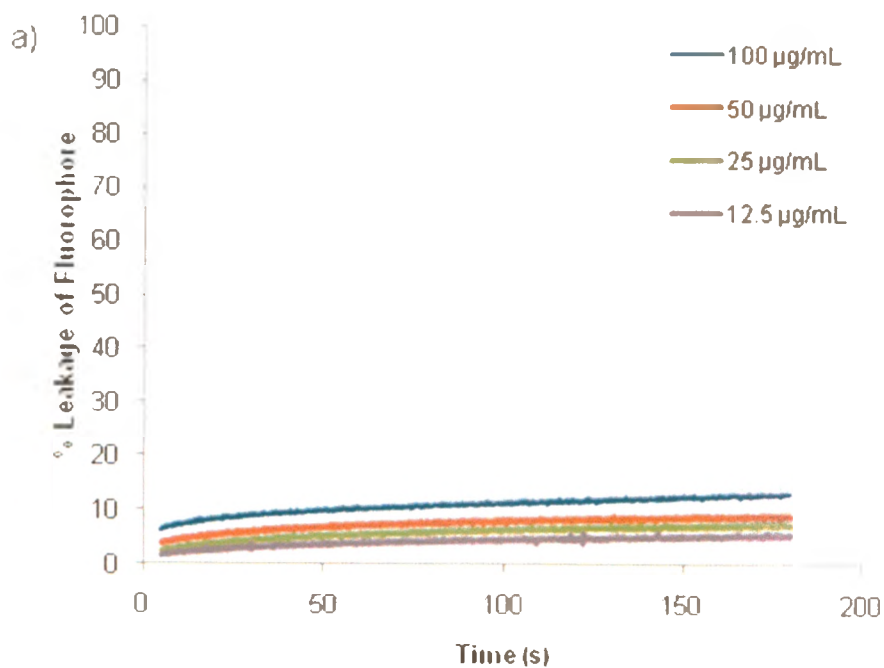


Figure 47. Detection of membrane lysis based on the leakage of encapsulated HPTS/DPX from vesicles: (a) oligomer **20** assessed in vesicles of 80/20 DOPE/DOPG (bacterial mimic); (b) oligomer **20** assessed in vesicles of DOPC (mammalian mimic).

Hexamer **20**, which is fully protected, was also examined against the bacterial and mammalian vesicle mimics. The DOPE/DOPG vesicles exhibited minimal leakage (Figure 47a), with the highest concentration of **20** generating just over 10% dye release. The same amount of dye release was observed for the DOPC vesicles (Figure 47b). This result was not surprising, as the heptamers **13** and **14** also showed a huge decrease in activity relative to the first generation of amphipathic @-tides, likely due to their increased hydrophobicity, and **20** is likely even more hydrophobic.

Overall, the vesicle lysis assays have shown that the anticipated improvement in activity, by increasing the degree of hydrophobicity by either the addition of another valine residue or an aliphatic tail, was not attainable with the oligomers that were prepared. This indicates that perhaps the Boc protecting group may play a specific role in the interaction of these oligomers with the bacterial mimic vesicles, as seen with the previous assay. However this result was not observed for the all lysine @-tides **15** and **16**, as the dicationic oligomer showed greater activity and selectivity than its Boc protected version. Tetramer **16** may however be in the correct balance of hydrophobic and hydrophilic components to display the expected activities, as those seen in natural host-defense antimicrobial peptides. Perhaps higher activity and selectivity may be attained through the preparation of longer oligomers containing only lysine residues. As well, it would be of interest to examine the differences in activities of an alternating D-/L-lysine @-tide and the all L-lysine @-tide.

The difference in activities between the first and second generation @-tides may also arise partly from the vesicle preparation. The first generation @-tides were tested on one batch of vesicles and the second generation was tested on another batch. Although

the batches were expected to be similar to one another, it is possible that there may be small differences from batch to batch in the concentrations of phospholipids and this should be quantified in the future. The shelf life of the lipids used to make these oligomers must also be accounted for, with the older lipids perhaps forming less stable vesicles, allowing them to be lysed more easily.

Part Three: Conclusions and Future Work

3.1 Contributions

β -strand mimetic oligomers based on alternating α -amino acids and azacyclohexenone units were designed as potential membrane disruptive antibiotics. In the first series of molecules D-valine and L-lysine were incorporated in an alternating manner with the aim of obtaining amphipathic structures having a cationic and a hydrophobic face in the linear β -strand conformation. The molecules were successfully synthesized by a solution phase convergent approach. Using NMR dilution studies, it was demonstrated that these new oligomers containing both D- and L-amino acids could dimerize to β -sheet mimics in $\text{CDCl}_3/\text{CD}_3\text{OH}$ solutions with similar affinities to the oligomers containing all L-amino acids, which were previously reported. This indicates that the incorporation of D-amino acids likely does not dramatically alter the conformation preferences of the molecules, and that they are capable of exhibiting amphipathic conformations. In vesicle leakage assays using membranes designed to mimic those of bacteria, it was found that several oligomers exhibited moderate membrane disruptive activity. No significant effects based on oligomer length were observed in this series of molecules ranging from tetramers to hexamers, although the hexamer exhibited slower leakage kinetics. Surprisingly, the oligomers with the ϵ -Boc protecting groups on the lysine units were as active or more active than the corresponding deprotected oligomers with pendant cationic amines, demonstrating that a cationic charge was not essential for activity in this class of molecules, and suggesting that there may be some advantage to the increased hydrophobicity of the protected oligomers. In addition, it was found that oligomers based on alternating D- and L-amino acids generally exhibited significantly higher activity than the corresponding oligomers containing all L-amino

acids. This indicated that there is some advantage to having the amino acid side chains diverging to opposite sides of the strand. Furthermore, much lower activity was observed for all of the oligomers with membranes mimicking those of eukaryotic cells in comparison with those of bacterial cells, suggesting that this class of molecules may be capable of selectively killing bacteria in the presence of mammalian cells.

Based on the results obtained with the first series of molecules, three new series of β -strand mimetic @-tide oligomers were designed to potentially provide greater activity. Two of the new series, based on the facially amphipathic @-tides, were synthesized with the aim of obtaining a more hydrophobic but still facially amphipathic structure. The other series was designed to contain only D- and L-lysine residues. Short versions of oligomers, ranging from tetramers to heptamers were successfully synthesized, but attempts at the syntheses of longer oligomers were unfortunately unsuccessful. In vesicle leakage assays, it was found that all of the new oligomers exhibited negligible activities except for the tetramer containing only lysine residues, which exhibited modest activity, and was more active in its deprotected than protected form. Unexpectedly, no significant improvements were observed resulting from the increases in hydrophobicities of the other series. The higher activity of the ϵ -Boc protected amine residue @-tides was again observed for these more hydrophobic oligomers, as previously seen in the initially examined @-tides. The reasons for this are still unclear. Additionally, the oligomers exhibited minimal lysis towards membranes mimicking those of eukaryotes; however, compared to the activities of the same oligomers towards membranes mimicking bacterial membranes, significant selectivity was not obtained.

Overall, this work represents the first example of membrane disruptive oligomers developed from a β -strand mimic based on α -amino acids. Although the membrane disruptive activities obtained thus far are relatively modest and some structure-activity relationships are still unclear, several important insights were gained into the features that are important for activity, providing the groundwork for further exploration of @-tides as potential antimicrobials. These structures are highly tunable as a diverse range of α -amino acids and oligomer terminal functionalities can be readily incorporated using the same synthetic routes described here. Thus the careful design, syntheses and evaluation of additional series of @-tides based on the discoveries described here can likely lead to new molecules with high antimicrobial activity and selectivity.

Part Four: Experimental

4.1 General Procedures and Materials.

All dry solvents were obtained from a solvent purification system. All other chemicals were obtained from commercial sources and used without further purification, unless otherwise indicated. Lipids were obtained from Avanti Polar Lipids as chloroform solutions and were used without further purification. Column chromatography was performed using silica gel (0.063-0.200 mm particle size, 70-230 mesh). Sonication was performed at ambient temperature using a Branson Digital Sonifier Model P/S Module 400W 20kHz at 25% amplitude. Extrusion was performed using a 1 mL Lipex™ Extruder from Northern Lipids, equipped with a polycarbonate membrane having a 1 μm pore size. ¹H NMR data were obtained at 400 or 600 MHz and ¹³C NMR data were obtained at 100 or 150 MHz. All chemical shifts are reported in ppm and are calibrated against residual solvent signals of CDCl₃ (δ 7.26, 77.2) or CD₃OD (δ 3.31, 48.9). All coupling constants (J) are reported in Hz. Mass spectrometry data were obtained using a Finnigan MAT 8200 instrument in TOF ES+ mode. IR spectra were obtained using films from dichloromethane or THF on NaCl plates. Fluorescence data were obtained on a QM-4 SE spectrofluorometer equipped with double excitation and emission monochromators from Photon Technologies International. All HPLC was performed on a Waters 2695 Separations Module with a Waters 2998 Photodiode Array Detector at a wavelength of 285 nm. Analytical HPLC traces were obtained using a Luna C18 3 μm (150 mm x 4.6 mm) column from Phenomenex, equipped with the corresponding guard column. The HPLC gradient was as follows: equilibration in either 30/70, 20/80, or 10/90 MeCN/H₂O at 1 mL/min flow rate, followed by ramping to 95/5 MeCN-H₂O over 15 min. The solvent mixture was then run for an additional 5 minutes for a total elution time

of 20 min. Retention times were recorded for this gradient. Preparative HPLC purification was accomplished using a Luna C18 5 μm (10 mm x 250 mm) column from Phenomenex, equipped with the corresponding guard column. The gradient for preparative HPLC purification was as follows: equilibration in 20/80 MeCN/H₂O at 3 mL/min flow rate for 10 min, followed by ramping to 95/5 MeCN/H₂O over 15 min. The solvent mixture was then run an additional 5 min for a total elution time of 20 min. Solvent mixtures for all chromatographic analyses and purifications contained 0.1% TFA.

4.2 Experimental Section

Synthesis of compound 1. This molecule was prepared by the previously reported method. ¹H NMR spectroscopic data agreed with those previously reported and were used to verify the compound's identity and purity.¹⁴⁶

Synthesis of dimer 2. Compound 1¹⁴⁶ (3.0 g, 12 mmol, 1.0 equiv.) and D-valine (1.6 g, 13 mmol, 1.1 equiv.) were dissolved in dry MeOH (180 mL) under a N₂ atmosphere. The solution was heated at 60 °C overnight. The reaction mixture was then cooled to room temperature and concentrated in vacuo. The crude product was redissolved in EtOAc/MeOH (147 mL/6 mL) and washed with 1M KHSO₄ and brine. The organic fractions were combined, dried over MgSO₄, filtered and concentrated. The crude product was purified by silica gel chromatography using a gradient of CH₂Cl₂/MeOH from 98/2 to 90/10 to remove impurities, followed by CH₂Cl₂/MeOH (1/1) to elute the product (2.2 g, 52 %) as an off white solid. ¹H NMR (400 MHz, CDCl₃/CD₃OD (2/1)): δ 0.97 (dd, 6H, J=13.1, 6.5), 2.06-2.20 (m, 1H), 3.67-3.73 (m, 1H), 3.94-4.12 (m, 2H), 4.23-4.43 (m, 2H), 5.11 (s, 2H), 5.15 (s, 1H), 7.26-7.40 (m, 5H). ¹³C NMR (100 MHz, CDCl₃): δ 18.4,

18.7, 30.5, 43.9, 50.0, 61.4, 67.8, 94.5, 127.8, 128.2, 128.4, 135.7, 154.8, 163.0, 173.2, 192.1. IR (cm⁻¹, film from CH₂Cl₂): 3287, 3062, 2961, 2928, 2863, 1719, 1663, 1553. HRMS calcd. for [M+H]⁺ (C₁₈H₂₃N₂O₅): 347.1607. Found (ES⁺): 347.1624.

Synthesis of dimer 3. Compound **1**¹⁴⁶ (4.5 g, 18 mmol, 1.0 equiv.) and ε-Boc-L-lysine^{164, 165} (4.8 g, 20 mmol, 1.1 equiv.) were dissolved in dry MeOH (270 mL) under a N₂ atmosphere. The reaction was heated to 60 °C and maintained at this temperature overnight. The solution was then cooled to room temperature and concentrated. The crude product was redissolved in EtOAc/MeOH (220 mL/9 mL) and extracted with 1M KHSO₄ followed by brine. The organic layer was isolated, dried with MgSO₄, filtered and concentrated. The product was purified by silica gel chromatography using a gradient of EtOAc/Hexane (95/5) to remove impurities followed by EtOAc/MeOH (90/10) to elute the product (5.97 g, 68 %) as a viscous oil. The product was taken to the next step without further purification. ¹H NMR (400 MHz, CDCl₃/CD₃OD (2/1)): δ 1.31-1.57 (m, 13H), 1.68-1.95 (m, 2H), 3.02 (t, 2H, J=6.3), 3.83-3.94 (m, 1H), 3.96-4.12 (m, 2H), 4.25-4.37 (m, 2H), 5.04-5.11 (m, 1H), 5.12-5.18 (m, 2H), 7.29-7.39 (m, 5H).

Synthesis of dimer 4. The acid **3** (6.0 g, 13 mmol, 1.0 equiv.) was dissolved in THF/H₂O (386 mL/45 mL) with stirring. A 20% solution of Cs₂CO₃ was added to the reaction mixture slowly until a pH of 7 was obtained. The mixture was then concentrated, redissolved in THF and concentrated again. Methyl iodide (0.94 mL, 15 mmol, 1.2 equiv.) in DMF (162 mL) was added to the resulting oil and the reaction was stirred at room temperature for 30 min. The solvent was evaporated and the viscous oil was triterated with distilled water to remove salts. The product was filtered and taken back up in MeOH and then concentrated. The product was further purified by silica gel

chromatography using a gradient of CH₂Cl₂ to CH₂Cl₂/MeOH (98/2) to remove the impurities, followed by CH₂Cl₂/MeOH (90/10) to elute the product (2.9 g, 48 %) as a glassy solid. ¹H NMR (600 MHz, CD₃OD): δ 1.26-1.51 (m, 13H), 1.69-1.90 (m, 2H), 2.97-3.07 (m, 2H), 3.71 (s, 3H), 3.96 (t, 1H, J=6.9), 4.00-4.07 (m, 2H), 4.24-4.33 (m, 2H), 5.04 (s, 1H), 5.12 (s, 2H), 7.26-7.37 (m, 5H). ¹³C NMR (150 MHz, CDCl₃/CD₃OD (2/1)): δ 23.9, 29.0, 30.5, 32.2, 40.9, 48.9, 51.4, 53.1, 56.7, 68.7, 79.7, 95.2, 128.9, 129.2, 129.6, 137.5, 156.1, 158.2, 173.1, 193.3. IR (cm⁻¹, film from CH₂Cl₂): 3269, 3056, 2925, 2859, 1739, 1658. HRMS calcd. for [M+H]⁺ (C₂₅H₃₅N₃O₇): 489.2475. Found (ES⁺): 489.2480.

Synthesis of dimer 5 and general hydrogenation procedure. The dimer 4 (0.75 g, 1.5 mmol, 1.0 equiv.) was dissolved in MeOH (20 mL) and 10% Pd/C (75 mg) was added. The mixture was placed in a Parr shaker and was reacted using 4.5 bar of H₂ pressure for approximately 1 hour. The solution was then filtered through celite and the filtrate was concentrated to yield the product (0.53 g, 100%) as a glassy solid. The product was taken to the next step without further purification. ¹H NMR (400 MHz, CDCl₃/CD₃OD (2/1)): δ 1.29-1.53 (m, 13H), 1.72-1.91 (m, 2H), 3.04 (q, 2H, J=6.5), 3.31 (s, 2H), 3.56 (d, 2H, J=2.9), 3.74 (s, 3H), 3.99 (dd, 1H, J=8.0, 5.5), 5.01 (s, 1H), 5.81 (br s, 1H).

Synthesis of tetramer 6. The dimer 2 (1.0 g, 2.9 mmol, 1.1 equiv), dimer 5 (0.93 g, 2.6 mmol, 1.0 equiv.), HATU (3.6 g, 9.5 mmol, 3.3 equiv.) and DIPEA (1.1 mL, 6.4 mmol, 2.2 equiv.) were dissolved in dry DMF (84 mL) under N₂ and the reaction mixture was stirred for 24 hours. The reaction progress was monitored by thin layer chromatography (100% EtOAc) and upon completion the solution was concentrated, redissolved in EtOAc

(124 mL) and washed with 1M KHSO₄ followed by sat. NaHCO₃. The organic layer was isolated, dried over MgSO₄, filtered and evaporated to yield a glassy solid. The product was purified by silica gel chromatography using EtOAc to elute the impurities, followed and EtOAc/MeOH (95/5) to elute the product (1.1 g, 63 %) as a glassy solid. ¹H NMR (600 MHz, CD₃OD): δ 0.81-1.09 (m, 6H), 1.25-1.55 (m, 15H), 1.71-1.95 (m, 2H), 2.02-2.16 (m, 1H), 2.96-3.09, (m, 2H), 3.66-3.78 (m, 3H), 3.94-4.14 (m, 3H), 4.14-4.25 (m, 1H), 4.28-4.62 (m, 5H), 4.73 (t, 1H, J=17.0), 5.06-5.28 (m, 4H), 6.52 (br s, 1H), 7.24-7.38 (m, 5H). ¹³C NMR (150 MHz, CD₃OD): δ 18.7, 19.6, 24.0, 28.9, 30.5, 32.5, 41.0, 43.7, 45.1, 51.5, 53.1, 56.9, 59.0, 68.8, 79.8, 95.0, 95.5, 129.0, 129.3, 129.7, 137.6, 156.4, 158.4, 163.4, 164.9, 170.8, 171.2, 173.0, 173.2, 192.4, 193.7. IR (cm⁻¹, film from CH₂Cl₂): 3283, 3057, 2960, 2927, 2862, 1736, 1689. HRMS calcd. for [M+Na]⁺ (C₃₅H₄₉N₅O₉Na)⁺: 706.3422. Found (ES⁺): 706.3428. HPLC tR 9.7 min (MeCN/H₂O (20/80)).

Synthesis of tetramer 7. Hydrogenolysis of tetramer **6** was performed as described above for the preparation of the dimer **5**, providing the tetramer **7** (99%) as a glassy solid. The product was taken to the next step without further purification. ¹H NMR (400 MHz, CDCl₃): δ 0.68-1.09 (m, 6H), 1.19-1.62 (m, 13H), 1.70-1.94 (m, 2H), 1.97-2.10 (m, 1H), 3.00-3.15 (m, 2H), 3.66-3.83 (m, 3H), 3.88-5.27 (m, 10H).

Synthesis of the pentamer 8. Tetramer **7** (0.69 g, 1.3 mmol, 1.0 equiv), α-acetyl-ε-Boc-L-lysine¹⁵⁴ (0.40 g, 1.4 mmol, 1.1 equiv.), HATU (1.6 g, 4.2 mmol, 3.3 equiv.) and DIPEA (0.50 mL, 3.0 mmol, 2.4 equiv.) were dissolved in dry DMF (22 mL) under a N₂ atmosphere and the reaction mixture was stirred for 24 hours. The reaction progress was monitored TLC. Upon completion, the solution was concentrated and the product was

redissolved in EtOAc (75 mL) and washed with 1M KHSO₄ followed by sat. NaHCO₃. The organic layer was isolated, dried over MgSO₄, filtered, and concentrated. The product was purified by silica gel chromatography using a gradient from CH₂Cl₂/MeOH (95/5) to elute impurities, followed by CH₂Cl₂/MeOH (93/7) to elute the product (0.63 g, 61%) as a light brown glassy solid. ¹H NMR (400 MHz, CDCl₃/CD₃OD (2/1)): δ 0.93-1.09 (m, 6H), 1.28-1.55 (m, 26H), 1.56-1.64 (m, 1H), 1.64-1.73 (m, 1H), 1.75-1.85 (m, 1H), 1.87-1.93 (m, 1H), 1.97 (d, 3H, J=11.1), 2.08-2.20 (m, 1H), 2.96-3.08 (m, 4H), 3.70-3.80 (m, 3H), 4.10-4.75 (m, 11H), 5.06-5.30 (m, 2H). IR (cm⁻¹, thin film from CH₂Cl₂): 3277, 3056, 2963, 2926, 2859, 1732, 1684, 1635, 1549. HRMS calcd. for [M+H]⁺ (C₄₀H₆₆N₇O₁₁): 820.4820. Found (ES⁺): 820.4794. HPLC tR 8.6 min (MeCN/H₂O (20/80)).

Synthesis of hexamer 9. Tetramer 7 (0.40 g, 0.73 mmol, 1.0 equiv), dimer 3 (0.38 g, 0.80 mmol, 1.1 equiv.), HATU (0.37 g, 2.4 mmol, 3.3 equiv.) and DIPEA (0.28 mL, 1.6 mmol, 2.2 equiv.) were dissolved in dry DMF (15 mL) under a N₂ atmosphere and the reaction mixture was stirred for 24 hours. The reaction progress was monitored by TLC. Upon completion, the solution was concentrated and the product was redissolved in EtOAc (44 mL) and washed with 1M KHSO₄ followed by sat. NaHCO₃. The organic layer was isolated, dried over MgSO₄, filtered, and concentrated in vacuo. The product was purified by silica gel chromatography using a gradient from EtOAc/Hexanes (95/5) to EtOAc/Hexanes (97/3) to remove impurities, followed by EtOAc to elute the product (0.16 g, 22 %). ¹H NMR (400 MHz, CDCl₃/CD₃OD (2/1)): δ 0.92-1.01 (m, 6H), 1.29-1.56 (m, 26H), 1.63-1.95 (m, 4H), 2.04-2.13 (m, 1H), 2.94-3.07 (m, 4H), 3.71-3.75 (m, 3H), 3.91-4.76 (m, 15H), 5.02-5.21 (m, 5H), 6.03 (br s, 1H), 7.26-7.38 (m, 5H). IR (cm⁻¹

¹, thin film from CH₂Cl₂): 3352, 3056, 2964, 2927, 2863, 1631, 1548. HRMS calcd. for [M+Na]⁺ (C₅₁H₇₄N₈O₁₃Na): 1029.5273. Found (ES⁺): 1029.5273. HPLC tR 9.1 min (MeCN/H₂O (30/70)).

Synthesis of deprotected pentamer 10 and general procedure for removal of Boc protecting groups. Pentamer **8** (99 mg, 0.12 mmol, 1.0 equiv.) was dissolved in a 2 mL solution of TFA/CH₂Cl₂ (1/1) and the reaction mixture was stirred at room temperature for 2 hours. The solution was then concentrated in vacuo to provide the product (76 mg, 94 %) as a glassy solid. ¹H NMR (400 MHz, CDCl₃/CD₃OD (2/1)): δ 0.83-1.10 (m, 6H), 1.27-1.55 (m, 4H), 1.57-1.80 (m, 6H), 1.83-2.01 (m, 5H), 2.09-2.21 (m, 1H), 2.84-3.06 (m, 4H), 3.74 (s, 3H), 4.03-5.37 (m, 12H). IR (cm⁻¹, thin film from CH₂Cl₂): 3499, 3243, 3052, 2948, 2921, 2845, 1675, 1630, 1556. HRMS calcd. for [M+H]⁺ (C₃₀H₅₀N₇O₇): 620.3772. Found (ES⁺): 620.3773. HPLC tR 4.2 min (MeCN/H₂O (10/90)).

Synthesis of deprotected hexamer 11. Treatment of hexamer **9**, as described above for the preparation of the pentamer **10**, provided hexamer **11** (56 mg, 93 %) as a glassy solid. A sample was purified further using preparative reverse-phase HPLC. ¹H NMR (400 MHz, CD₃OD): δ 0.93-1.08 (m, 6H), 1.38-1.57 (m, 4H), 1.59-1.77 (m, 5H), 1.80-2.02 (m, 3H), 2.07-2.22 (m, 1H), 2.83-3.00 (m, 4H), 3.75 (s, 3H), 2.96-4.80 (m, 15H), 5.11-5.21 (m, 2H), 7.27-7.41 (m, 5H). IR (cm⁻¹, thin film from CH₂Cl₂): 3496, 3452, 3038, 2938, 2896, 2838, 1672, 1549. HRMS calcd. for [M+H]⁺ (C₄₁H₅₉N₈O₉): 807.4405. Found (ES⁺): 807.4413. HPLC tR 3.9 min (MeCN/H₂O 10/90).

Syntheses of oligomers containing all L-amino acids. The oligomers **6'**, **8'**, **9'**, **10'**, and **12'** containing all L-amino acids were prepared by identical procedures to those

described above for the preparation of the corresponding oligomers **6**, **8**, **9**, **10**, and **12** containing alternating D and L-amino acids. Their characterization data are reported below.

Dimer 2'. All spectral data were identical to those of **2** (its enantiomer).

Tetramer 6'. ^1H NMR (400 MHz, CDCl_3): δ 0.84-1.02 (m, 6H), 1.31-1.52 (m, 13H), 1.76-1.91 (m, 2H), 2.20-2.48 (m, 1H), 3.00-3.13 (m, 2H), 3.78, (s, 3H), 3.92-4.06 (m, 2H), 4.11-4.23 (m, 2H), 4.33-4.52 (m, 3H), 4.63 (t, 2H, $J=15.4$), 4.74 (t, 1H, $J=5.5$), 5.05-5.22 (m, 3H), 5.40-5.54 (m, 1H), 7.01 (d, 1H, $J=9.4$), 7.18 (d, 1H, $J=7.0$), 7.28-7.40 (m, 5H). ^{13}C NMR (400 MHz, CDCl_3): δ 14.2, 17.8, 19.2, 21.0, 22.7, 28.37, 29.6, 31.42, 32.4, 39.9, 41.8, 42.48, 44.3, 50.6, 52.3, 52.8, 55.4, 56.4, 60.4, 67.8, 79.2, 95.0, 127.4, 128.2, 128.5, 135.7, 155.3, 156.0, 160.9, 169.8, 171.2, 172.2, 188.9, 191.6. IR (cm^{-1} , film from CH_2Cl_2): 3272, 3058, 2957, 2929, 2863. HRMS calcd. for $[\text{M}^+]$ ($\text{C}_{35}\text{H}_{49}\text{N}_5\text{O}_9$) $^+$: 683.3530. Found (ES $^+$): 683.3574. HPLC tR 9.7 min (MeCN/ H_2O (20/80)).

Pentamer 8'. ^1H NMR (400 MHz, CD_3OD): δ 0.95-1.06 (m, 6H), 1.25-1.55 (m, 26H), 1.56-1.63 (m, 1H), 1.63-1.74 (m, 1H), 1.76-1.86 (m, 1H), 1.87-1.94 (m, 1H), 1.96 (d, 3H, $J=11.13$), 2.09-2.18 (m, 1H), 2.95-3.10 (m, 4H), 3.71-3.77 (m, 3H), 3.98-4.76 (m, 11H), 5.05-5.18 (m, 2H). IR (cm^{-1} , film from CH_2Cl_2): 3278, 3061, 2961, 2928, 2862, 1719, 1632, 1552. HRMS calcd. for $[\text{M}+\text{Na}]^+$ ($\text{C}_{40}\text{H}_{65}\text{N}_7\text{O}_{11}\text{Na}$) $^+$: 842.4640. Found (ES $^+$): 842.4615. HPLC tR 8.6 min (MeCN/ H_2O (20/80)).

Hexamer 9'. ^1H NMR (400 MHz, CDCl_3): δ 0.83-1.01 (m, 6H), 1.06-2.01 (m, 30H), 2.10 (s, 1H), 2.84-3.09 (m, 4H), 3.64 (s, 3H), 3.81-5.00 (m, 15H), 5.09 (s, 2H), 5.19 (s, 1H), 5.45 (br s, 1H), 5.75 (br s, 1H), 7.06 (br s, 1H), 7.09-7.40 (m, 5H), 7.47 (br s, 1H), 7.64 (br s, 1H). IR (cm^{-1} , film from CH_2Cl_2): 3294, 3059, 2955, 2924, 2863, 1680, 1634,

1556. HRMS calcd. for $[M+Na]^+$ ($C_{51}H_{74}N_8O_{13}Na$): 1029.5273. Found (ES+): 1029.5298. HPLC tR 9.1 (MeCN/H₂O (30/70)).

Pentamer 10'. ¹H NMR (400 MHz, CD₃OD): δ 0.95-1.09 (m, 6H), 1.25-1.57 (m, 4H), 1.60-1.82 (m, 6H), 1.83-2.02 (m, 5H), 2.09-2.21 (m, 1H), 2.87-3.01 (m, 4H), 3.72-3.79 (m, 3H), 4.05-4.79 (m, 10H), 5.06-5.23 (m, 2H). IR (cm⁻¹, film from CH₂Cl₂): 3416, 3250, 3055, 2958, 1718, 1674. HRMS calcd. for $[M+H]^+$ ($C_{30}H_{50}N_7O_7$): 620.3772. Found (ES+); 620.3798. HPLC tR 6.0 min (MeCN/H₂O (10/90))

Hexamer 11'. ¹H NMR (400 MHz, CD₃OD): δ 0.94-1.10 (m, 6H), 1.19-1.58 (m, 4H), 1.60-1.79 (m, 5H), 1.81-2.06 (m, 3H), 2.07-2.20 (m, 1H), 2.85-2.98 (m, 4H), 3.71-3.77 (m, 3H), 3.98-4.86 (m, 17H), 5.07-5.26 (m, 3H), 7.29-7.44 (m, 5H), 7.59-7.66 (m, 1H), 7.70-7.75 (m, 1H). IR (cm⁻¹, film from CH₂Cl₂): 3464, 3241, 3049, 2935, 2921, 2851, 1674, 1550. HRMS calcd. for $[M+H]^+$ ($C_{41}H_{59}N_8O_9$): 807.4405. Found (ES+): 807.4421. HPLC tR 4.1 min (MeCN/H₂O 10/90).

Synthesis of Hexamer 12. Hydrogenolysis of the hexamer **9** was performed as described above for the preparation of the dimer **5**, providing the hexamer **9** (99%) as a glassy solid. The product was taken to the next step without further purification.

Synthesis of Heptamer 13. Hexamer **12** (0.10 g, 0.15 mmol, 1.0 equiv.), α -acetylvaline¹⁶⁶ (0.032 g, 0.20 mmol, 1.3 equiv.), HATU (0.98 g, 0.50 mmol, 3.3 equiv.) and DIPEA (0.30 mL, 0.33 mmol, 2.2 equiv.) were dissolved in dry DMF (5 mL) under a N₂ atmosphere and the reaction mixture was stirred for 24 hours. The reaction progress was monitored TLC. Upon completion, the solution was concentrated and the product was redissolved in EtOAc (8 mL) and washed with 1M KHSO₄ followed by sat. NaHCO₃. The organic layer was isolated, dried over MgSO₄, filtered, and concentrated. The

product was purified by silica gel chromatography using a gradient from 100% EtOAc then CH₂Cl₂/MeOH (90/10) to elute impurities, followed by CH₂Cl₂/MeOH (80/20) to elute the product (0.045 g, 29%) as a light brown glassy solid. ¹H NMR (600 MHz, CDCl₃): δ 0.63-0.99 (m, 12H), 1.11-1.52 (m, 26H), 1.56-1.67 (m, 1H), 1.68-1.87 (m, 3H), 1.88-2.07 (m, 4H), 2.88-3.11 (m, 4H), 3.63-3.76 (m, 3H), 3.83-5.60 (m, 18H). IR (cm⁻¹, thin film from CH₂Cl₂): 3283, 3051, 2934, 2924, 2857, 1719, 1669, 1629, 1552. HRMS calcd. for [M+Na]⁺ (C₅₀H₇₉N₉NaO₁₃): 1036.5695. Found (ES⁺): 1036.5674. HPLC tR 6.3 min MeCN/H₂O (30/70).

Synthesis of Heptamer 14. Treatment of hexamer **9**, as described above for the preparation of the pentamer **10**, provided heptamer **14** (20 mg, 99 %) as a glassy solid. ¹H NMR (600 MHz, CDCl₃:CD₃OD(2:1)): δ 0.77-1.03 (m, 12H), 1.16-1.33 (m, 7H), 1.39-1.54 (m, 4H), 1.57-1.73 (m, 5H), 1.74-1.80 (m, 1H), 1.88-1.95 (m, 1H), 1.95-2.06 (m, 3H), 2.06-2.20 (m, 1H), 2.80-3.0 (m, 4H), 3.63-3.83 (m, 3H), 3.99-4.30 (m, 6H), 4.33-5.00 (m, 10H), 5.01-5.74 (m, 3H). IR (cm⁻¹, thin film from THF): 3237, 2978, 2915, 2845, 1634, 1447, 1414. HRMS calcd. for [M]⁺ (C₄₀H₆₅N₉O₉): 815.4894. Found (ES⁺): 815.4886. HPLC tR 5.2 min MeCN/H₂O (10/90).

Synthesis of Dimer 3'. Dimer **3'** prepared by the identical procedure to that described above for the preparation of the corresponding dimer **3**. All spectral data was identical to that of **3**.

Synthesis of Tetramer 15. Dimer **3'** (0.35 g, 0.73 mmol, 1.25 equiv.), amine **5** (0.20 g, 0.56 mmol, 1 equiv.), HATU (0.71g, 1.9mmol, 3.3 equiv.) and DIPEA (0.22 mL, 1.2 mmol, 2.2 equiv.) were dissolved in dry DMF (20 mL) under a N₂ atmosphere and the reaction mixture was stirred for 24 hours. The reaction progress was monitored by TLC.

Upon completion, the solution was concentrated and the product was redissolved in EtOAc (20 mL) and washed with 1M KHSO₄ followed by sat. NaHCO₃. The organic layer was isolated, dried over MgSO₄, filtered, and concentrated. The product was purified by silica gel chromatography using a gradient from 100% EtOAc to elute impurities, followed by EtOAc/MeOH (97/3) to elute the product (0.17 g, 36%) as a light brown glassy solid. ¹H NMR (600 MHz, CDCl₃): δ 1.17-1.54 (m, 26H), 1.58-1.70 (m, 1H), 1.71-1.93 (m, 3H), 2.91-3.97 (m, 4H), 3.59-3.81 (m, 3H), 3.87-4.18 (m, 4H), 4.18-4.58 (m, 4H), 4.58-5.00 (m, 2H), 5.04-5.35 (m, 4H), 7.25-7.43 (m, 5H). IR (cm⁻¹, thin film from CH₂Cl₂): 3297, 3047, 2945, 2920, 2853, 1684, 1628, 1551. HRMS calcd. for [M+Na]⁺ (C₄₁H₆₀N₆O₁₁Na): 835.4218. Found (ES⁺): 835.4191. HPLC tR 10.4 min MeCN/H₂O (20/80).

Synthesis of Tetramer 16. Treatment of tetramer **15**, as described above for the preparation of the pentamer **10**, provided tetramer **16** (7 mg, 99 %) as a glassy solid. ¹H NMR (600 MHz, CDCl₃:CD₃OD(2:1)): δ 1.17-1.31 (m, 6H), 1.32-1.52 (m, 5H), 1.55-2.01 (m, 10H), 2.62-2.93 (m, 4H), 3.67-3.76 (m, 3H), 3.93-4.43 (m, 10H), 4.44-4.59 (m, 2H), 4.99-5.15 (m, 2H). IR (cm⁻¹, thin film from THF): 3405, 2951, 1634, 1427. HRMS calcd. for [M]⁺ (C₃₁H₄₆N₆O₇): 614.3417. Found (ES⁺): 614.3503. HPLC tR 2.2 min (MeCN/H₂O (10/90)).

Synthesis of Tetramer 17. Tetramer **6** (0.21 g, 0.30 mmol, 1 equiv.) was dissolved in 20 mL of THF/water (1:1) and LiOH·H₂O (0.025 g, 0.60 mmol, 2 equiv.) was added. The reaction mixture was stirred for 1 hr, then was diluted with 1M KHSO₄ and extracted with EtOAc. The organic fractions were combined, dried over MgSO₄, and concentrated

generating **17** in quantitative yield. The product was taken to the next step without further purification.

Synthesis of Tetramer 18. The tetramer acid **17** (0.17 g, 0.26 mmol, 1 equiv.), 1-octanol (0.060 mL, 1.5 mmol, 1.5 equiv.), DCC (0.21 g, 1.02 mmol, 4.0 equiv), DPTS (0.038 g, 0.13 mmol, 0.5 equiv.) and DMAP (0.016 g, 0.13 mmol, 0.5 equiv.) were dissolved in dry CH₂Cl₂ (10 mL) and stirred under N₂ for 6 hours. The solution was then filtered through cotton and concentrated. The crude product was then redissolved in EtOAc and refiltered until all of the visible precipitate was removed, followed by a final concentration. The product was further purified by silica gel chromatography using EtOAc/MeOH (90:10) to remove impurities and to elute the product (0.072 g, 36%) as an off-white foam. ¹H NMR (600 MHz, CDCl₃): δ 0.75-1.03 (m, 9H), 1.14-1.52 (m, 23H), 1.54-1.63 (m, 2H), 1.69-1.92 (m, 2H), 1.95-2.14 (m, 1H), 2.94-3.19 (m, 4H), 3.89-4.03 (m, 2H), 4.03-4.17 (m, 3H), 4.18-4.45 (m, 4H), 4.46-4.63 (m, 1H), 4.67-5.03 (m, 2H), 5.13 (s, 2H), 5.26-5.47 (m, 1H), 6.50 (s, 1H), 7.12 (s, 1H), 7.20-7.45 (m, 5H), 8.18 (s, 1H). IR (cm⁻¹, thin film from CH₂Cl₂): 3405, 2934, 2925, 2852, 1636, 1436, 1363. HRMS calcd. for [M+Na]⁺ (C₄₂H₆₃N₅NaO₉): 804.4523. Found (ES⁺): 804.4517. HPLC tR 13.3 min MeCN/H₂O (30/70).

Synthesis of Tetramer 19. Hydrogenolysis of the tetramer **18** was performed as described above for the preparation of the dimer **5**, providing the tetramer **19** (99%) as a glassy solid. The product was taken to the next step without further purification.

Synthesis of Hexamer 20. Tetramer **19** (0.050 g, 0.077 mmol, 1.0 equiv.), dimer **3** (0.048 g, 0.10 mmol, 1.3 equiv.), HATU (0.097 g, 0.26 mmol, 3.3 equiv.) and DIPEA

(0.030 mL, 0.17 mmol, 2.2 equiv.) were dissolved in dry DMF (8 mL) under a N₂ atmosphere and the reaction mixture was stirred for 24 hours. The reaction progress was monitored by TLC. Upon completion, the solution was concentrated and the product was redissolved in EtOAc (5 mL) and washed with 1M KHSO₄ followed by sat. NaHCO₃. The organic layer was isolated, dried over MgSO₄, filtered, and concentrated. The product was purified by silica gel chromatography using EtOAc/MeOH (94/6) to elute the product (23 mg, 26%) as a light brown glassy solid. ¹H NMR (600 MHz, CDCl₃): δ 0.82-0.91 (m, 6H), 0.91-1.01 (m, 3H), 1.23-1.34 (m, 15H), 1.40-1.48 (m, 15H), 1.55-1.68 (m, 21H), 1.74-1.96 (m, 2H), 1.98-2.13 (m, 1H), 2.97-3.18 (m, 4H), 3.72-3.83 (m, 2H), 3.86-4.55 (m, 12H), 4.56-4.89 (m, 3H), 4.91-5.46 (m, 5H), 7.3-7.42 (m, 5H). IR (cm⁻¹, thin film from CH₂Cl₂): 3412, 2939, 2920, 2847, 1630, 1432. HRMS calcd. for [M+Na]⁺ (C₅₈H₈₈N₈NaO₁₃): 1127.6363. Found (ES⁺): 1127.6437. HPLC tR 8.4 min MeCN/H₂O (40/60).

¹H NMR dilution experiment. The pentamer **8** was dissolved in CDCl₃ at a concentration of 50 mM and serial two-fold dilutions were carried out to a concentration of 0.78 mM. ¹H NMR spectra were obtained at 600 MHz for each concentration. The upper concentration was limited by broadness of peaks at higher concentrations in CDCl₃. The same procedure was carried out for pentamer **8** in 99/1 CDCl₃/CD₃OH and 97.5/2.5 CDCl₃/CD₃OH but at concentrations ranging from 125 mM to 1 mM. The tetramer **6** and hexamer **9** were evaluated in 97.5/2.5 CDCl₃/CD₃OH at concentrations ranging from 125 mM to 1 mM.

Vesicle Leakage Assay. Vesicles formed from DOPC were used as models for mammalian cell membranes and vesicles formed from an 80/20 mixture of DOPE/DOPG

were used as models for bacterial membranes. HPTS and its quencher DPX were encapsulated in these vesicles. The following solutions were used in the vesicle experiments: 4-(2-hydroxyethyl)piperazine-1-ethanesulfonic acid (HEPES) buffer (10 mM HEPES, 145 mM NaCl, 0.1mM EDTA, NaHCO₃ pH 7.25), HPTS (10 mM) in HEPES buffer, DPX (100 mM) in HEPES buffer, and HPTS/DPX/HEPES buffer (3.0 mL, 1.8 mL, and 5.2mL respectively of the HPTS, DPX, and HEPES buffers). 1.1 mL of a DOPC stock solution (25 mg/mL) was dried under N₂, and then dried under high vacuum for 2 hours. 0.88 mL of a DOPE stock solution (25 mg/mL) in chloroform was mixed with 0.22 mL of a DOPG stock solution (25 mg/mL) in chloroform to a total volume of 1.1 mL and then the resulting solution was dried under N₂, followed by under high vacuum for 2 hours. The resulting films were hydrated with 0.6 mL HPTS/DPX/HEPES buffer for 2 hours. The suspensions were then subjected to five freeze-thaw/sonication cycles and were subsequently extruded through a 1 μm Whatman polycarbonate membrane >10 times yielding about 0.5mL, which was then diluted to 2.5mL with HEPES buffer. The excess dye was removed by gel filtration chromatography (Nap-10 columns, GE Healthcare) using HEPES buffer, resulting in 4.5 mL of vesicle solution. 20 μL of this solution was added to 1.98 mL of HEPES buffer in a quartz fluorescence cuvette. Solutions of the oligomers in DMSO (5-40 μL of a 5 mg/mL solution) were added to provide final oligomer concentrations ranging from 12.5 to 100 μg/mL in the 2mL of vesicle solution. The solutions were stirred and the fluorescence emission intensities I_t ($\lambda_{em} = 520$ nm, $\lambda_{ex} = 460$ nm) were monitored as a function of time (t). 20 μL of 20 % Triton X-100 in DMSO was then added to provide complete vesicle lysis. The curves were normalized to percent leakage $[(I_t - I_0)/(I_\infty - I_0)] \times$

100. I_0 is the emission intensity before the addition of any of the polymers, and I_∞ is the emission intensity after the addition of Triton X-100.

Part Five: References

- (1) Russell, A. D. *J. Appl. Microbiol. Symp. Suppl.* **2002**, *92*, 1S-3S.
- (2) Levy, S. B. In *The Antibiotic Paradox. How Miracle Drugs Are Destroying the Miracle*. Plenum Press: New York, 1992.
- (3) Chopra, I. *Curr. Opin. Microbiol.* **1998**, *1*, 495.
- (4) Russel, A. D. *Prog. Med. Chem.* **1998**, *35*, 133.
- (5) Russel, A. D.; Chopra, I. In *Understanding Antibacterial Action and Resistance*; Ellis Horwood: Chichester, 1996.
- (6) Zasloff, M. *Nature* **2002**, *415*, 389.
- (7) Brogden, K. A. *Nat. Rev. Microbiol.* **2005**, *3*, 238.
- (8) Zasloff, M. *Proc. Natl. Acad. Sci. U. S. A* **1987**, *84*, 5449.
- (9) Steiner, H.; Hultmark, D.; Engstrom, A.; Bennich, H.; Boman, H. G. *Nature* **1981**, *292*, 246.
- (10) Lai, J. R.; Huck, B. R.; Weisblum, B. Gellman, S. H. *Biochemistry* **2002**, *41*, 12835.
- (11) Ganz, T. *Nat. Rev. Immunol.* **2003**, *3*, 710.
- (12) Falla, T. J.; Karunaratne, N.; Hancock, R. E. W. *J. Biol. Chem.* **1996**, *271*, 19298.
- (13) Choi, S.; Isaacs, A.; Clements, D.; Liu, D.; Kim, H.; Scott, R. W.; Winkler, J. D.; DeGrado, W. F. *Proc. Natl. Acad. Sci. U. S. A* **2009**, *106*, 6968.
- (14) Epand, R. F.; Umezawa, N.; Porter, E. A.; Gellman, S. H.; Epand, R. M. *Eur. J. Biochem.* **2003**, *270*, 1240.
- (15) Shai, Y.; Oren, Z. *J. Biol. Chem.* **1997**, *272*, 14543.
- (16) Westerhoff, H. V.; Juretic, D.; Hendler, R. W.; Zasloff, M. *Proc. Natl. Acad. Sci. U. S. A* **1989**, *86*, 6597.
- (17) Ludtke, S.; He, K.; Huang, H. *Biochemistry* **1995**, *34*, 16764.
- (18) Shai, Y.; Oren, Z. *Biol. Chem.* **1996**, *271*, 7305.
- (19) Matsuzaki, K.; Murase, O.; Fujii, N.; Miyajima, K. *Biochemistry* **1995**, *34*, 6521.
- (20) Huang, H. W. *Biochemistry* **2000**, *39*, 8347.
- (21) Oren, Z.; Shai, Y. *Biochemistry* **1997**, *36*, 1826.
- (22) Tew, G. N.; Liu, D.; Chen, B.; Doerksen, R. J.; Kaplan, J.; Carroll, P. J.; Klein, M. L.; DeGrado, W. F. *Proc. Natl. Acad. Sci. U. S. A* **2002**, *99*, 5110.
- (23) Moore, A. J.; Beazley, W. D.; Bibby, M. C.; Devine, D. A. *J. Antimicrob. Chemother.* **1996**, *37*, 1077.
- (24) Steinberg, D. A.; Hurst, M. A.; Fujii, C. A.; Kung, A. H.; Ho, J. F.; Cheng, F. C.; Loury, D. J.; Fiddes, J. C. *Antimicrob. Agents Chemother.* **1997**, *41*, 1738.
- (25) Selsted, M. E.; Harwig, S. S.; Ganz, T.; Schilling, J. W.; Lehrer, R. I. *J. Clin. Invest.* **1985**, *76*, 1436.
- (26) Ganz, T. *J. Clin. Invest.* **1985**, *76*, 1427.
- (27) Zeya, H. I.; Spitznagel, J. K. *Science* **1963**, *142*, 1085.
- (28) Kostoulas, G.; Horler, D.; Naggi, A.; Casu, B.; Caici, A. *Biol. Chem.* **1997**, *378*, 1481.
- (29) Fromm, J. R.; Hileman, R. E.; Caldwell, E. E.; Weiler, J. M.; Linhardt, R. J. *Arch. Biochem. Biophys.* **1995**, *323*, 279.
- (30) Hileman, R. E.; Fromm, J. R.; Weiler, J. M.; Linhardt, R. J. *Bioessays* **1998**, *20*, 156.
- (31) Wimley, W. C.; Selsted, M. E.; White, S. H. *Protein Sci* **1994**, *3*, 1362.
- (32) Lohner, K.; Latal, A.; Lehrer, R. I.; Ganz, T. *Biochemistry* **1997**, *36*, 1525.
- (33) Fujii, G.; Selsted, M. E.; Eisenberg, D. *Protein Sci* **1993**, *2*, 1301.
- (34) Kagan, B. L.; Selsted, M. E.; Ganz, T.; Lehrer, R. I. *Proc. Natl. Acad. Sci. U. S. A*

1990, 87, 210.

- (35) Boman, H. G.; Marsh, J.; Goode, J. A., Eds.; In *Antimicrobial Peptides*; John Wiley & Sons: Chichester, U.K., 1994; pp 1-272.
- (36) Yang, L.; Harroun, T. A.; Weiss, T. M.; Ding, L.; Huang, H. W. *Biophys. J.* **2001**, 81, 1475.
- (37) Wade, D.; Boman, A.; Wahlin, B.; Drain, C. M.; Andreu, D.; Boman, H. G.; Merrifield, R. B. *Proc. Natl. Acad. Sci. U. S. A* **1990**, 87, 4761.
- (38) Bessalle, R.; Kapitkovsky, A.; Gorea, A.; Shalit, I.; Fridkin, M. *FEBS Lett.* **1990**, 274, 151.
- (39) Yasin, B.; Lehrer, R. I.; Harwig, S. S. L.; Wagar, E. A. *Infect. Immun* **1996**, 64, 4869.
- (40) Cho, Y.; Turner, J. S.; Dinh, N.; Lehrer, R. I. *Infect. Immun* **1998**, 66, 2486.
- (41) Hancock, R. E. W. *Lancet* **1997**, 349, 349.
- (42) Melo, M. N.; Ferre, R.; Castanho, M. A. R. B. *Nature* **2009**, 7, 245.
- (43) Chen, X.; Tang, H.; Even, M. A.; Wang, J.; Tew, G. N.; Chen, Z. *J. Am. Chem. Soc.* **2006**, 128, 2711.
- (44) Yang, L.; Gordon, V. D.; Mishra, A.; Som, A.; Purdy, K. R.; Davis, M. A.; Tew, G. N.; Wong, G. C. L. *J. Am. Chem. Soc.* **2007**, 129, 12141.
- (45) Epand, R. F.; Umezawa, N.; Porter, E. A.; Gellman, S. H.; Epand, R. M. *Eur. J. Biochem.* **2003**, 270, 1240.
- (46) Frackenhohl, J.; Arvidsson, P. I.; Schreiber, J. V.; Seebach, D. *ChemBioChem* **2001**, 2, 445.
- (47) Chen, Y.; Mant, C. T.; Farmer, S. W.; Hancock, R. E. W.; Vasil, M. L.; Hodges, R. S. *J. Biol. Chem.* **2005**, 280, 12316.
- (48) Won, H. S.; Jung, S. J.; Kim, H. E.; Seo, M. D.; Lee, B. J. *J. Biol. Chem.* **2004**, 279, 14784.
- (49) Hamuro, Y.; Schneider, J. P.; DeGrado, W. F. *J. Am. Chem. Soc.* **1999**, 121, 12200.
- (50) Porter, E. A.; Wang, X.; Lee, H. S.; Weisblum, B.; Gellman, S. H. *Nature* **2000**, 404, 565.
- (51) Schmitt, M. A.; Weisblum, B.; Gellman, S. H. *J. Am. Chem. Soc.* **2007**, 129, 417.
- (52) Schmitt, M. A.; Weisblum, B.; Gellman, S. H. *J. Am. Chem. Soc.* **2004**, 126, 6848.
- (53) Chongsiriwatana, N. P. *Proc. Natl. Acad. Sci. U. S. A* **2008**, 105, 2794.
- (54) Liu, D.; Choi, S.; Chen, B.; Doerksen, R. J.; Clements, D. J.; Winkler, J. D.; Klein, M. L.; DeGrado, W. F. *Angew. Chem. Int. Ed.* **2004**, 43, 1158.
- (55) Tew, G. N.; Liu, D.; Chen, B.; Doerksen, R. J.; Kaplan, J.; Carrol, P. J.; Klein, M. L.; DeGrado, W. F. *Proc. Natl. Acad. Sci. U. S. A* **2002**, 99, 5110.
- (56) Tang, H.; Doerksen, R. J.; Tew, G. N. *Chem. Commun.* **2005**, 1537.
- (57) Kuroda, K.; DeGrado, W. F. *J. Am. Chem. Soc.* **2005**, 127, 4128.
- (58) Tang, H.; Doerksen, R. J.; Jones, T. V.; Klein, M. L.; Tew, G. N. *Chem. Biol.* **2006**, 13, 427.
- (59) Kuroda, K.; DeGrado, W. F. *J. Am. Chem. Soc.* **2005**, 127, 4128.
- (60) Ilker, M. F.; Nusslein, K.; Tew, G. N.; Coughlin, E. B. *J. Am. Chem. Soc.* **2004**, 126, 15870.
- (61) Gelman, M. A.; Weisblum, B.; Lynn, D. M.; Gellman, S. H. *Org. Lett.* **2004**, 6, 557.
- (62) Tang, H.; Doerksen, R. J.; Tew, G. N. *Chem Commun* **2005**, 1537.
- (63) Lienkamp, K.; Madkour, A. E.; Musante, A.; Nelson, C. F.; Nusslein, K.; Tew, G. N.

- J. Am. Chem. Soc.* **2008**, *130*, 9836.
- (64) Mowery, B. P.; Lee, S. E.; Kissounko, D. A.; Epand, R. F.; Epand, R. M.; Weisblum, B.; Stahl, S. S.; Gellman, S. H. *J. Am. Chem. Soc.* **2007**, *129*, 15474.
- (65) Tossi, A.; Sandri, L.; Giangaspero, A. *Biopolymers* **2000**, *55*, 4.
- (66) Lai, J. R.; Huck, B. R.; Weisblum, B.; Gellman, S. H. *Biochemistry* **2002**, *41*, 12835.
- (67) Raguse, T. L.; Porter, E. A.; Weisblum, B.; Gellman, S. H. *J. Am. Chem. Soc.* **2002**, *124*, 12774.
- (68) Gellman, S. H. *Acc. Chem. Res.* **1998**, *31*, 173.
- (69) Dado, G. P.; Gellman, S. H. *J. Am. Chem. Soc.* **1994**, *116*, 1054.
- (70) Appella, D. H.; Christianson, L. A.; Karle, I. L.; Rowell, D. R.; Gellman, S. H. *J. Am. Chem. Soc.* **1996**, *118*, 13071.
- (71) Porter, E. A.; Weisblum, B.; Gellman, S. H. *J. Am. Chem. Soc.* **2002**, *124*, 7324.
- (72) Guichard, G.; Seebach, D. *Chimia* **1997**, *51*, 315.
- (73) Hintermann, T.; Seebach, D. *Synlett* **1997**, 437.
- (74) Seebach, D.; Ciceri, P. E.; Overhand, M.; Jaun, B.; Rigo, D.; Oberer, L.; Hommel, U.; Amstutz, R.; Widmer, H. *Helv. Chim. Acta* **1996**, *79*, 2043.
- (75) Seebach, D.; Overhand, M.; Kuhnle, F. N. M.; Martinoni, B.; Oberer, L.; Hommel, U. W., H. *Helv. Chim. Acta* **1996**, *79*, 913.
- (76) Hintermann, T.; Seebach, D. *Chimia* **1997**, *51*, 244.
- (77) Muller, H. -.; Seebach, D. *Angew. Chem. Int. Ed.* **1993**, *32*, 477.
- (78) Hintermann, T.; Gademann, K.; Jaun, B.; Seebach, D. *Helv. Chim. Acta* **1998**, *81*, 932.
- (79) Watterson, M. P.; Fleet, G. W. J. *Tetrahed. Lett.* **2001**, *42*, 4251.
- (80) LePlae, P. R.; Fisk, J. D.; Porter, E. A.; Weisblum, B.; Gellman, S. H. *J. Am. Chem. Soc.* **2002**, *124*, 6820.
- (81) Chen, H.; Brown, J. H.; Morell, J. L.; Huang, C. M. *FEBS Lett.* **1988**, *236*, 462.
- (82) Habermann, E. *Science* **1972**, *177*, 314.
- (83) Porter, E. A.; Weisblum, B.; Gellman, S. H. *J. Am. Chem. Soc.* **2002**, *124*, 7324.
- (84) Liu, D.; DeGrado, W. F. *J. Am. Chem. Soc.* **2001**, *123*, 7553.
- (85) LePlae, P. R.; Umezawa, N.; Lee, H. -.; Gellman, S. H. *J. Org. Chem.* **2001**, *66*, 5629.
- (86) Porter, E. A.; Weisblum, B.; Gellman, S. H. *J. Am. Chem. Soc.* **2005**, *127*, 11516.
- (87) Dathe, M.; Wieprecht, T.; Nikolenko, H. H., L.; Maloy, W. L.; MacDonald, D. L.; Beyermann, M.; Bienert, M. *FEBS Lett.* **1997**, *403*, 208-212.
- (88) Seebach, D.; Abele, S.; Schreiber, J. V.; Martinoni, B.; Nussbaum, A. K.; Schild, H.; Schulz, H.; Hennecke, H.; Woessner, R.; Bitsch, R. *Chimia* **1998**, *52*, 734-?.
- (89) Appella, D. H.; Barchi Jr., J. J.; Durell, S. R.; Gellman, S. H. *J. Am. Chem. Soc.* **1999**, *121*, 2309-2310.
- (90) Zhang, L.; Benz, R.; Hancock, R. E. W. *Biochemistry* **1999**, *38*, 8102-8111.
- (91) Oren, Z.; Shai, Y. *Biochemistry* **1997**, *36*, 1826.
- (92) Dathe, M.; Schumann, M.; Wieprecht, T.; Winkler, A.; Beyermann; Krause, E.; Matsuzaki, K.; Murase, O.; Bienert, M. *Biochemistry* **1996**, *35*, 12612-12622.
- (93) De Pol, S.; Zorn, C.; Klein, C. D.; Zerbe, O.; Reiser, O. *Angew. Chem. Int. Ed.* **2004**, *43*, 511.
- (94) Hayen, A.; Schmitt, M. A.; Ngassa, K. A.; Gellman, S. H. *Angew. Chem. Int. Ed.* **2004**, *43*, 505.

- (95) Giangaspero, A.; Sandri, L.; Tossi, A. *Eur. J. Biochem.* **2001**, *268*, 5589.
- (96) Epand, R. F.; Schmitt, M. A.; Gellman, S. H.; Sen, A.; Auger, M.; Hughes, D. W.; Epand, R. M. *Mol. Membr. Biol.* **2005**, *22*, 457.
- (97) Engelmann, B.; Streich, S.; Schonthier, U. M.; Richter, W. O.; Duhm, J. *Biochim. Biophys. Acta* **1992**, *1165*, 32.
- (98) Epand, R. F.; Schmitt, M. A.; Gellman, S. H.; Epand, R. M. *Biochim. Biophys. Acta* **2006**, *1758*, 1343.
- (99) Rathinakumar, R.; Wimley, W. C. *J. Am. Chem. Soc.* **2008**, *130*, 9849.
- (100) Sambhy, B.; Peterson, B. R.; Sen, A. *Angew. Chem. Int. Ed.* **2008**, *47*, 1250.
- (101) Allison, B.; Applegate, B. M.; Youngblood, J. P. *Biomacromolecules* **2007**, *8*, 2995.
- (102) Sellenet, P. H.; Allison, B.; Applegate, B. M.; Youngblood, J. P. *Biomacromolecules* **2007**, *8*, 19.
- (103) Lewis, K.; Klibanov, A. M. *Trends Biotechnol.* **2005**, *23*, 343.
- (104) Tiller, J. C.; Liao, C. -; Lewis, K.; Klibanov, A. M. *Proc. Natl. Acad. Sci. U. S. A* **2001**, *98*, 5981.
- (105) Hashimoto, K. *Prog. Polym. Sci.* **2000**, *25*, 1411.
- (106) Lee, M.; Stahl, S. S.; Gellman, S. H. *Org. Lett.* **2008**, *10*, 5317-5319.
- (107) Epand, R. F.; Mowery, B. P.; Lee, S. E.; Stahl, S. S.; Lehrer, R. I.; Gellman, S. H.; Epand, R. M. *J. Mol. Biol.* **2008**, *379*, 38.
- (108) Mowery, B. P.; Lindner, A. H.; Weisblum, B.; Stahl, S. S.; Gellman, S. H. *J. Am. Chem. Soc.* **2009**, *131*, 9735.
- (109) Zhang, J.; Kissounko, D. A.; Lee, S. E.; Gellman, S. H.; Stahl, S. S. *J. Am. Chem. Soc.* **2009**, *131*, 1589.
- (110) Ilker, M. F.; Schule, H.; Coughlin, E. B. *Macromolecules* **2004**, *37*, 694.
- (111) Tew, G. N.; Clements, D.; Tang, H.; Arnt, L.; Scott, R. W. *Biochim. Biophys. Acta - Biomembranes* **2006**, *1758*, 1387.
- (112) Arnt, L.; Nusslein, K.; Tew, G. N. *J. Polym. Sci Part A: Polym. Chem.* **2004**, *42*, 3860.
- (113) Arnt, L.; Tew, G. N. *Langmuir* **2003**, *19*, 2404.
- (114) Yang, L.; Gordon, V. D.; Mishra, A.; Som, A.; Purdy, K. R.; Davis, M. A.; Tew, G. N.; Wong, G. C. L. *J. Am. Chem. Soc.* **2007**, *128*, 12141.
- (115) Chen, S.; Tang, H.; Even, M. A.; Wang, J.; Tew, G. N.; Chen, Z. J. *J. Am. Chem. Soc.* **2006**, *128*, 2711.
- (116) Al-Badri, Z. M.; Som, A. L., S.; Nelson, C. F.; Nusslein, K.; Tew, G. N. *Biomacromolecules* **2008**, *9*, 2805.
- (117) Al-Badri, Z. M.; Tew, G. N. *Macromolecules* **2008**, *41*, 4173.
- (118) Gabriel, G. J.; Madkour, A. E.; Dabrowski, J. M.; Nelson, C. F.; Nusslein, K.; Tew, G. N. *Biomacromolecules* **2008**, *9*, 2980.
- (119) Arnt, L.; Tew, G. N. *J. Am. Chem. Soc.* **2002**, *124*, 7664.
- (120) Colak, S.; Nelson, C. F.; Nusslein, K.; Tew, G. N. *Biomacromolecules* **2009**, *10*, 353.
- (121) Gabriel, G. J.; Maegerlein, J. A.; Nelson, C. F.; Dabkowski, J. M.; Eren, T.; Nusslein, K.; Tew, G. N. *Chem. Eur. J.* **2009**, *15*, 433.
- (122) Hennig, A.; Gabriel, G. J.; Tew, G. N.; Matile, S. *J. Am. Chem. Soc.* **2008**, *130*, 10338.

- (123) Doerksen, R. J.; Chen, B.; Liu, D.; Tew, G. N.; DeGrado, W. F.; Klein, C. D. *Chem. Eur. J.* **2004**, *10*, 5008.
- (124) Pophristic, V.; Vemparala, S.; Ivanov, I.; Liu, Z.; Klein, M. L.; DeGrado, W. F. *J. Phys. Chem. B* **2006**, *110*, 3517.
- (125) Vemparala, S.; Ivanov, I.; Pophristic, V.; Spiegel, K.; Klein, M. L. *J. Comput. Chem* **2006**, *27*, 693.
- (126) Scott, R. W.; DeGrado, W. F.; Tew, G. N. *Curr. Opin. Biotechnol.* **2008**, *19*, 620.
- (127) Ishitsuka, Y.; Lachelle, A.; Majewski, J.; Frey, S.; Ratajczek, M.; Kjaer, K.; Tew, G. N.; Lee, K. Y. C. *J. Am. Chem. Soc.* **2006**, *128*, 13123.
- (128) Yang, L.; Gordon, V. D.; Trinkle, D. R.; Schmidt, N. W.; Davis, M. A.; CeVries, C.; Som, A.; Cronan Jr., G. E.; Tew, G. N.; Wong, G. C. L. *Proc. Natl. Acad. Sci. U. S. A* **2008**, *105*, 20595.
- (129) Slutsky, M. M.; Phillip, J. S.; Tew, G. N. *New J. Chem.* **2008**, *32*, 670.
- (130) Ishitsuka, Y.; Arnt, L.; Ratajczek, M.; Frey, S.; Majewski, J.; Kjaer, K.; Tew, G. N.; Lee, K. Y. C. *J. Am. Chem. Soc.* **2006**, *128*, 13123.
- (131) Jones, T. V.; Slutsky, M. M.; Laos, R.; de Greef, T. F. A.; Tew, G. N. *J. Am. Chem. Soc.* **2005**, *127*, 17235.
- (132) Gabriel, G. J.; Tew, G. N. *Org. Biomol. Chem* **2008**, *5*, 417.
- (133) Blazyk, J.; Wiegand, R.; Klein, J.; Hammer, J.; Epanand, R. M.; Epanand, R. F.; Maloy, W. L.; Kari, U. P. *J. Biol. Chem.* **2001**, *276*, 27899.
- (134) Srinivas, N.; Moehle, K.; Abou-Hadeed, K.; Obrecht, D.; Robinson, J. A. *Org. Biomol. Chem* **2007**, *2007*, 3100.
- (135) Nowick, J. S. *Acc. Chem. Res.* **2008**, *41*, 1319.
- (136) Nowick, J. S.; Powell, N. A.; Martinex, E. J.; Smith, E. M.; Noronha, G. *J. Org. Chem.* **1992**, *57*, 3763.
- (137) Nowick, J. S.; Smith, E. M.; Pairish, M. *Chem. Soc. Rev.* **1996**, *25*, 401.
- (138) Nowick, J. S. *Acc. Chem. Res.* **1999**, *32*, 287.
- (139) Nowick, J. S. *Org. Biomol. Chem* **2006**, *4*, 3869.
- (140) Nowick, J. S.; Insaf, S. *J. Am. Chem. Soc.* **1997**, *119*, 10903.
- (141) Chou, P. Y.; Fasman, G. D. *Biochemistry* **1974**, *13*, 211.
- (142) Nowick, J. S.; Chung, D. M.; Maitra, K.; Stigers, K. D.; Sun, Y. *J. Am. Chem. Soc.* **2000**, *122*, 7654.
- (143) Nowick, J. S.; Holmes, D. L.; Mackin, G.; Noronha, G.; Shaka, A. J.; Smith, E. M. *J. Am. Chem. Soc.* **1996**, *118*, 2764.
- (144) Smith, E. M.; Holmes, D. L.; Shaka, A. J.; Nowick, J. S. *J. Org. Chem.* **1997**, *62*, 7906.
- (145) Khasanova, T. V.; Khakshoor, O.; Nowick, J. S. *Org. Lett.* **2008**, *10*, 5293.
- (146) Phillips, S. T.; Piersanti, G.; Ruth, M.; Gubernator, N.; van Lengerich, B.; Bartlett, P. A. *Org. Lett.* **2004**, *6*, 4483.
- (147) Phillips, S. T.; Rezac, M.; Abel, U.; Kossenjans, M.; Bartlett, P. A. *J. Am. Chem. Soc.* **2002**, *124*, 58.
- (148) Hammond, M. C.; Harris, B. Z.; Lim, W. A.; Bartlett, P. A. *Chem. Biol.* **2006**, *13*, 1247.
- (149) Phillips, S. T.; Rezac, M.; Abel, U.; Kossenjans, M.; Bartlett, P. A. *J. Am. Chem. Soc.* **2002**, *124*, 58.
- (150) Porter, E. A.; Wang, X.; Lee, H. S.; Weisblum, B.; Gellman, S. H. *Nature* **2000**,

404, 565.

- (151) Rossmeis, J.; Kristensen, I.; Gregersen, M.; Jacobsen, K. W.; Norskov, J. K. *J. Am. Chem. Soc.* **2003**, *125*, 16383.
- (152) Fasman, G. D. In *Fasman, G. D. In Prediction of Protein Structure and the Principles of Protein Conformation*; Plenum Publishing: New York, 1989.
- (153) Arvidsson, P. I.; Ryder, N. S.; Weiss, H. M.; Gross, G.; Kretz, O.; Woessner, R.; Seebach, D. *ChemBioChem* **2003**, *4*, 1345.
- (154) Zheng, Y.; Duanmu, C.; Gao, Y. *Org. Lett.* **2006**, *8*, 3215.
- (155) Phillips, S. T.; Blasdel, L. K.; Bartlett, P. A. *J. Am. Chem. Soc.* **2005**, *127*, 4193.
- (156) Schneider, H. J., Durr, H., Eds. In *Wilcox, D. S. In Frontiers in Supramolecular Organic Chemistry and Photochemistry*; VCH: New York, 1991, pp 123-143.
- (157) Brock, T. D. In *Biology of Microorganisms, 2nd ed.* Prentice Hall: Englewood Cliffs, NJ, 1974.
- (158) Bai, Y.; Louis, K. L.; Murphy, R. S. *J. Photochem Photobiol. A* **2007**, *192*, 130.
- (159) Daleke, K. L.; Hong, K.; Papahadjopoulos, D. *Biochim. Biophys. Acta* **1990**, *1024*, 352.
- (160) Oren, Z.; Shai, Y. *Biochemistry* **1997**, *36*, 1826.
- (161) Cuervo, J. H.; Rodriguez, B.; Houghten, R. A. *Pept. Res.* **1988**, *1*, 81.
- (162) Li, Z. Q.; Merrifield, R. B.; Boman, I. A.; Boman, H. G. *FEBS Lett.* **1988**, *231*, 299.
- (163) Bechinger, B.; Zasloff, M.; Opella, S. J. *Protein Sci.* **1993**, *2*, 2077.
- (164) Scott, J. W.; Parker, D.; Parrish, D. R. *Synth. Commun.* **1981**, *11*, 303.
- (165) Nowshuddin, S.; Reddy, A. R. *Tetrahed. Lett.* **2006**, *47*, 5159.
- (166) Erdelyi, M.; Langer, V.; Karlen, A.; Gogoll, A. *New J. Chem.* **2002**, *26*, 834.

Part Six: Appendix (NMR Spectra)

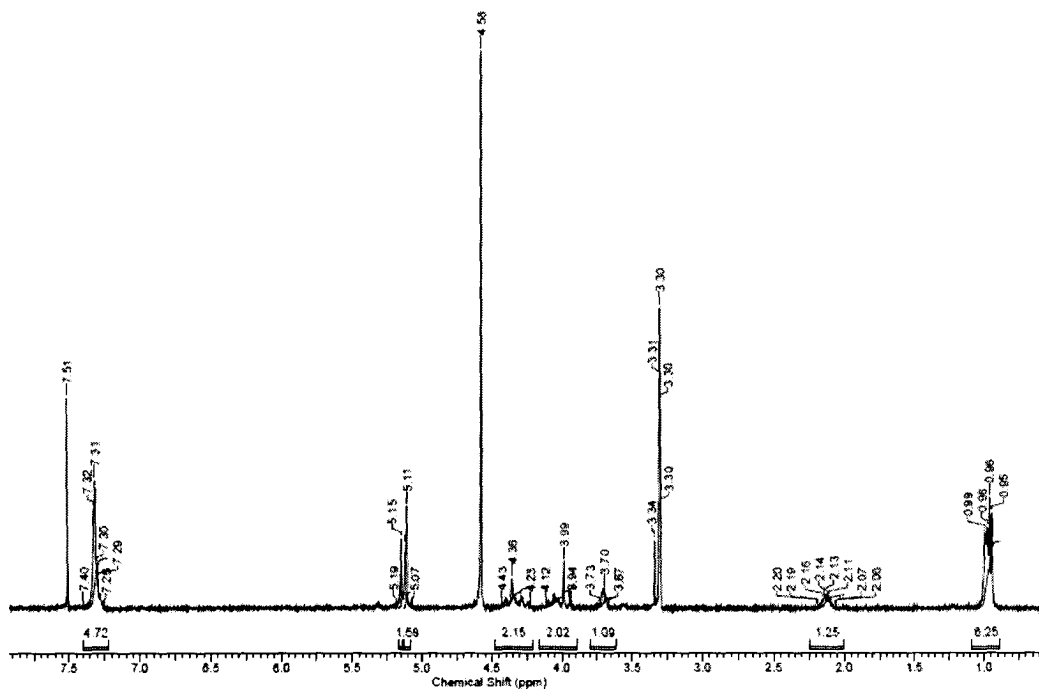


Figure A1. ¹H NMR spectrum of compound 2/2' (400 MHz, CDCl₃/CD₃OD (2/1)).

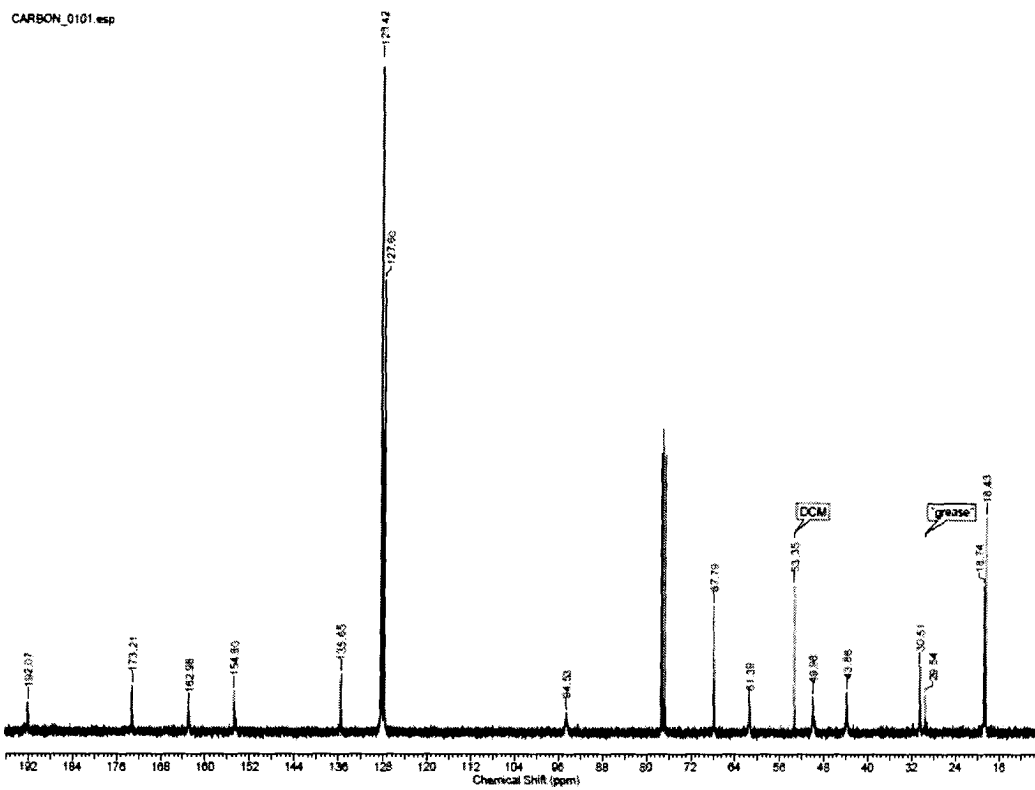


Figure A2. ¹³C NMR spectrum of compound 2/2' (100 MHz, CDCl₃).

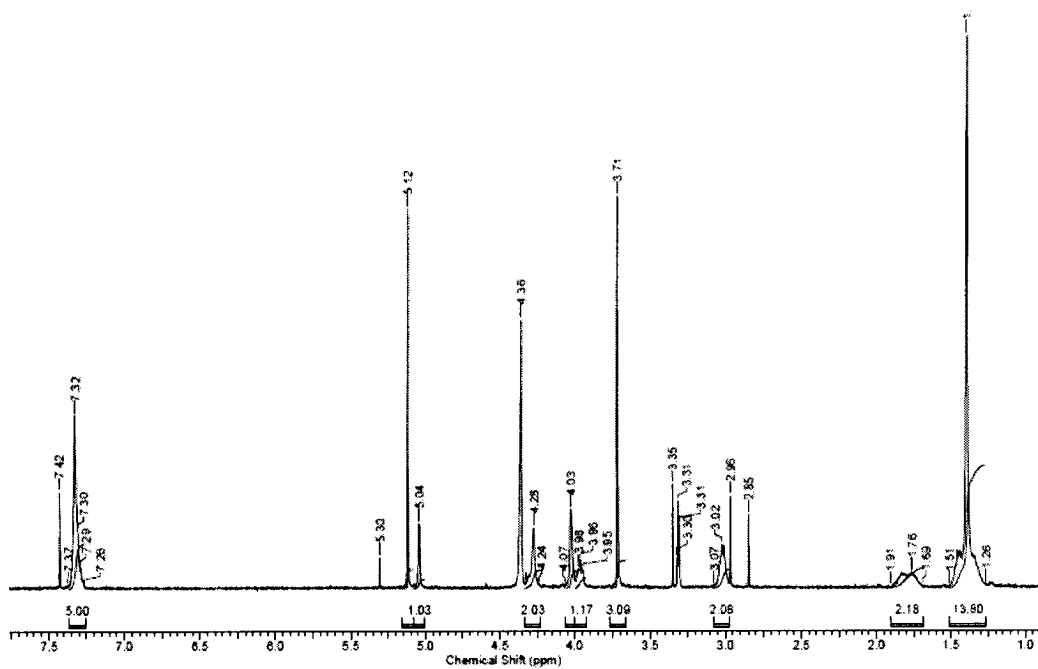


Figure A3. ^1H NMR spectrum of compound 4 (400 MHz, $\text{CDCl}_3/\text{CD}_3\text{OD}$ (2/1)).

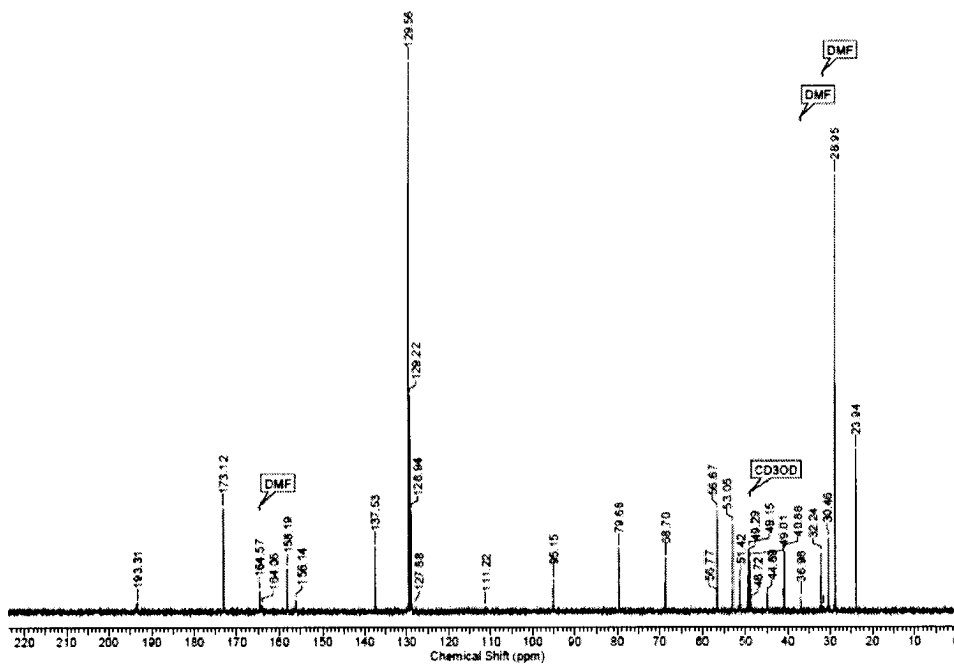


Figure A4. ^{13}C NMR spectrum of compound 4 (150 MHz, $\text{CDCl}_3/\text{CD}_3\text{OD}$ (2/1)).

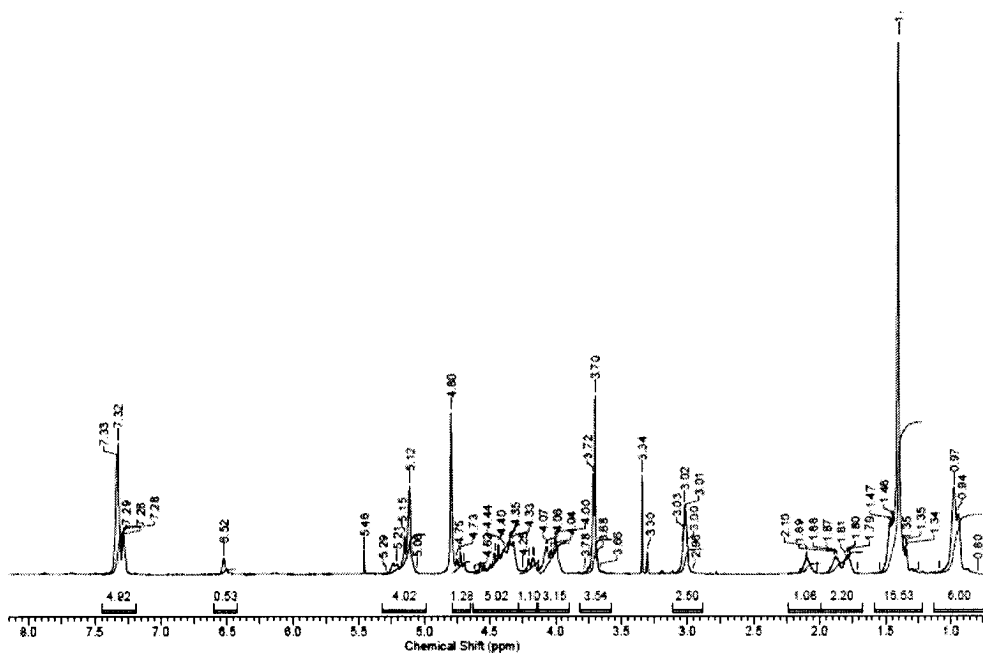


Figure A5. ^1H NMR spectrum of compound 6 (600 MHz, CD_3OD)

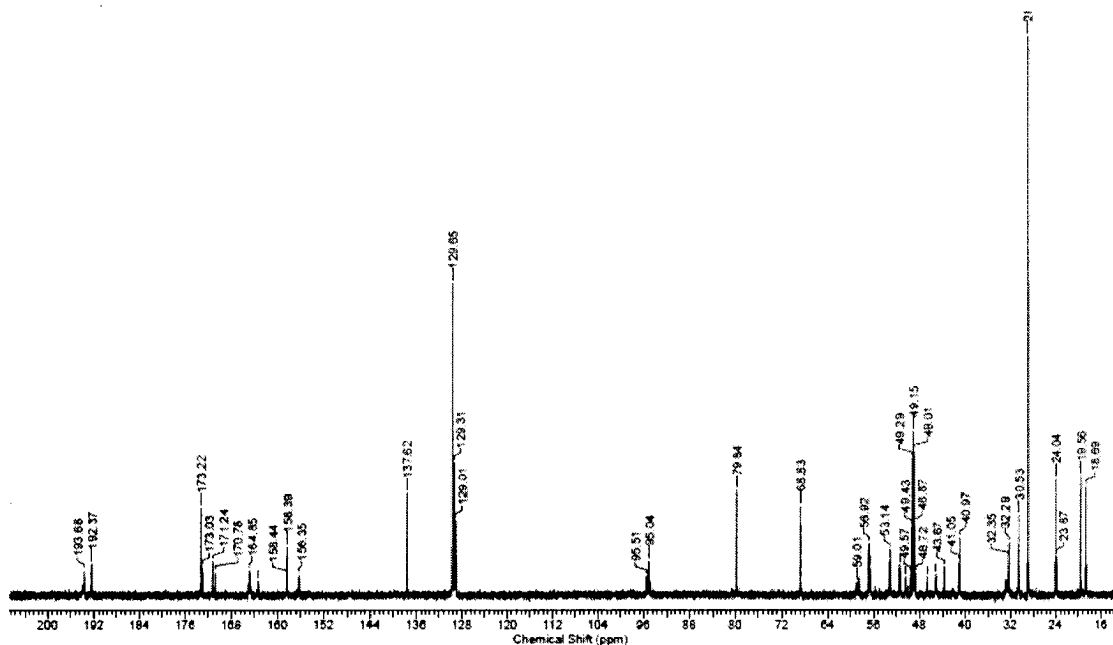


Figure A6. ^{13}C NMR spectrum of compound 6 (150 MHz, CD_3OD)

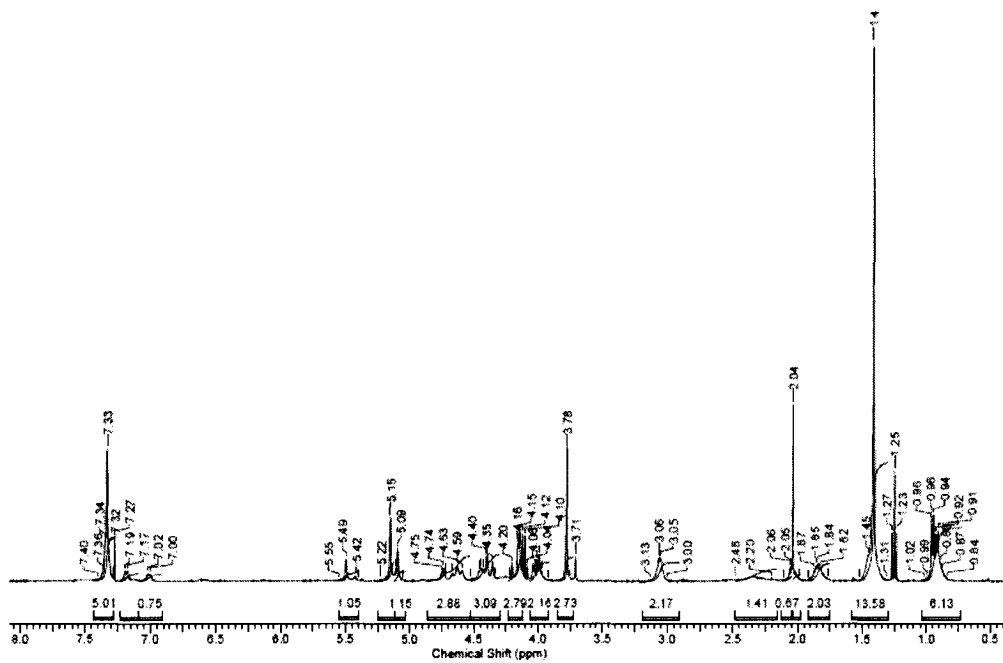


Figure A7. ^1H NMR spectrum of compound **6'** (400 MHz, CDCl_3)

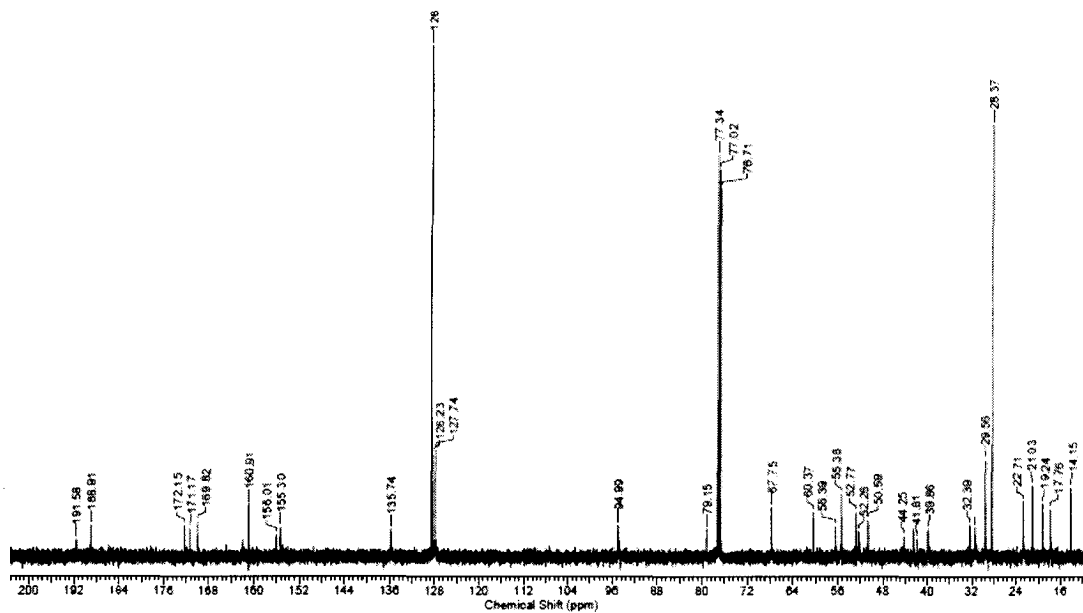


Figure A8. ^{13}C NMR spectrum of compound **6'** (100 MHz, CDCl_3)

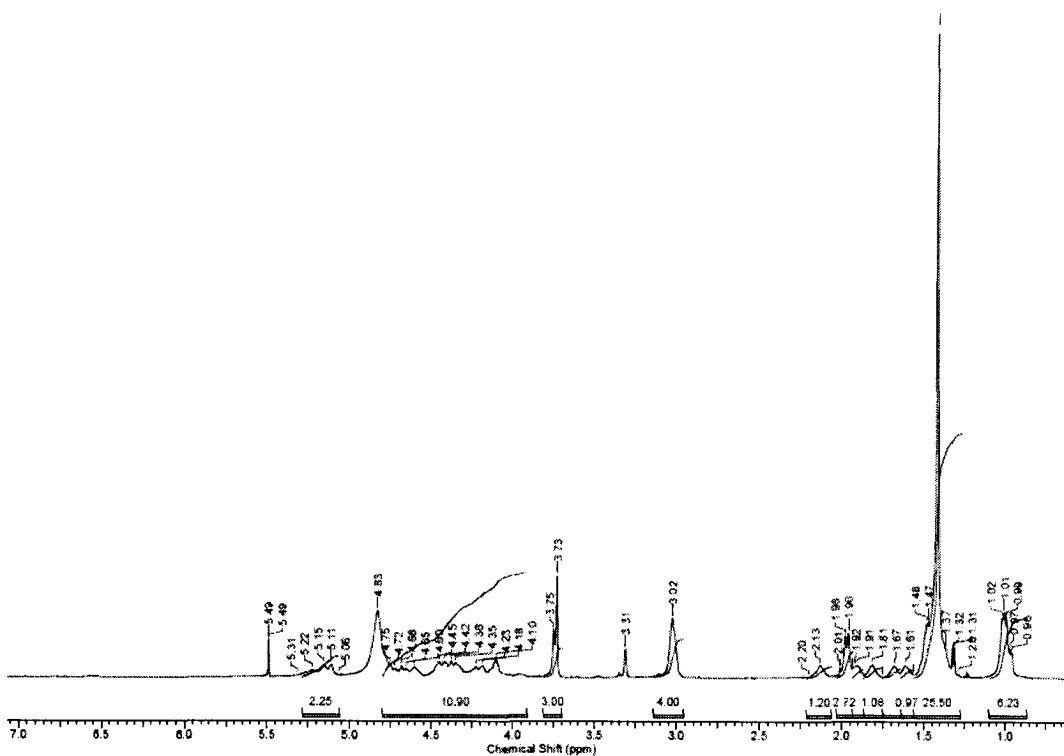


Figure A9. ^1H NMR spectrum of compound **8** (400 MHz, $\text{CDCl}_3/\text{CD}_3\text{OD}$ (2/1))

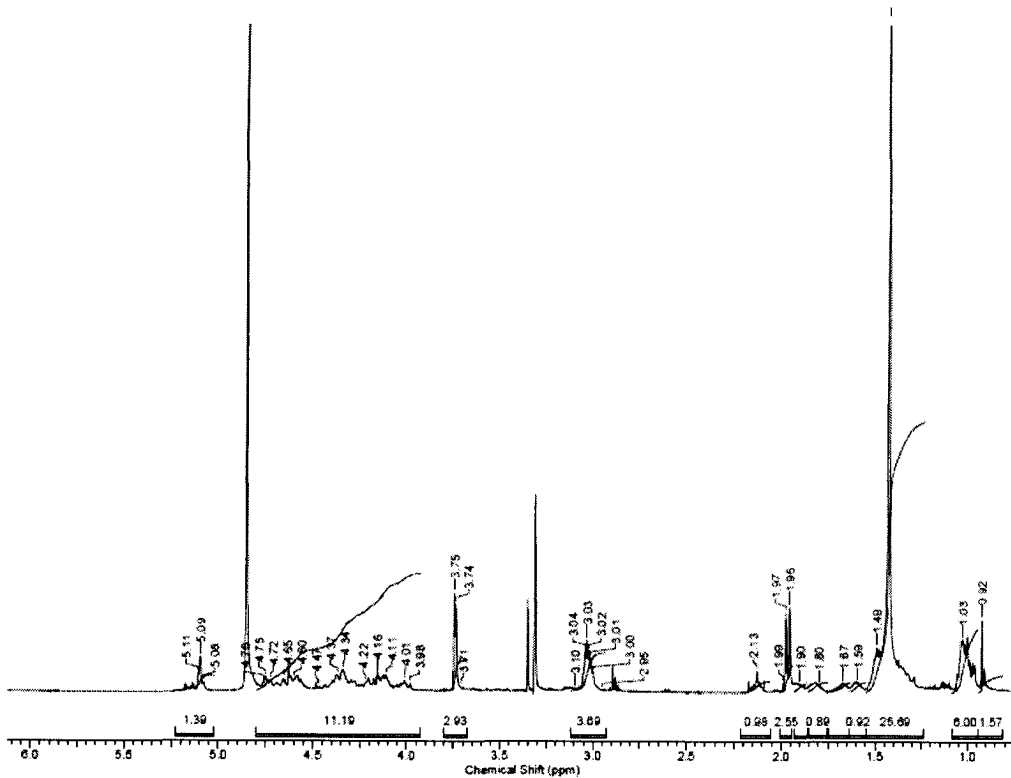


Figure A10. ^1H NMR spectrum of compound **8'** (400 MHz, CD_3OD)

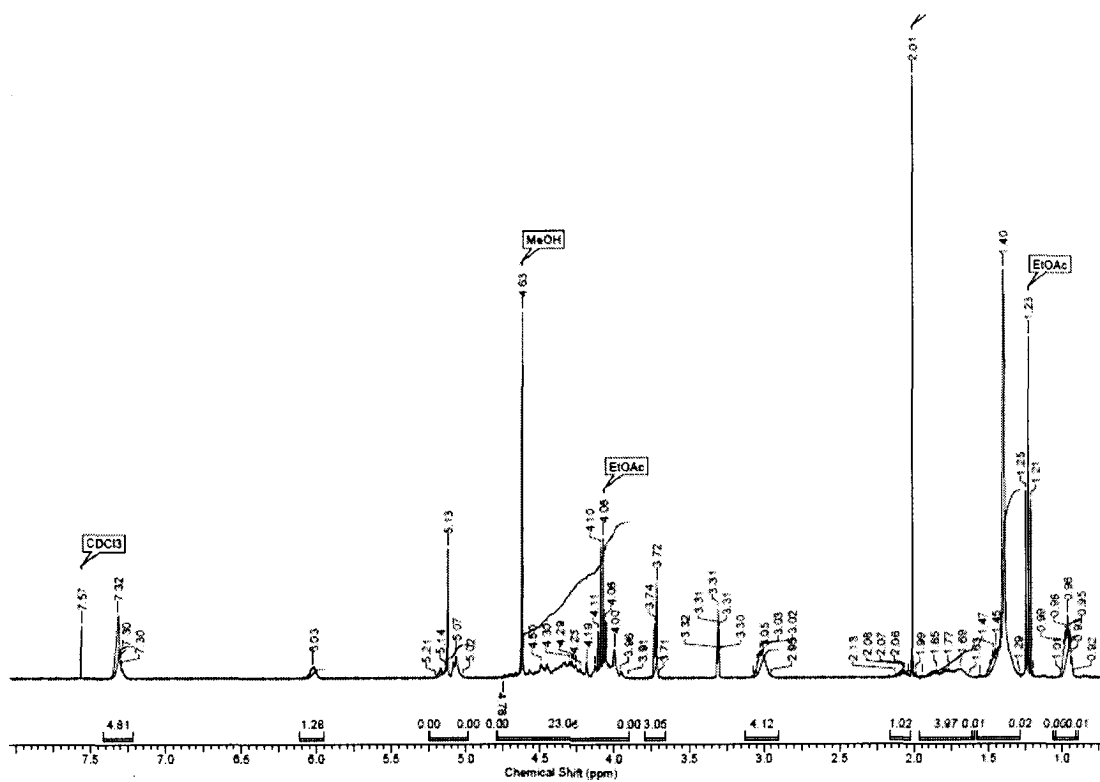


Figure A11. ^1H NMR spectrum of compound **9** (400 MHz, $\text{CDCl}_3/\text{CD}_3\text{OD}$ (2/1))

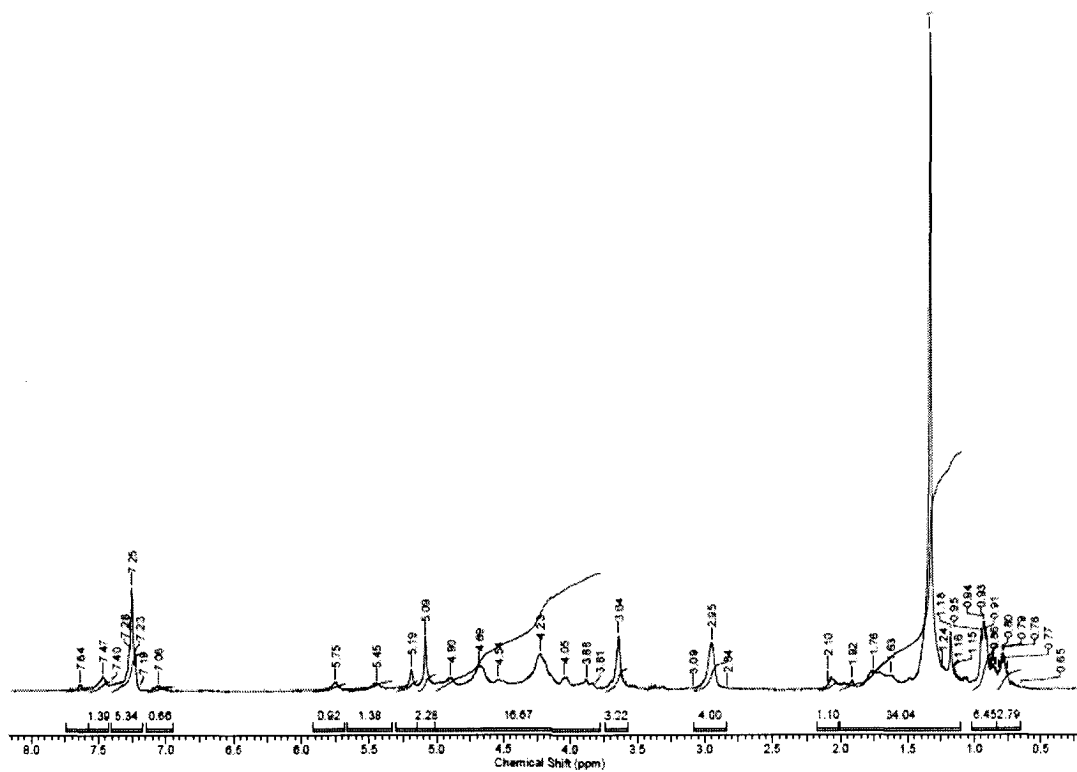


Figure A12. ^1H NMR spectrum of compound **9'** (400 MHz, CDCl_3)

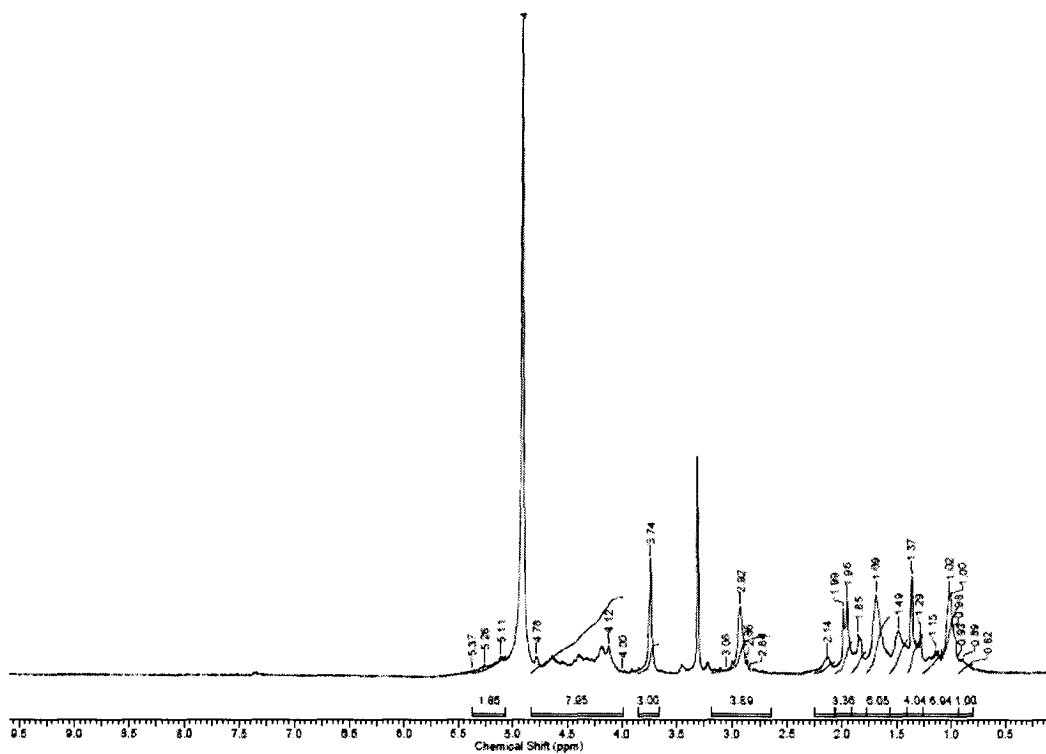


Figure A13. ^1H NMR spectrum of compound **10** (400 MHz, $\text{CDCl}_3/\text{CD}_3\text{OD}$ (2/1))

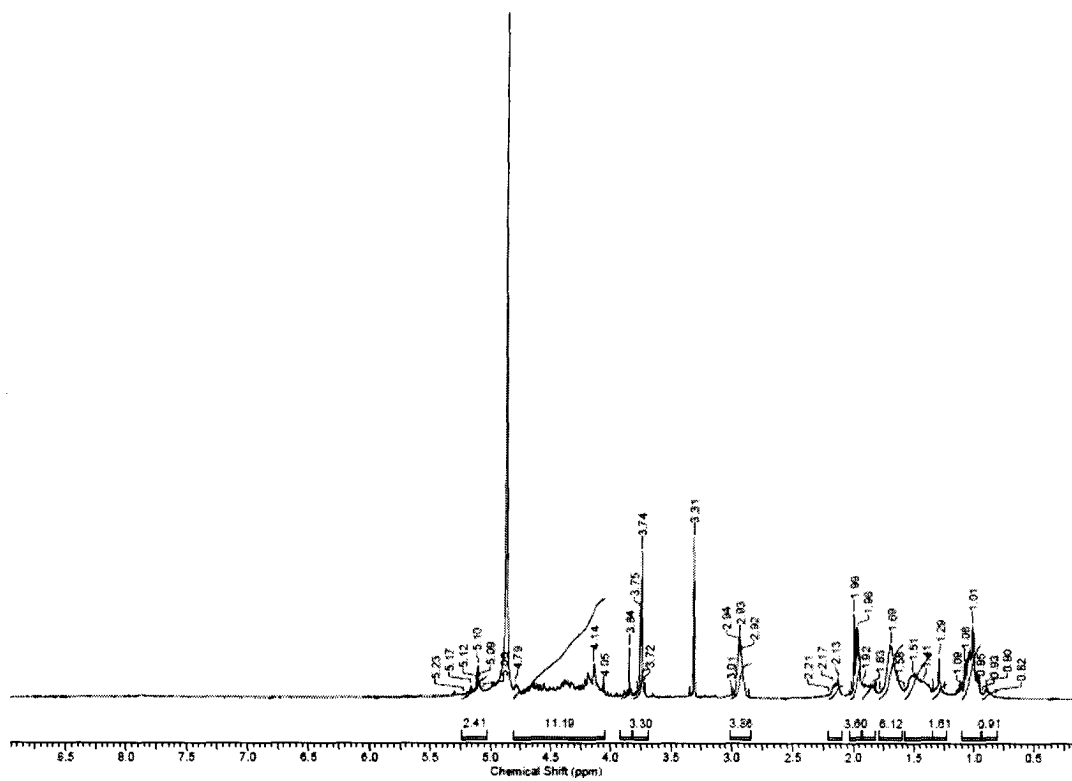


Figure A14. ^1H NMR spectrum of compound **10'** (400 MHz, CD_3OD)

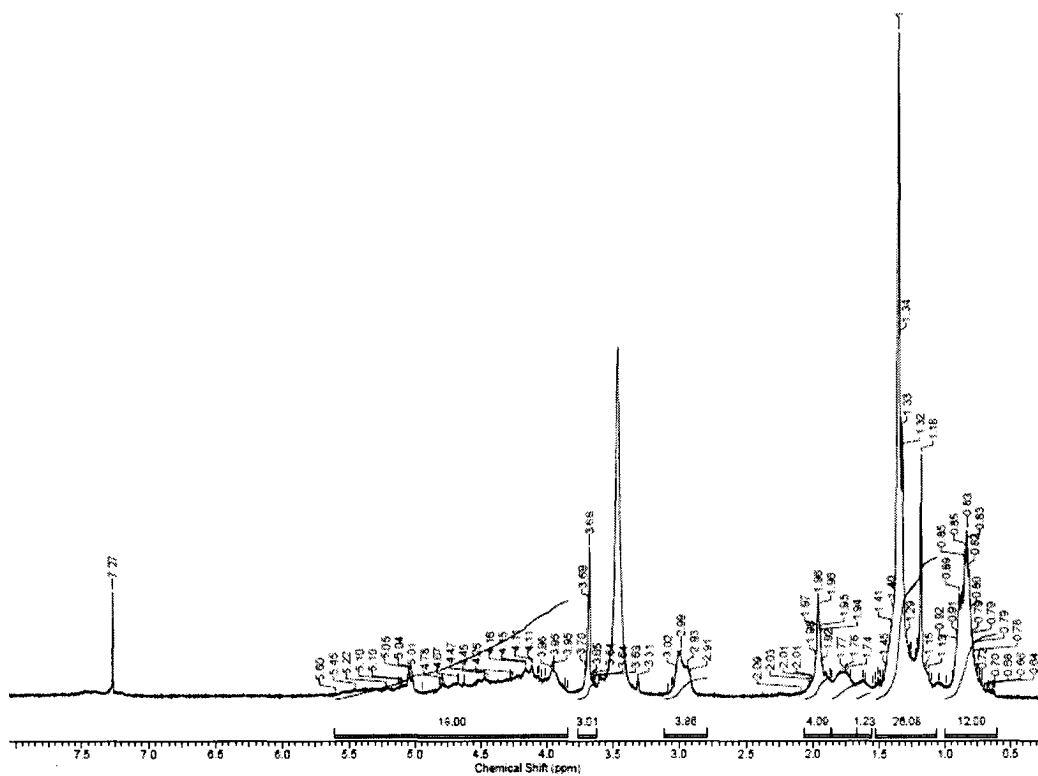


Figure SA17. ^1H NMR spectrum of compound 13 (600 MHz, $\text{CDCl}_3/\text{CD}_3\text{OD}$ (2/1))

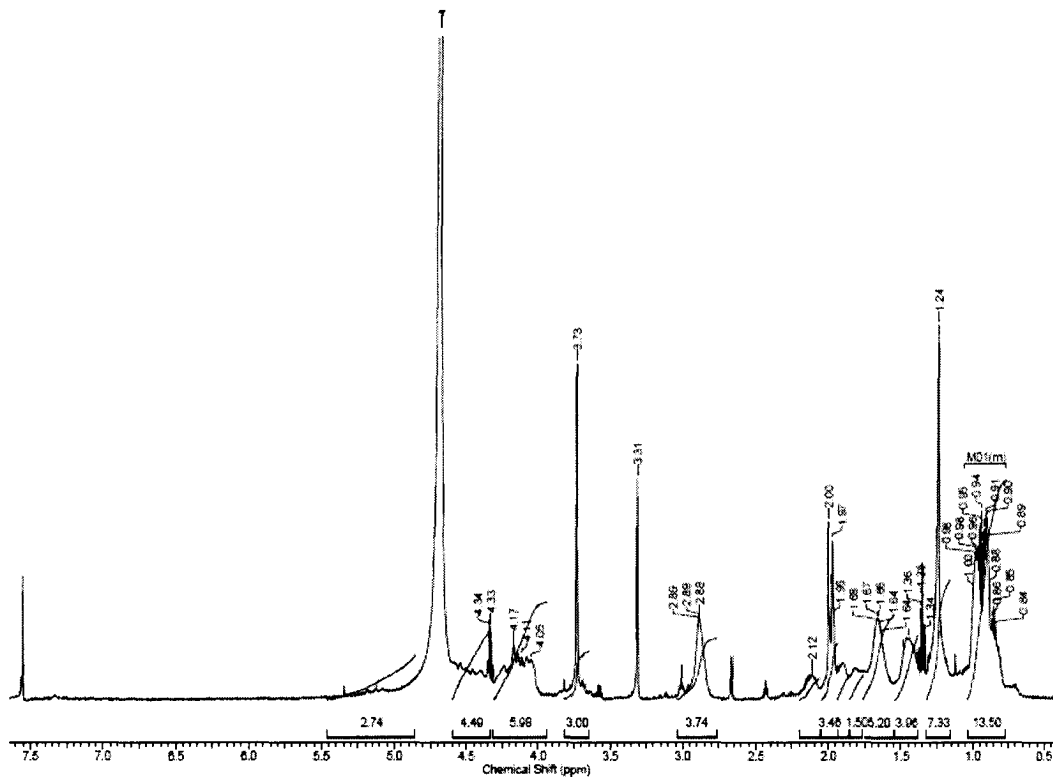


Figure A18. ^1H NMR spectrum of compound 14 (600 MHz, $\text{CDCl}_3/\text{CD}_3\text{OD}$ (1/2))

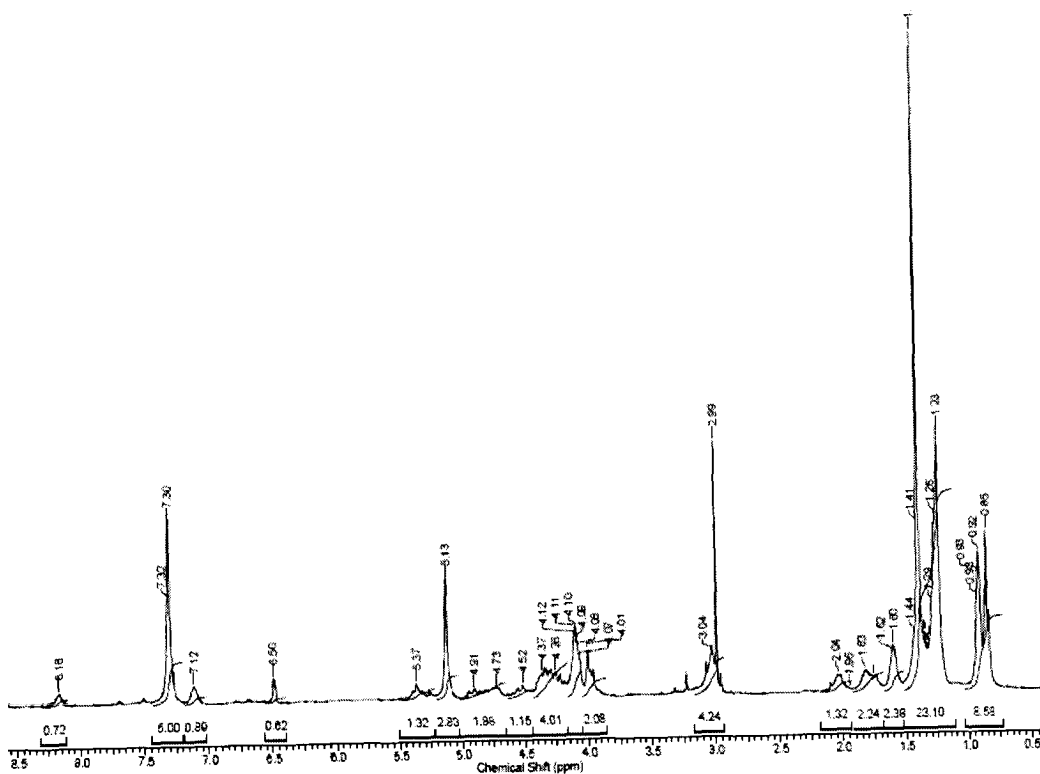


Figure A21. ^1H NMR spectrum of compound **18** (600 MHz, CDCl_3)

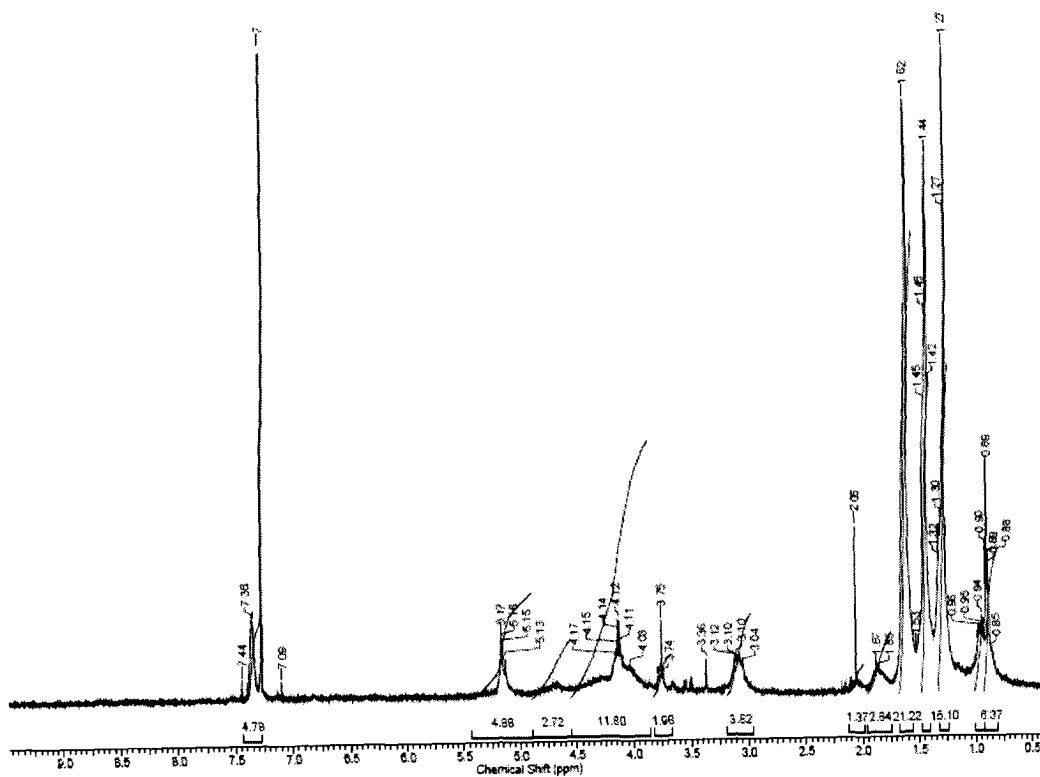


Figure A22. ^1H NMR spectrum of compound **20** (600 MHz, CDCl_3)